Technical Report

Final Report for Annex II— Assessment of Solar Radiation Resources in Saudi Arabia 1998–2000

Daryl R. Myers
Stephen M. Wilcox
William F. Marion
Naif M. Al-Abbadi
Mohammed bin Mahfoodh
Zaid Al-Otaibi

King Abdulaziz City for Science and Technology
Energy Research Institute

NREL

National Renewable Energy Laboratory

Final Report for Annex II—Assessment of Solar Radiation Resources in Saudi Arabia 1998–2000

Daryl R. Myers
Stephen M. Wilcox
William F. Marion
Naif M. Al-Abbadi
Mohammed bin Mahfoodh
Zaid Al-Otaibi

King Abdulaziz City for Science and Technology
Energy Research Institute

NREL

National Renewable Energy Laboratory

NOTICE

NOTICE

This document was produced and printed as an account of work performed by the National Renewable Energy Laboratory under the Joint U.S./Saudi Arabia Renewable Energy Agreement between the United States of America and the Kingdom of Saudi Arabia. This work was performed under Annex II of the agreement, "Assessment of Solar Radiation Resources in Saudi Arabia." The project was funded by the Saudi Arabian Ministry of Finance programs supporting the King Abdulaziz City for Science and Technology, Energy Research Institute, Riyadh, Saudi Arabia. Neither the United States nor the United States Department of Energy, nor any of their employees, nor any of their contractors, subcontractors, or their employees, makes any warranty, express or implied, or assumes any legal liability or responsibility for the accuracy, completeness, or usefulness of any information, apparatus, product, or process disclosed, or represents that its use would not infringe privately owned rights.

Preface

The *Final Report for Annex II – Assessment of Solar Radiation Resources in Saudi Arabia 1998-2000* summarizes the accomplishment of work performed, results achieved, and products produced under Annex II, a project established under the Agreement for Cooperation in the Field of Renewable Energy Research and Development between the Kingdom of Saudi Arabia and the United States. The report covers work and accomplishments from January 1998 to December 2000. A previous progress report, *Progress Report for Annex II – Assessment of Solar Radiation Resources in Saudi Arabia 1993-1997*, NREL/TP-560-29374, summarizes earlier work and technical transfer of information under the project. A brief synopsis of the progress report is contained in this final report. The work was performed in at the National Renewable Energy Laboratory (NREL) in Golden, Colorado, at the King Abdulaziz City for Science and Technology (KACST) in Riyadh, Saudi Arabia, and at selected weather stations of the Saudi Meteorological and Environmental Protection Administration (MEPA). The primary objectives of Annex II were to upgrade the assessment of solar radiation resources in Saudi Arabia, and to transfer NREL's solar radiation resource assessment technology to KACST in the form of hardware, software, and staff training. These objectives have been substantially achieved.

Direct financial support for Annex II came from KACST through the Joint Economic Commission Office in Riyadh (JECOR), and the United States Department of Energy (DOE). Substantial indirect support was received from MEPA and from several resource assessment research and development projects at NREL. In particular, MEPA performs operational control and maintenance of the solar radiation measurement equipment at 11 of the 12 stations in the Saudi Arabian solar radiation monitoring network (designed and established under this project). MEPA also transfers meteorological and METEOSAT satellite data to KACST at no cost to the project. In addition to direct support for hardware and software development, the Annex II project benefited from technology developments achieved under independent NREL research and development projects, including the technology to produce high resolution (40 kilometer spacing) solar radiation data grids, vital to the production of the new Solar Radiation Atlas for Saudi Arabia.

Acknowledgements

Approved for the National Renewable Energy Laboratory

Tony Schaffhauser, Director
Distributed Energy Resources Center

Daryl Myers, Leader
Saudi Arabian Annex II Task
Center for Renewable Energy Resources

Approved for the King Abdulaziz City for Science and Technology

AbudlRahman M. Al-Ibrahim, Director
KACST Energy Research Institute

Ali I. Al-Rubian, Supervisor
Renewable Energy Department
KACST Energy Research Institute

Contents

List of Tables

List of Figures

List of Acronyms and Abbreviations

ACR	Absolute Cavity Radiometers
AOD	Aerosol Optical Depth
ARM	DOE's Atmospheric Radiation Measurement program
ASES	The American Solar Energy Society
BSRN	Baseline Surface Radiation Network
CERES	Clouds and Earth Radiant Energy Sensor
CSR	Climatological Solar Radiation
DOE	United States Department of Energy
DQMS	Data Quality Management System
EOS	Earth Observing System
ETR	Extraterrestrial radiation
GIS	Geographical Information System
IPC	International Pyrheliometer Comparisons (sponsored by WMO)
KACST	King Abdulaziz City for Science and Technology
METEOSAT	Meteorological Satellite (European Space Agency)
MEPA	The Saudi Meteorological and Environmental Protection Agency
MPA	Multi-pyranometer array
METSAT	Meteorological data
NASA	National Aeronautics and Space Administration
NIP	Normal Incidence Pyrheliometer (Eppley Laboratory instrument model)
NOAA	National Oceanic and Atmospheric Administration
NREL	National Renewable Energy Laboratory
NSRDB	National Solar Radiation Database (United States of America)
NVAP	NASA Water Vapor Project
OD	Optical depths
PMOD	Physical Meteorological Observatory, Davos, Switzerland
PSP	Precision Spectral Pyranometer (Eppley Laboratory instrument model)
PV	Photovoltaic
QA	Quality assessment
RCC	Radiometer Calibration and Characterization
RTNEPH	Real Time Nephanalysis
SANCST	Saudi Arabian National Center for Science and Technology
SOLPOS	Solar position calculation
SRDB	Solar radiation database
TOMS	Total Ozone Mapping Spectrometer
TUVR	Total Ultraviolet Radiometer (Eppley Laboratory instrument model)
uV	Microvolts
UV	Ultraviolet
UVA	Ultraviolet A spectral region, 315 nm to 400 nm
UVB	Ultraviolet B spectral region, 285 nm to 315 nm
W/m²	Watts per square meter
WCF	Window Correction Factor
WCRF	World Climate Research Program
WMO	World Meteorological Organization

WRC	World Radiation Center
WRG	World Reference Group
WRR	World Radiometric Reference
WSG	World Standard Group
YES	Yankee Environmental Systems

1.0 Overview

In 1987, the United States Department of Energy (DOE) and the King Abdulaziz City for Science and Technology (KACST) signed a five-year *Agreement for Cooperation in the Field of Renewable Energy Research and Development.* [1, 2] This agreement was extended to the year 2000. Under this agreement, in 1993 a four-year (1994-1997) project (Annex II) was initiated to improve the assessment of solar radiation resources in Saudi Arabia. Annex II is a joint effort carried out by KACST and the DOE's National Renewable Energy Laboratory (NREL). A previous progress report covers accomplishments from 1993 to 1997 [3]. This report briefly summarizes the accomplishments covered in the previous progress report, and summarizes accomplishments under the Annex II project through the year 2000.

The original objectives of the project, set out in 1993, included the following tasks and objectives [3].

Task 1.   Update solar radiation measurements in Saudi Arabia

Task 2.   Assemble a database of concurrent solar radiation, satellite (METEOSAT) and meteorological data (with a period of record of 10 years, to the extent possible)

Task 3.   Adapt NREL model and other software for use in Saudi Arabia

Task 4.   Develop procedures, algorithms, and software to estimate solar irradiance at locations and times for which measured solar radiation was not available.

Task 5.   Prepare a uniformly spaced grid of solar radiation data to prepare maps and atlases, and to estimate solar radiation resources and system performance at any location in Saudi Arabia.

A brief summary of the accomplishments regarding each task is given here. In addition, Annex II research and development activities have resulted in significant advances in solar radiometry and solar radiation resource assessment. Continuation of the work begun under Annex II into the future will ensure that Saudi Arabia will have an excellent knowledge of their solar radiation resources and some of the most outstanding solar radiation resource assessment capabilities in the world.

Task 1 was fully accomplished. NREL provided training in the theory and application of solar radiation measurements (Six week *Introduction to Solar Radiometry* course, at NREL, June 1994; on-site radiometry training at KACST, October, 1994; *Advanced Solar Radiometry*, at NREL, March 1996). A 12-station solar radiation-monitoring network with a wide variety of representative characteristics was established. Each station collects direct normal, global horizontal, and diffuse horizontal solar radiation data, as well as temperature and relative humidity. The data recovery from the sites has been exceptional

for the duration of the project. An excellent radiometer calibration facility has been established at the Solar Village solar research site near Riyadh. Direct traceability to the World Radiometric Reference was established in 1995 at the World Radiation Center, Davos, Switzerland, during the eighth International Pyrheliometer Comparisons. [4] An overview article describing the Saudi network and operations was drafted and submitted to the journal *Renewable Energy* in May 2000 [5]. Joint publications on the aging of pyranometers in the Saudi network, and application of zenith angle dependent corrections to network data, were prepared for presentation at the April 2001 meeting of the American Solar Energy Society (ASES) in Washington, D.C. [6, 7]

Task 2 has been accomplished, though not exactly in the manner planned. At first, the project solicited the support of the Saudi Meteorological and Environmental Protection Agency (MEPA). MEPA did not begin digitizing meteorological data until 1995. A method of digitizing historical solar radiation data from analog chart recordings produced by bi-metallic actinograph recorders was developed and transferred to KACST. However, the resources to accomplish the digitization of years of daily graphs were not available. Transfer of both meteorological and METEOSAT data from MEPA to KACST was irregular and fraught with technical roadblocks. In the end, a historical, and frequently upgraded, worldwide data set of meteorological data, used in conjunction with Task 5 (DATSAV2) was obtained by NREL. Saudi Arabian meteorological data for the period from 1973 to 2000 were extracted and validated against existing MEPA data. These data were used to address tasks 4 and 5.

Task 3 was accomplished by the transfer to KACST of software packages for the calibration and characterization of radiometers (Radiometer Calibration and Characterization, or RCC) [8], and a Data Quality Management System (DQMS) [9]. These packages are essential to maintaining and operating the 12-station monitoring network. Further improvements and upgrades to these software systems were also shared with KACST. Models for estimating hourly solar radiation from meteorological data (METSAT) [10], and Climatological Solar Radiation (CSR) [11] were provided to KACST. These models were developed under other NREL projects.

Under task 4, NREL developed and provided courses for training in the radiation models mentioned above (*Estimation of Monthly Mean Daily Total Radiation on a Uniform Grid,* at NREL, March 1997; *NREL's Meteorological and Statistical Solar Radiation Model METSTAT,* February 2000). A short course on Annex II activities (Part I: *Summary of Annex II Activities Accomplishments,* and Part II: *Application of Annex II Products,* and Part III: *Solar Radiation Resource Assessment Fundamentals)* was given at KACST September 13- October 1, 1997.

Task 5 was accomplished by the production of a Solar Radiation Atlas for Saudi Arabia [12] in 1999. A uniformly spaced grid of monthly mean daily total solar radiation was produced using the CSR model, in conjunction with the DATSAV2 data set. This approach (completely different than envisioned in 1992) was developed and supported by independent DOE funding supporting worldwide resource assessment research during 1995 and 1996. The data sets were processed using NREL and KACST Geographical

Information System (GIS) software and hardware to produce the maps for the Saudi solar radiation atlas. The ArcView GIS software algorithms developed by NREL to produce the atlas maps was transferred to KACST during 1997 and 1998. The atlas was reprinted in 1999.

The synergism afforded by combining Annex II, NREL, and projects in concert with the National Aeronautics and Space Administration (NASA) Earth Observing System (EOS) program and DOE's Atmospheric Radiation Measurement (ARM) program has produced superior solar radiation data and products to the benefit of both Saudi Arabia Energy Research Institute and the DOE Energy Efficiency and Renewable Energy programs.

2.0 Summary of 1993-1997 Progress Report

2.1 Establishing a Saudi Solar Radiation Network

Prior to the Annex II project, Saudi Arabian solar radiation measurements were carried out by several organizations, such as universities, MEPA, and the Saudi Ministry of Agriculture and Water. Some measurements were made using thermopile instruments such as pyrheliometers and pyranometers, but most historical data were collected with bi-metallic actinographs. These instruments recorded daily solar radiation profiles on strip charts.

Early in the project, it was decided to provide each solar radiation measurement site with Eppley Precision Spectral Pyranometers (PSP) for measuring global horizontal and diffuse horizontal (under tracking shading disks) radiation, and Normal Incidence Pyrheliometers (NIP) on Eppley Model ST-1 solar trackers (driven with synchronous motors) for direct normal radiation measurements. NREL worked with the Eppley Laboratory and KACST to design modified tracking shading disks for more reliable shading disk operation. A standard mounting platform was designed to carry all solar and meteorological instruments, as well as the Campbell Scientific CR-10 data loggers. Special tools were designed to reduce cable twisting in the NIP tracking units, evaluate the radiometric level (or geometric tilt) of the sensors, and to align the mounting platforms with true north.

Station sites were selected on the criteria of (1) available personnel for maintenance, (2) reliable power and telephone service, (3) uniform spatial coverage of the Kingdom, (4) representative climates found in the Kingdom, (5) representative albedo variations in the Kingdom, and (6) unobstructed horizon. [13] Maps and satellite photos of the Kingdom were examined to establish prospective sites. KACST researchers visited prospective sites to assess the suitability for installation of the equipment. Twelve sites were selected, and site preparation, such as power and telephone line extensions, were executed as necessary. These constraints led to the selection of 12 MEPA stations distributed across the Kingdom as shown in Figure 2.1 and Table 2.1. The NREL-designed instrument platform is shown in Figure 2.2.
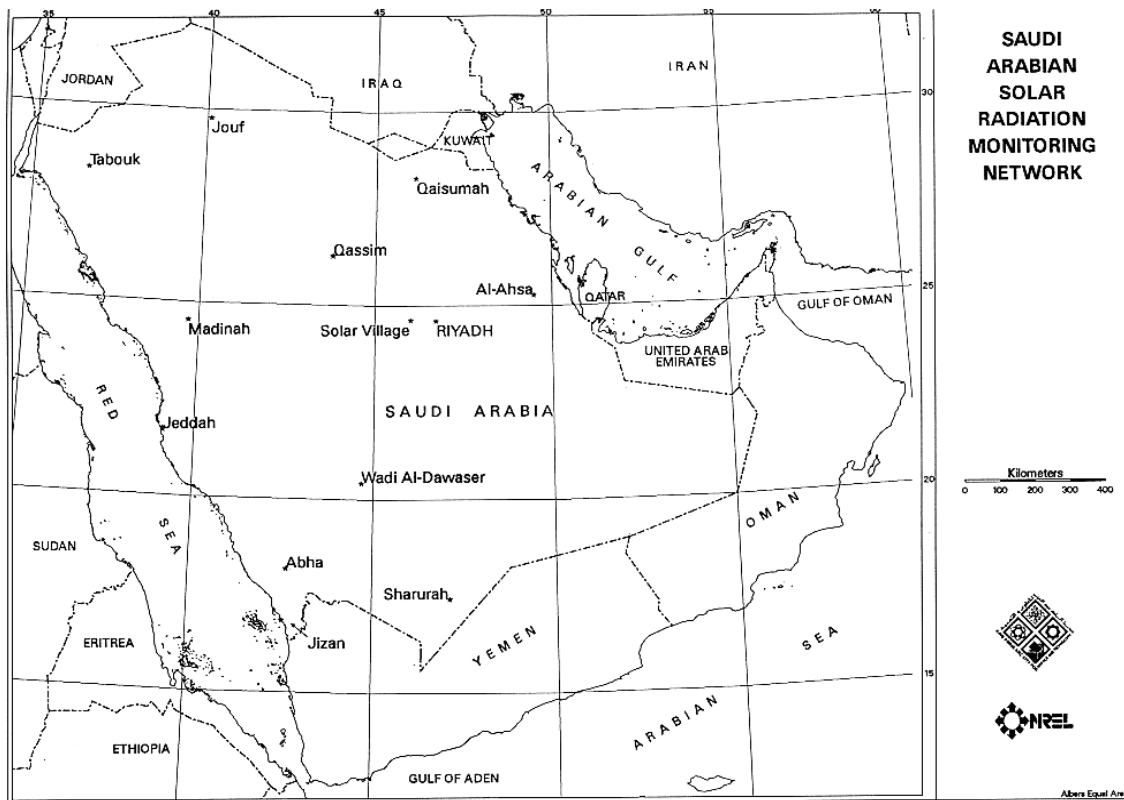
Figure 2.1. The 12-station Saudi Solar Radiation Monitoring Network.

Table 2.1. Station Locations and Operational Dates

STATION	LATITUDE	LONGITUDE	ELEVATION (meters)	Date Initial Operation
SolarVillage	24.91	46.41	650	NOV 1994
Qassim	26.31	43.77	647	NOV 1994
Al Ahsa	25.30	49.48	178	JAN 1995
Wadi Al-Dawasser	20.44	44.68	701	APR 1995
Abha	18.23	42.66	2039	JUN 1995
Gizan	16.90	42.58	7	JUN 1995
Sharurah	17.47	47.11	725	JUN 1995
Jouf	29.79	40.10	669	AUG 1995
Qaisumah	28.32	46.13	358	AUG 1995
Tabouk	28.38	36.61	768	AUG 1995
Madinah	24.55	39.70	66	SEP 1995
Jeddah	21.68	39.15	4	MAY 1996

Figure 2.2. Profile of Saudi Arabian Instrumentation Platform. Instruments (left to right) are tracking shading disk, diffuse (shaded) pyranometer, north-south alignment sight, Normal Incidence Pyrheliometer in ST-1 Tracker, temperature and relative humidity sensor housing, global horizontal pyranometer, and data logger environmental housing.

2.2 Network Instrumentation Calibration Traceability

The World Radiometric Reference (WRR), maintained by the World Meteorological Organization (WMO), defines the international reference scale for solar radiation measurements [14]. The WRR is maintained at the World Radiation Center (WRC), at the Physical Meteorological Observatory, Davos (PMOD), Switzerland. The WRR is defined as the mean of group (the World Reference Group, WRG) of six highly accurately characterized Absolute Cavity Radiometers (ACR). These radiometers are calibrated using the principle of (highly accurately measured) electrical heating to reproduce the temperature rise in a blackened cavity heated by exposure to the sun.

Similar commercially available radiometers are used by individual nations to embody the WRR scale. The WRR is transferred to the working ACRs every five years during International Pyrheliometer Comparisons conducted by WMO/WRC/PMOD [4]. The WRR uncertainty is declared to be ±0.3% of reading. The repeatability of the transfer process from the WRG to a working reference ACR is on the order of 0.15% [15]. Ultimately, field radiometers are calibrated using the ACR as a reference. The calibrated radiometers thus become traceable to the WRR.

KACST purchased an Eppley Laboratory Hickey-Frieden ACR, serial number 30110 to use as their calibration reference. The KACST reference ACR has been compared with similar cavity radiometers, first at the Eppley Laboratory; then against the NREL reference ACR 28968, and at WMO/WRDC/PMOD IPC VIII in October 1995 [4]. The correction factor to produce the WRR direct normal irradiance for the KACST reference ACR is 0.96682 ±0.3%.

NREL developed radiometer calibration and characterization procedures and software for using off the shelf, high-resolution data logger in conjunction with an ACR to calibrate pyrheliometers and pyranometers. RCC includes real time checking of atmospheric stability, alarms and flagging for poor quality data, an integrated report generator, and calibration database for maintaining radiometer calibration history. The method for calibrating pyrheliometers is direct comparison of pyrheliometer signals with the ACR WRR readings in Watts per square meter (W/m²). Pyranometers are calibrated using the so-called "Component Summation" technique. [16, 17]

The component summation technique uses the ACR reference to measure the direct beam, and a pyranometer shaded with a tracking disk (subtending the same 5.0° field of view as the ACR) to measure the diffuse sky radiation. The reference irradiance, Iref, is computed from the vertical component of the direct beam (Id) multiplied by the cosine of the solar zenith angle, Z, added to the diffuse sky irradiance, (Idf), or $Iref = Idn Cos(Z) + Idf$. The pyranometer responsivity, Rs, is the ratio of the signal, Vu, to the reference irradiance, Iref; or $Rs = Vu/ [Idn Cos (Z) + Idf]$.

This method requires determining the responsivity, Rsd, of the diffuse measuring pyranometer by comparing the difference between an unshaded, Vu, and shaded, Vs, reading with the vertical component of the direct beam – or $Rsd = (Vu-Vs)/[Idn Cos(z)]$. This is referred to as a shade/unshade calibration, as documented in [18, 19].

RCC reports the individual responsivities of pyranometers as a function of zenith angle, where the zenith angle is binned in ten, 9-degree-wide bins from 0° to 90°. This allows one to map the non-lambertian cosine response of the pyranometer. Figure 2.3 shows a typical cosine response map for a pyranometer. Table 2.2 shows the responsivities determined for each bin. Control instruments, never used except during calibration events, are included in each outdoor calibration exercise to monitor the calibration process for changes and repeatability. The historical data on these control instruments show no changes greater than 1.25% over the course of 10 calibration events conducted since 1994. The overall uncertainties in the RCC derived responsivities has been estimated as a function of the zenith angle and diffuse irradiance conditions as better than 2.5%. [17]

The mean responsivity in each Z-bin is plotted as a horizontal bar, as shown in Figure 2.3. The 45-55 and cosine-weighted composite responsivities are plotted as horizontal lines spanning the total zenith angle range. The 45-55 bin represents an average responsivity for homogenous, isotropic sky conditions. The "composite" result is the response of the pyranometer computed as the average of all responsivities weighted by the cosine of Z.

31548F3
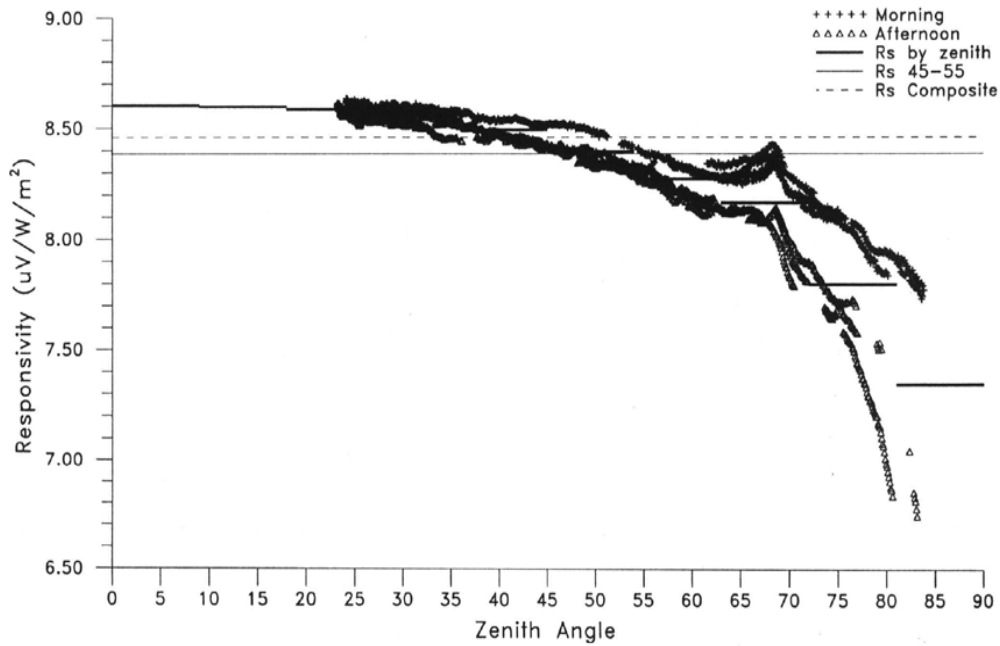
Figure 2.3. RCC plot of zenith angle

Network data are collected using the composite responsivity. We have developed a method of correcting the data based on using the zenith-angle based "vector" described in sections 3 and 10.

Table 2.2. RCC report of mean pyranometer responsivity within zenith angle bins

Bin	Rs	Unc	Pct
45-55	8.262	0.18	2.2
Composite	8.328	0.45	5.4
Zen 00–09	8.406	0.18	2.1
Zen 09–18	8.408	0.17	2.0
Zen 18–27	8.387	0.18	2.1
Zen 27–36	8.353	0.19	2.2
Zen 36–45	8.314	0.20	2.4
Zen 45–54	8.265	0.18	2.2
Zen 54–63	8.214	0.18	2.2
Zen 63–72	8.208	0.25	3.0
Zen 72–81	8.118	0.28	3.4
Zen 81–90	7.972	0.27	3.3

Bin = Zenith angle bin identifier
Rs = Mean responsivity within bin (both morning and afternoon data) uV/W/m²
Unc = Uncertainty in units of Rs (uV/W/m²)
Pct = Uncertainty as a percent of mean responsivity (percent)
(see section 2.5 for discussion of uncertainty)
45-55 = bin for computing responsivity under isotropic conditions
Composite = cos (Z) weighted mean responsivity

Each BORCAL event contains control instruments used only during the calibration events to validate the calibration event. From 1994 until 1997, the responsivities of the two control instruments (NIP 30174E6 and PSP 30205F3) show slight increases in responsivity, however, the change is no more than 1.25%. Section 3 will describe research results and improvements regarding RCC and BORCAL data.

2.3 Operating the Solar Radiation Network

As described in Sections 2.1 and 2.2, each of the 12 network stations measures three components of solar radiation, ambient temperature, and relative humidity. Observations are recorded as five-minute averages of 10-second samples. Network operations consist of installation and daily maintenance of the instrumentation, data acquisition and data quality assessment, archiving and calibration, and installation of the radiometers. MEPA operators perform daily maintenance of the solar trackers and sensor windows. Data collection is managed remotely from the Solar Village operations center.

Data acquisition uses the Campbell Scientific CR-10 data logger. The programmable data logger samples and averages the data, using calibration factors for each sensor to produce data in engineering units. Data are downloaded nightly to the central network operations center at the KACST Solar Village using telephone modem (Campbell Scientific Model DC 112) access. Downloading does not affect data collection. Data may also be accessed, viewed, or downloaded in real time, using Campbell Scientific PC208 software. Raw data are archived on magnetic media at the operations center; and transferred to another computer at the KACST offices in Riyadh. All raw data files for the network are transferred to NREL monthly, and KACST and NREL perform data quality assessment and archiving.

Data quality assessment is performed using DQMS software developed by Augustyne+Company based on NREL specifications. SERI-QC and QCFIT are two data quality assessment tools developed by NREL before the Annex II project that are incorporated into the DQMS package. [9] These tools evaluate the relationship between solar radiation components and generate flags attached to each data point indicating the magnitude, direction, and possible cause of erroneous data.

During the project, a computer application called SHADES was developed to convert measured data and flags into grayscale values that may be plotted graphically as a matrix of monthly or weekly values. The data and flags are presented with respect to clearness index values (Kt for global, Kn for direct, and Kd for diffuse). These clearness indices are the ratio of measured values to computed extraterrestrial values (derived from the solar constant, the eccentricity of the Earth's orbit, and the solar geometry for a location). Figure 2.4 displays a typical SHADES plot. The plot shows hours across each panel and days of the month from the top down in each panel. Hours with data flagged as bad are darker, the darker the gray, the worse the error. Data are indicated by shades of gray from white to black representing high to low clearness index (i.e., irradiances).

Saudi Annex II Network: Abha

Monthly Quality Assessment Summary for July, 1998

| | SERI QC Flags | Kt | Kn | Kd |
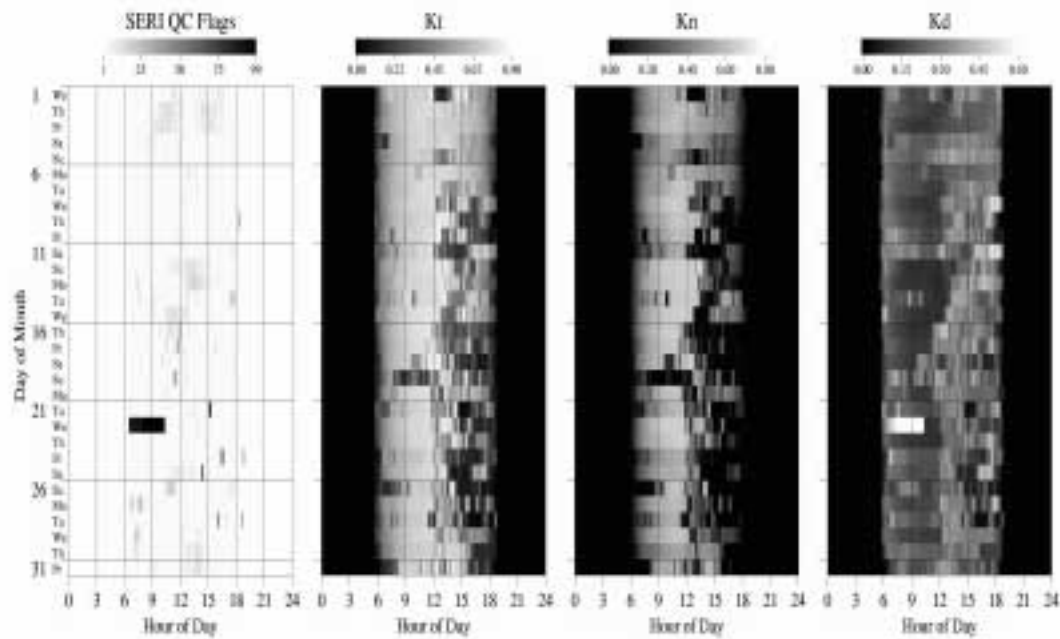
Summary Statistics

Percent of data	Daytime					Nighttime					Site Information
	Glo	Dir	Dif	Temp	RelHum	Glo	Dir	Dif	Temp	RelHum	
Present	100.0	100.0	100.0	100.0	100.0	100.0	100.0	100.0	100.0	100.0	Identifier: AB1
*Flags <= 5%	99.0	98.8	98.4	100.0	99.9	100.0	100.0	100.0	100.0	99.5	Latitude: 18.23
*Flags > 10%	0.5	0.5	0.5	0.0	0.0	0.0	0.0	0.0	0.0	0.0	Longitude: 42.66
*Below empirical limit	0.0	0.2	0.0	0.0	0.0	0.0	0.0	0.0	0.0	0.0	Elevation: 2079 meters
*Above empirical limit	0.1	0.0	0.5	0.0	0.1	0.0	0.0	0.0	0.0	0.5	Time Zone: 3.0
*Strange but true	0.4	0.4	0.4	0.0	0.0	0.0	0.0	0.0	0.0	0.0	Data Resolution: 5 min

* Flag statistics indicate percent of present data

Developed by the National Renewable Energy Laboratory

Figure 2.4. Visual display of quality assessment (QA) flags and normalized radiation values of one month of five-minute solar data. The dark rectangle of larger QA flags (large errors) on Wednesday, July 22 from 6:30 AM to 10:00 AM corresponds to a failed diffuse-shade tracker, indicated by the high (white) diffuse value in Kd.

As shown in the figure, flagged data and possible problems are easy to identify. Efforts are made to correct problems through direct communications either with MEPA operators, or in the case of persistent problems, site visits by KACST engineers to troubleshoot and rectify problems.

2.4 Network Data Summary as of December 1997

The data quality assessment tools described in the previous section allow one to monitor the performance of individual stations and the network regarding the collection of good quality data. The SERI_QC and DQMS flags compare measured data with both expected values and the balance between solar radiation components. Historical data are used to provide an envelope of expected values within which each solar radiation component is expected to fall. QCFIT is the software that is used to establish the envelopes.

DQMS produces reports of the magnitude of discrepancies between global, direct, and diffuse solar radiation components. Given the uncertainty in calibrations and instrumental sources of errors, the relative contributions of errors by each component could amount to 5% of a reading. DQMS begins flagging "bad" data above this threshold. Table 2.3 shows the percent of possible data that did not exceed this threshold of error for each station from 1995 to 1997.

The table shows that 85% to 90% of the data collected by the network up to 1997 have been within the instrumental uncertainty expected. This represents outstanding network performance for any national measurement network.

Table 2.3. Percentage of station data falling within 5% threshold for correct data by year from 1995 to 1997

STATION	1995	1996	1997
SolarVillage	94.2	98.7	98.6
Qassim	85.3	91.7	93.0
Al Ahsa	92.1	88.3	90.3
Wadi Al-Dawasser	91.2	92.6	94.7
Abha	93.9	89.8	92.1
Gizan	85.0	86.1	94.0
Sharurah	82.9	82.0	79.0
Jouf	94.1	93.4	93.4
Qaisumah	94.9	90.4	79.1
Tabouk	62.8	87.6	86.8
Madinah	76.8	94.1	91.5
Jeddah	NA	75.1	83.5
NETWORK	**86.6**	**88.8**	**89.7**

The previous progress report [3] presented a summary of the monthly mean daily total solar radiation in units of kilowatt-hours per square meter. Rather than repeat that data here, a summary of the network monthly mean data is discussed in sections 6 and 8, in the light of the measured network data as a validation tool for the Solar Radiation Atlas, and development of the Saudi Arabian solar radiation database. A summary of monthly mean station data is also presented in Al-Abbadi, et al. [5]

2.5 Acquiring Meteorological and Satellite Data

Task II of the project called for the assembly of a database of concurrent METEOSAT satellite data, meteorological surface observations, and solar radiation data, and for the development of a 10-year solar/meteorological database. A significant effort to acquire METEOSAT data was made by KACST, in conjunction with MEPA, with NREL guidance. Obstacles included insufficient resources, inadequate technical communications, and data format variations that prevented the assembly of an adequate data set of METEOSAT images and data. These obstacles are described in the previous progress report. As a result, some data and images were collected and archived, but not in sufficient quantity to satisfy the project needs. KACST will continue to explore the possibilities for deriving solar radiation estimates from geosynchronous satellite data in the future.

MEPA provided KACST with hourly or three-hourly surface meteorological observations from January 1995 to June 1997. The data were provided in WMO synoptic format, and NREL had to develop a decoder program to extract the data of interest.   Upper air radiosonde data for the period from January 1994 to December 1998 were also supplied by MEPA. These data were important for determining total precipitable water vapor, and deriving aerosol optical depth profiles for the kingdom. Format changes and intermittent delivery limited access to useful data in this period, but KACST has made a concerted effort to improve the exchange of data with MEPA.

The United States Air Force and the National Climatic Data Center have collaborated to acquire and archive a worldwide database of surface meteorological observations called DATSAV2. NREL acquired a complete set of DATSAV2 data covering the period from 1973 to 2000, as part of other DOE renewable energy programs. The Annex II project extracted data for all Saudi MEPA stations. These data were then evaluated with respect their usefulness in generating a Saudi Solar Radiation Database, using the NREL Meteorological and Statistical (METSTAT) solar radiation model. [10, 11, 20, 21] See sections 7 and 9 below.

2.6 Evaluating Bimetallic Actinograph Data

As reported in the previous progress report, it was hoped that historical solar radiation data could be derived from analog strip chart recordings made with bi-metallic actinograph instrumentation (Pyranograph Model 5-3850A, Belfort Instrument Company). A technique of digital scanning and transformation into digital columnar data with five-minute resolution was developed and validated by NREL. The validation included comparison of digitized results with simultaneous thermopile radiometer digital data. Normalized differences between daily total irradiances measured with the two instruments ranged from 2% to 10% depending on season. Individual hourly differences could be as large as 25% to 50%, and were examined as a function of solar zenith and azimuth angles. The results show that under clear or completely overcast skies, the digitized actinograph data compared favorably with the pyranometer data. However, under partly cloudy skies there could be significant differences. Daily total values derived from the two instruments were comparable, but useful hourly data under partly cloudy skies was much more problematic.

Further research into ways to correct the partly cloudy actinograph data is needed. The use of these data to provide historical solar radiation data for an hourly solar radiation database was not pursued.

2.7 Evaluating a Multi-Pyranometer Array Radiometer

As part of the technology transfer, instrumentation development, and resource assessment research and development components of the Annex II project, NREL and KACST jointly investigated the use of an MPA radiometer for estimating global, direct, and diffuse solar radiation components. The concept of using an array of pyranometers oriented to specific azimuth and tilt directions in combination with an algorithm to extract the solar radiation components is an extension of the work of Faiman, et al. [22]. Faiman and his group used an array of thermopile radiometers in their MPA experiment. They were able to estimate monthly mean direct normal estimates with mean bias errors of 4% and root-mean-square errors of 50 W/m² for 10-minute average data at Sede Boquer. NREL and KACST used low cost, silicon photodiode based pyranometers (LI-200 SB, available from Li-Cor Instruments, Inc.) to evaluate several aspects of the MPA approach.

MPA radiometers were designed, constructed, and deployed at the Solar Radiation Research Laboratory from July to August 1995, at NREL in Golden, Colorado, to develop and validate algorithms for extracting direct normal and diffuse radiation. Results comparable to those of Faiman were achieved. Two identical MPA arrays were deployed at the KACST Solar Village.

Details of the deployment and data analysis are reported in the previous progress report and summarized here. The two MPAs were used to investigate the effects of radiometer soiling as well as being evaluated for performance compared to thermopile sensors. In addition, subsets of the four-element MPA design were studied to establish the minimum pyranometer matrix needed to extract useful solar radiation data.

Evaluation of subsets of the four-pyranometer array showed that an array of three pyranometers was sufficient to extract useful solar radiation data. With respect to thermopile sensors, the MPA radiometers had a mean bias error of 4% or less in the direct normal for all months, and an annual Mean Bias Error (MBE) of zero. Root-mean-square differences ranged from 55 W/m² to more than 100 W/m², depending on month. These results were significantly higher than obtained at the NREL Solar Radiation Research Laboratory. We hypothesize that the differences are due to the limited spectral response of the Licor pyranometer (0.3 microns to 1.0 microns) and differing spectral conditions in Colorado and at the Solar Village.

The soiling study involved daily cleaning of one thermopile and MPA sensor combination, while letting the second accumulate dust and dirt. Two periods were used in the evaluation, August 1, 1996, to October 26, 1996, (86 days) and May 13, 1997, to July 22, 1997, (70 days). Depending on the location of the Licor pyranometers in the array, degradation of the data due to soiling ranged from 0.5% to 1% for the more resistant elements (east and west facing) to a maximum of 2.5% for the radiometers oriented to southeast and

southwest azimuths. The PSP thermopile radiometers showed degradation in data of up to 3.5% (for the 86-day period). This study established that low maintenance (unattended operation) of the MPA results in tolerable levels of soiling losses, and established the level of degradation due to soiling in both measurement systems under unattended operation in the Solar Village environment.

2.8 Creating a Solar Radiation Data Grid and Atlas for Saudi Arabia

A primary objective of the Annex II project was to update and upgrade the first edition Solar Radiation Atlas for Saudi Arabia. [23]   The first edition atlas was based on conversion of percent sunshine (S) and global (G) solar radiation data for 17 and 41 stations, respectively, in Saudi Arabia. The Angstrom relation between S and G; G = A+B*S was used to estimate global radiation from percent sunshine data. This older methodology was replaced by application of the NREL-developed CSR model, [11] itself an application of the NREL METSTAT model. Both of these models were developed at NREL using DOE funding. The CSR model is used to develop a "data-grid" of solar radiation values. A data-grid is a uniformly spaced network of grid points, or point locations, with a data value attached to each location.

The CSR model approach was used in place of the planned satellite-derived data approach, due to the obstacles encountered in acquiring and processing the satellite data described in section 2.5. The CSR model produces monthly mean daily total solar radiation values derived from monthly means of total and opaque cloud cover, aerosol optical depth, total precipitable water vapor, atmospheric pressure, ozone, and surface albedo. CSR computes unitless transmittances for the atmosphere defined by the input parameters and multiplies them by the extraterrestrial solar radiation to yield surface radiation in Wh/m^2. CSR model input data are derived from the following sources:

Cloud cover: Real Time Nephanalysis (RTNEPH) database, from the U.S. Air Force Global Weather Center, Offut Air Force Base, Nebraska. (Available from the U.S. national Climatic Data Center, Ashville, North Carolina). Data were available on a 40-kilometer worldwide grid of observations every three hours.

Aerosol Optical Depth (AOD):   Estimated from available direct solar radiation. Transmittances for ozone, total precipitable water, uniformly mixed gases, and Rayleigh scattering are estimated from the Bird & Hulstrom clear sky model. The aerosol transmittance is computed from direct normal irradiance. Monthly mean values of aerosol optical depth are computed. Finally a sine function is fit to the monthly data to produce AOD as a function of day of the year.

Total Precipitable Water Vapor: Monthly mean precipitable water vapor values were obtained from the NASA Water Vapor Project (NVAP) data set. These data were available on a 1° worldwide grid, and interpolated to the 40-km resolution of the RTNEPH data.

Atmospheric Pressure: Calculated from five-minute (9-kilometer grid) elevation data. Used to compute Rayleigh and uniform mixed gas transmissions.

Ozone: Obtained from the Total Ozone Mapping Spectrometer (TOMS) CD-ROM data set available from the National Oceanic and Atmospheric Administration (NOAA).

Albedo: Obtained from the Canadian Center for Remote Sensing. The center provides worldwide data on a 2.5° grid.

All input data were interpolated to match the RTNEPH 40-kilometer grid since cloud cover is the most prominent modifier of solar radiation in the atmosphere.

Model performance was evaluated by comparing CSR model results with values at 213 sites in the U.S. National Solar Radiation Database (NSRDB). [20, 21] Detailed results are presented in the previous progress report. The monthly mean bias differences are less than 3% of the typical monthly mean daily totals, and the standard deviation of the differences are less than half of the typical interannual variations. Mean differences between measured Saudi network data and CSR modeled data are less than 6%. Mean differences between measured and CSR model data were less than 3%, and the standard deviation of the differences ranged from 6% to 10%, depending on month for 10 stations in Egypt and Sudan (data available through the WMO World Radiation Data Center, St. Petersburg, Russia).

CSR data grids for Saudi Arabia produced monthly mean daily total solar radiation maps for each of the three components of solar radiation. These were assembled into a second Edition Saudi Arabian Solar Radiation Atlas. [12] Figure 2.5 is a gray-scale presentation of a representative map of monthly mean daily total direct normal radiation for October.
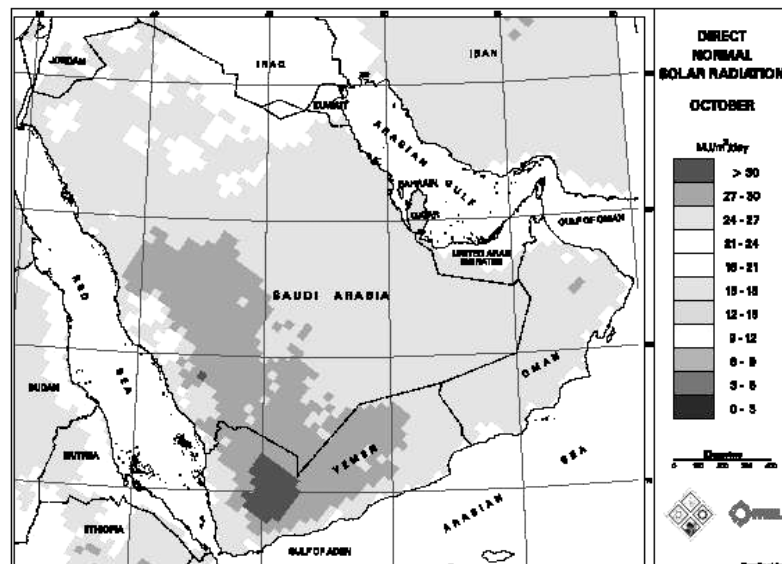
Figure 2.5. Grayscale version of CSR generated map of monthly mean daily total for October in the Kingdom of Saudi Arabia and surrounding areas.

The maps in the second edition Saudi Arabian Solar Radiation Atlas are printed in a full-page, color format.

2.9 Technology Transfer and Training

Technology transfer and training were conducted continuously throughout the project. This was to provide KACST scientists and technicians the ability to continue working on the project objectives to obtain a true climatological picture of solar radiation resources in Saudi Arabia. Such a true climatological picture requires collection and analysis of at least 30 years of high quality solar radiation and meteorological data; as well as an understanding of the measurement and modeling techniques used to develop the climatology.

Formal training and courses detailed in the previous progress report include:

- A course in Fundamentals of Solar Radiometry (6 weeks, June-August 1994, at NREL)
- Operational training at the KACST Solar Village (4 Weeks, October/November 1994)
- Advanced Radiometer Training at NREL (2 weeks, March 1996)
- Five Part Annex II Summary Course at KACST (2 weeks, September 1997)
- Data Grid Short Course at NREL (3 weeks, March 1997)

These courses covered 13 weeks, equivalent to two, 15-credit university semesters (or one academic year) of lecture and laboratory courses.

NREL visited KACST in May 1996, to perform on-site training in network operations, calibration operations, and network management. NREL assisted KACST in participating in the eighth International Pyrheliometer Comparison at WMO/WRC/PMOD in October 1995. Every month throughout the project, NREL provided feedback on the evaluation of network station data recovery and quality. NREL also produced quarterly reports highlighting Annex II activities and interactions and summarizing the status of the network data recovery and quality.

Hardware designed and/or developed at NREL that was transferred to KASCT included the radiometer mounting platforms, tracking shading disk balance arm, slip-ring assembly for pyrheliometers, and two tracker alignment tools. KACST purchased and installed the 24 pyranometers and 12 pyrheliometers for the station installation, plus 50% spares (an additional 12 pyranometers and 6 pyrheliometers), plus the control instruments for RCC/BORCAL validation. KACST also purchased and installed the Campbell Scientific CR-10 data loggers, modems, and associated data management software.

NREL developed and transferred to KACST the RCC/BORCAL calibration and calibration database management software, SERI_QC, QC_FIT, and DQMS software for network data quality assessment. The METSTAT and CSR models and the NREL-developed ArcInfo GIS macros, algorithm scripts, and input data sets were all transferred to KACST. NREL also provided copies of the Saudi Arabian subsets of DATSAV2 data

from 1973 to 1997 on CD-ROM to KACST, in preparation for development of the Saudi Solar Radiation Database.

This concludes the summary of the Progress Report for Annex II up to 1997. The following sections address further progress from 1997 and the status of the project at the termination of the Joint Technical Agreement and the Annex II project in June 2000.

3.0 Traceability and Transfer of World Radiometric Reference

As described in Section 2.2, The KASCT ACR has direct traceability to the 1995 IPC conducted by WMO at WRC/PMOD. In October 1999, KACST was invited to participate in an annual intercomparison of ACR's conducted at NREL.

3.1 NREL Pyrheliometer Comparison, October 1999

The WRR was transferred with an uncertainty of 0.39% from the World Standard Group (WSG) of absolute cavity radiometers to the KACST reference cavity radiometer AHF 30110 at the WRC at Davos, Switzerland, in 1995. NREL has documented the transfer process in [15]. KACST and NREL performed intermediate transfers of the WRR among working reference cavity radiometers during "NREL Pyrheliometer Comparisons" at NREL October 4-10, 1999. The root-sum-square of the 0.3% uncertainty in WRR and 0.25% random variation in the transfer of WRR to the working reference AHF 30110 result in the overall uncertainty in the direct beam irradiance of 0.39%. The correction factor to reduce AHF 30110 measured irradiance to WWR is 0.99692 ±0.39%. Figure 3.1 is a time series plot of the WRR reduction factor derived for the KACST AHF during the comparison. Figure 3.2 shows the distribution of the WRR reduction factor in the form of a histogram.
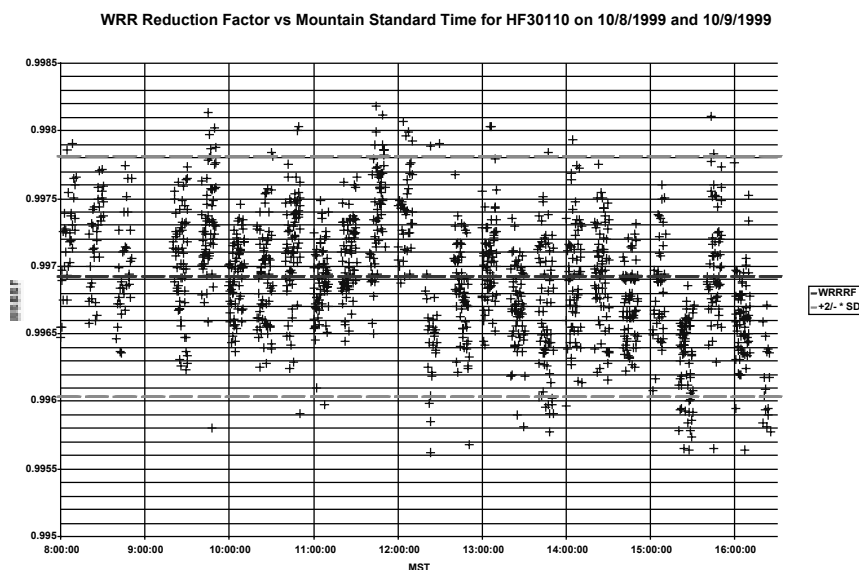
Figure 3.1. Time series development of the WRR reduction factor for the KACST RCC reference AHF 30110 during NREL pyrheliometer comparison, Oct 1999

16
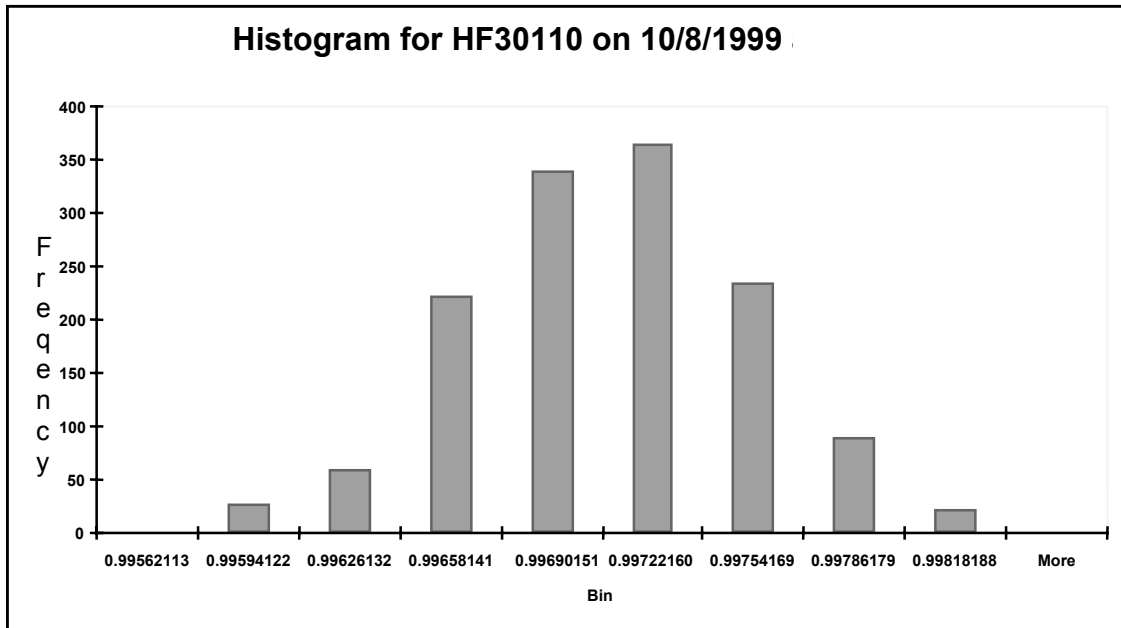
Figure 3.2. Distribution of WRR reduction factor for KACST AHF 30110 in histogram form.

Since the KACST RCC reference cavity radiometer is operated with a window in place (due to light, fine blowing dust at the Solar Village site), a window correction factor (WCF) was determined during the 1999 NREL pyrheliometer comparison. Using the same analysis technique that was used for determining the WRR Reduction Factors for the participating absolute cavity radiometers, the WCFs were computed for the windowed cavity radiometers. The resulting WRR/WCF Reduction Factors for the KACST windowed cavity radiometers is $1.06089 \pm 0.39\%$ as shown in table 3.1

Table 3.1. Windowed Cavity Results at NREL Pyrheliometer Comparison Oct 1999

SN	WCF	SD	SD%	2SD%	N. RDGS	U95% wrt WRR	wrt SI
29226	1.06373	0.00125	0.12	0.23	493	0.33	0.45
29227	1.06469	0.00093	0.09	0.17	492	0.29	0.42
30494	1.05059	0.00079	0.07	0.15	494	0.28	0.41
30110	**1.06089**	**0.00056**	**0.05**	**0.11**	**458**	**0.25**	**0.39**
30495	1.05083	0.00051	0.05	0.10	401	0.25	0.39
29222	1.05959	0.00063	0.06	0.12	401	0.26	0.40
31041	1.05602	0.00063	0.06	0.12	396	0.26	0.40

3.2 Recommendations

- The WRR Reduction Factor must not be used when operating a windowed cavity radiometer. Traceability to the WRR is maintained by using *only* the WCF.
- Always mount the window in the same orientation used during the transfer of WCF. This recommendation is based on a very limited data set to evaluate the possible sun light polarization due to the window.
- Always mount the same window on the same cavity radiometer that was used to determine the WCF.
- Based on our very limited data sets for determining the WCFs, further window characterization is needed to evaluate the spectral dependency(s) and orientation with respect to the receiving cavity.

4.0 Radiometer Characterization and Calibration Upgrade

4.1 Year 2000 (Y2K) and Solar Position Algorithm Upgrade

As the year 2000 approached, NREL performed an evaluation of the software developed in conjunction with the Annex II project to address possible year 2000 (Y2K) issues concerning the RCC computations of solar position and historical database updates as RCC reports were generated. In order to accommodate correct processing of dates in the RCC software, the date time stamp produced by the RCC software was modified to accept and record four-digit year.

RCC must compute solar zenith angle, Z, based upon time, date, and location, using a module called SOLPOS. From 1994 to 1999, an algorithm developed in 1977 by Walraven [24, 25] was used to compute Z. In 2000, NREL updated the SOLPOS routine using the algorithm of Michalsky [26, 27]. We also investigated Y2K issues that might arise in the SOLPOS module. NREL verified and validated the algorithm was functioning properly, and compared the old and new algorithms with respect to differences that would occur in using the two different algorithms. In the course of the changeover and validation, we found that the leap year correction computation needed to be corrected to account for the year 2000 being a leap year (since 2000 is divisible by 400).

4.2 Upgrading the Reference Irradiance Diffuse Measurement

Recent research on offsets in PSP radiometers led to a decision to replace the Eppley PSP [with an all black sensor] used to measure diffuse with an Eppley 8-48 "Black-and-White" instrument (S/N 32645). Figure 4.1 shows each type of radiometer deployed under a tracking-shading disk to measure sky diffuse radiation.

Studies have shown that a negative offset of up to 20 or more Watts exists in the PSP under clear skies due to the design and thermodynamics of the instrument [see figure 4.2].

Such an offset exists in the 8-48 also, but is smaller by an order of magnitude (2 W/m²)[28, 29]

Measuring diffuse sky radiation, particularly under clear skies when the diffuse irradiance is relatively small, the offset has been shown to be a source of significant error. Although the diffuse component of the global reference irradiance is typically small under clear skies, the offset can result in an error of 10% or more in the reference global irradiance used in the BORCAL process. Figure 4.2 is a plot of the clear sky diffuse irradiance measured simultaneously by the two different radiometers at NREL.

The responsivity of the new diffuse instrument was determined using a method developed by the NREL Metrology Laboratory. [19] Responsivities at a zenith angle of 45° are determined in three azimuth directions (0°, 120°, and 240°) with respect to south = 0°, using the shade-unshade technique. The measurement and timing sequence for the shade/unshade approach is shown in Figure 4.3. Period A is a 30-minute warm-up period for allowing the instrument to stabilize. Period B represents 20 to30 time constants (1/e, or 63% of final steady state values) for the instrument response. Period C represents 60 time constants for the instrument response. Period M is the time during which at least three readings of instrument response, Vs or Vu, and the direct beam irradiance, are recorded. The mean zenith angle and cavity pyrheliometer data during the measurement periods M are used in computing the $I_{dn} *$ Cosine(z) terms.

Figure 4.1. All-black (top unit) and black and white thermopile pyranometers under tracking shading disks.
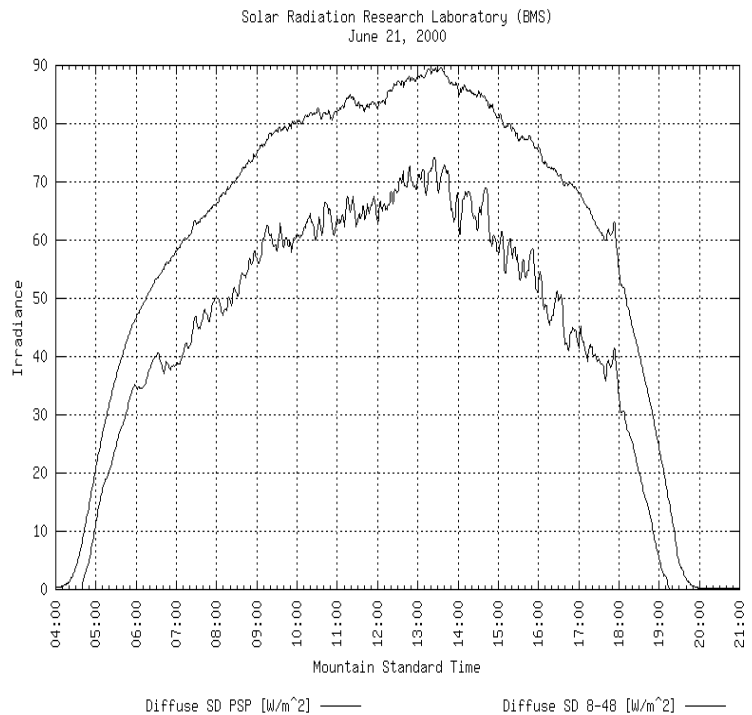
Figure 4.2. Clear sky diffuse irradiance under tracking shading disks for an all-black (lower line) and black-and-white (upper line) pyranometers.

19
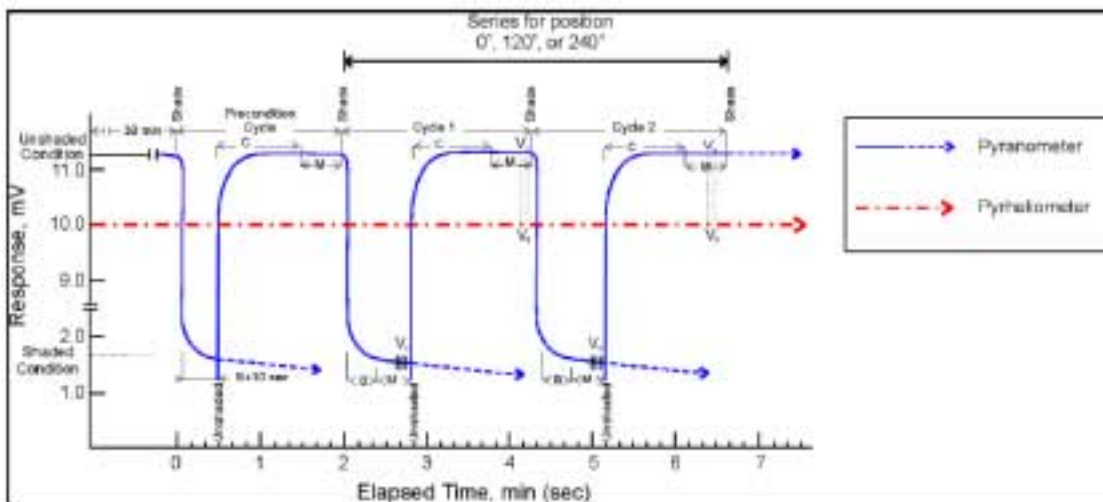
Figure 4.3. Sequence for shade/unshade calibration procedures

Detailed uncertainty analysis of this refined approach results in a total uncertainty of 2.5% in the calibration factor for measuring total sky diffuse irradiance (I_{df}) for an all black Eppley PSP under clear sky conditions. The above described thermal offsets in all-black thermopile pyranometer measurements imply that the uncertainty in the reference diffuse is actually ± 2.5% *of reading* + Woff, where the thermal offset, Woff, for a PSP is 20 W/m² and 2 W/m² for the model 8-48 Black and white pyranometer at NREL.

KACST purchased an Eppley Model 8-48 black and white pyranometer to replace the previously used all-black PSP pyranometer used to measure sky diffuse radiation during RCC/BORCAL activities. NREL calibrated the black-and-white unit in February 2000, and shipped it to KACST for use in all subsequent BORCAL operations.

4.3 Analysis of BORCAL/RCC events from 1998-2000

4.3.1 Background

In order to maintain Annex II network measurement traceability to world standards and to compensate for changes in instrument sensitivity, regular radiometer calibrations are scheduled as part of the Annex II project. The calibrations are performed by KACST at the Solar Village radiometer calibration facility. The process uses the RCC/BORCAL techniques developed at NREL

4.3.2 Traceability to World Reference Standards

The KACST reference radiometer (AHF 30110) has been compared four times to establish and maintain traceability to the WRR at the WRC in Davos, Switzerland:

1) In 1994, by the manufacturer, The Eppley Labs, Inc. prior to delivery
2) In 1994, with WRR traceable cavity radiometers at NREL
3) In 1995, as a participant at the International Pyrheliometer Comparison in Davos
4) 1998, at KACST (Solar Village) using a WRR traceable cavity radiometer from NREL
5) In 1999, at the NREL Pyrheliometer Comparison, NREL

4.3.3 Process Validation

As part of the calibration, two designated process control radiometers are included in each event. These two radiometers, a PSP (30305F3) and a NIP (30174E6), are kept in dark storage except during those days when the calibration is in progress. Because exposure to sunlight is a major contributor to instrument sensitivity degradation, these instruments are expected to show consistency from one BORCAL event to the next, even over a period of years. The results from these radiometers serve as an important validation of the BORCAL results.

4.3.4 Analysis of Results from BORCAL 1998-01 to 2000-01

The change in the method of measuring diffuse in 2000 ultimately resulted in a significant reduction in the calculated responsivity of the pyranometers under test. This is evident in Figure 4.4, a plot of the BORCAL control instruments. The responsivity of control PSP 30205F3 decreased by about 4% from previous BORCALs, whereas the control NIP 30174E6 shows insignificant change. Due to the change in responsivity of the PSP control instrument, a valid comparison with previous BORCALs for that instrument is no longer possible. However, the control NIP (which uses only the cavity radiometer for a reference irradiance) will continue to provide a process comparison with BORCALs prior
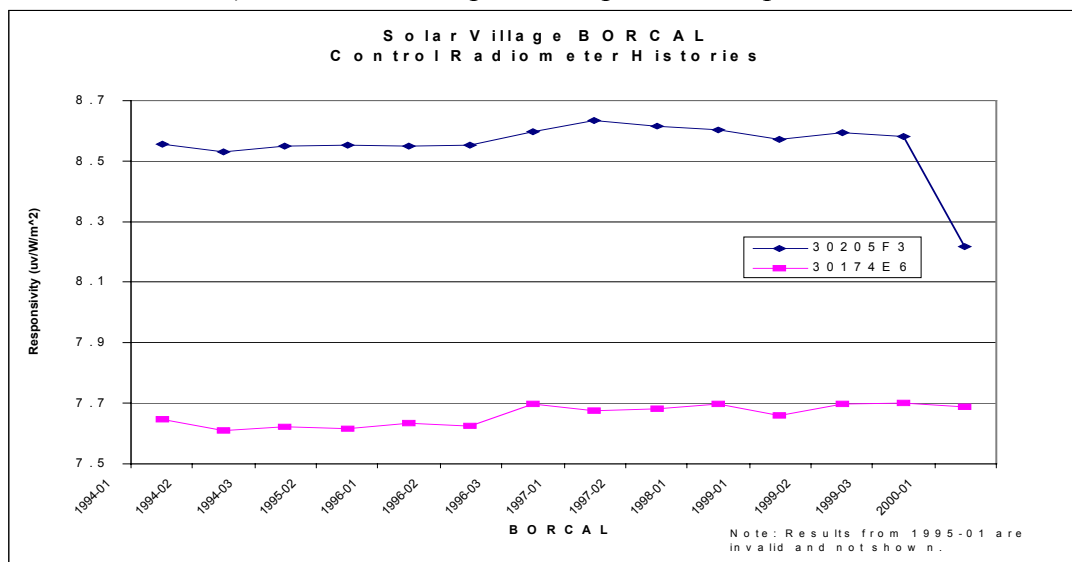
Figure 4.4. BORCAL control instrument calibration history from RCC data.
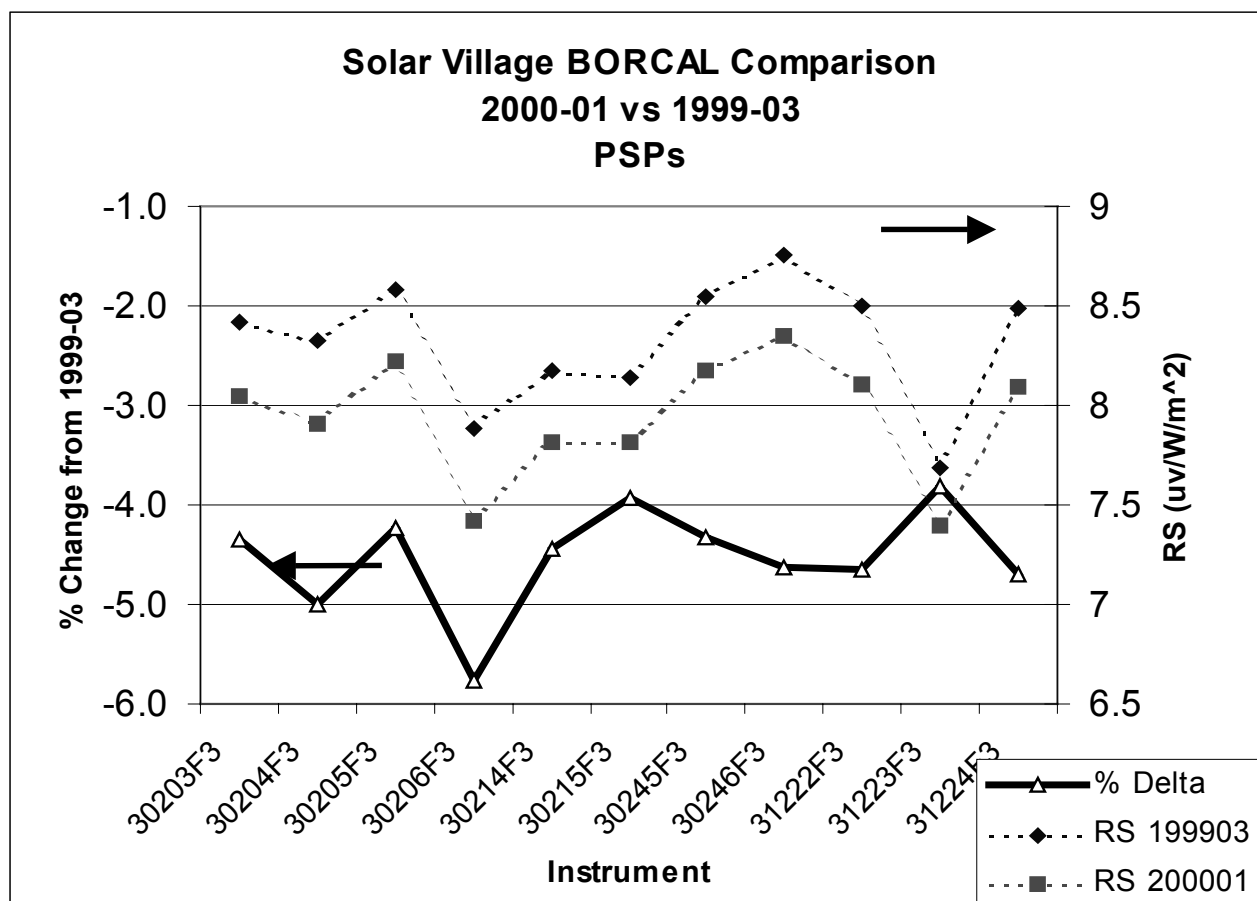
Figure 4.5. Comparison of PSP responsivities determined with all-black PSP (1999-03) and black and white model 8-48 (2000-01) diffuse sky measurement in RCC reference irradiance.

to 2000-01. In this regard, the plot of the control NIP, as well as comparisons with other NIPs explained below, indicates that BORCAL 2000-01 was well controlled.

In an effort to evaluate the effects attributable to the change in diffuse measurements, this BORCAL included all instruments that were calibrated in BORCAL 1999-03 (which used a PSP for the diffuse measurement). Figure 4.5 compares the two BORCALs and the responsivity changes in the eleven pyranometers included in both BORCALs.

The mean shift in responsivity was -4.5%, with a range of about -4% to about -6%. Average change for the six NIPs common to both BORCALs (results not shown) was about 0.3%.

Because of the *expected* change in the responsivity of the control PSP, and because the control PSP is used for real-time process validation, the RCC software was modified for the first BORCAL using the new diffuse measurements. The usual threshold of +-6% between the calculated global reference and the global measured by the control PSP was relaxed to 15%. This would prevent the unwanted flagging of data due to the mismatch of the existing responsivity of the control PSP. Unfortunately, the instructions provided by NREL to install the new software were incorrect, resulting in a significant amount of data being flagged. To correct this problem, the flags were removed from the data sets and the

report was generated without benefit of that process control. The resulting report indicates that the data set has few if any bad data points that would have otherwise been removed. In addition, the history of the Solar Village calibrations indicates that site personnel run a well-controlled process. In short, there is no evidence to suggest that bypassing the control instrument flagging has degraded the results of BORCAL 2000-01.

4.3.5 Revised Uncertainty in RCC Upgrade

Another modification to the RCC software implemented changes in the calculation of measurement uncertainty to better account for the uncertainty associated with the diffuse measurement. The uncertainty values for each pyranometer now include varying contributions of uncertainty of the diffuse measurement, depending on the ratio of diffuse to direct in the calculated global irradiance. Because of implementing a more accurate computation of solar zenith angles and measurement of sky diffuse irradiance, our estimates of uncertainty base on earlier BORCAL procedures and instrumentation must be revised. The "base uncertainty" of 1.3% used previously for the reference irradiance calculation for pyranometers is now reduced by a factor of approximately two. A detailed uncertainty analysis and new prescription for computing the uncertainty for subsequent BORCAL events is described below. The new methods will be incorporated into subsequent RCC versions.

4.3.5.1 Data Acquisition

RCC uses hardware comprised of a Fluke Helios Plus 2287A data logger, with a high performance Analog-to-Digital (A /D) converter, and Isothermal voltage input cards. The one-year accuracy specification for this configuration on the DC voltage range used ($\pm$ 64 mV) is 0.03% of reading + 9 microvolts (uV). NREL tests the "zero" input voltage level, measured by putting a high quality short circuit between the high and low terminals and the 9 uV offset is typical. For a nominal 10 mV (=10,000 uV) thermopile pyranometer signal, this amounts to 9+3= 12uV/ 10000 uV or 0.12% for data logger contributions to measurement uncertainty.

4.3.5.2 Zenith Angle Computation

Additional uncertainty in the reference irradiance for pyranometers is due to computing the solar zenith angle, Cos (Z). This computation depends on knowledge of the latitude, longitude, local standard time, solar equation of time (difference between True Solar Time and Local Standard Time), and solar declination (the angle between the center of the solar disk and the projection of the Earth's equator on the sky dome). NREL determined the location of the KACST BORCAL calibration platform to within 0.001°, or $\pm$ 100 feet. RCC software uses the local standard time accurate to within $\pm$ 2 second. The current version of RCC utilizes the algorithm of Michalsky, accurate to within 0.01° in Z. For Z less than 75°, the uncertainty in Cos (Z) is less than 0.06%. For Z greater than 75°, an atmospheric refraction correction is applied [27], to compute an effective zenith angle to an accuracy of 0.05°. The resulting 0.06° uncertainty in Z= 85° produces a 1.0% uncertainty in Cos (Z), growing to 6% at Z= 89°.

4.3.5.3   Reference Diffuse Sky Irradiance

The thermal offset in a black and white (model 8-48) pyranometer is no more than -2 W/m², but the uncertainty in determining the responsivity at 45° is still on the order of 2.5% of reading (usually less than 200 W/m², or 5 W/m²; thus 0.5% of reference irradiance of 1000 W/.m²).

4.3.5.4   Total Uncertainty Calculation

Summing uncertainty from the data logger (0.12%), WRR and transfer of WRR (0.39%), and cosine of the zenith angle (0.06% for z< 75°); uncertainty in the computation of the vertical component of the direct beam is 0.57%. For a typical clear sky diffuse irradiance of 100 W/m², measured with an all black detector pyranometer, the uncertainty in the diffuse component of the reference irradiance is ± 2.5% of reading + 20 W/m², or ±2.5 W/m² + 20 W/m² = 22.5 W/m². Using the black and white pyranometer, the uncertainty in the diffuse is ±2.5% of reading + 2 W/m² = 2.5 W + 2 W/m² = 4.5 W/m², or 0.50% of the reference irradiance.

Using a pyranometer with an all black detector to measure diffuse, assuming a clear sky global irradiance of 900 W/m², with diffuse component of 100 W/m², the 22.5 W/m² diffuse uncertainty is 22.5/900 = 2.5%. Combining the diffuse uncertainty with the 0.55% direct beam uncertainty by root-sum-squaring, the total "base" uncertainty in the determination of a single responsivity measurement using an all black detector for Z < 70° before adding in variability in each instrument is:

$$U_{tot} = \sqrt{0.57^2 + 2.5^2} = 2.6\%$$

Using a pyranometer with a black and white sensor the uncertainty in the diffuse (as a percentage of the total reference irradiance) is 0.50%, and the "base" total uncertainty in each individual responsivity for Z< 70° is reduced to:

$$U_{tot} = \sqrt{0.57^2 + 0.50^2} = 0.75\%$$

Since the uncertainty, U_i, for each responsivity, Rs_i, is a function of the zenith angle and the magnitude of the diffuse irradiance, RCC computes the uncertainty for each individual Rs_i using:

$$U_{dn} = 0.57\%$$

$$U_Z = 100 \bullet \frac{(Cos(Z) - Cos(Z + 0.03^O))}{Cos(Z)} \%$$

$$U_{df} = 100 \bullet \frac{(2 + 0.025 \bullet I_{df})}{(I_{dn} \bullet Cos(Z) + I_{df})} \%$$

$$U_i = \sqrt{U_{dn}^2 + U_Z^2 + U_{df}^2} \%$$

After each of the 10 zenith angle bins is completed, the mean responsivity for the 10 (9° wide) zenith angle bin is computed. The total uncertainty for the mean responsivity, U_{Rs}, in each bin is the root-sum-square of the mean of the U_i, and 1/2 of the range $\overline{U}_i$, (maximum - minimum), R, as a percentage of the mean Rs for the bin. The range term reflects the fact that for the same zenith angle bins, morning and afternoon responsivities may not overlap, as shown in figure 2.3.

$$U_{Rs} = \sqrt{\overline{U}_i^2 + (100 \bullet 0.5 \bullet \frac{R}{R_s})^2}$$

For computing the uncertainty in the determination of the responsivities of pyrheliometers, the sum of data logger and absolute cavity radiometer uncertainty is 0.47% (no zenith angle term). After the mean responsivity, Rs, and the standard deviation , σ, as a percentage of the mean are computed, the uncertainty in Rs is computed as

$$U_{Rs} = \sqrt{(0.47)^2 + (2 \bullet \sigma)^2}$$

4.3.5.5   Results and impact of RCC/BORCAL revisions
The above described improvements in RCC/BORCAL operations and procedures have the following specific impacts:

(1) *Measurements of clear sky total global solar radiation made with pyranometers calibrated at KACST before March 2000 are approximately 2.5% to 3% (of reading) too low. This amounts to 25 W/m² to 30 W/m² at "1-sun" of 1000 W/m².*

(2) Absolute uncertainty in responsivities of pyranometers and pyrheliometers has been reduced by about 15%.

(3) Absolute accuracy of total global pyranometer measurements has been improved by removing a negative bias (due to thermal offsets in all black pyranometers measuring the sky diffuse irradiance) of up to 20 W/m² in the calibration reference irradiance during calibrations.

(4) Total global pyranometer measurements made using previous versions of BORCAL/RCC, or any component summation technique method using an all black pyranometer for diffuse sky measurements, have an inherent negative bias (approximately 20 W/m² at NREL) built into the derived responsivity, and hence in the measured data.

(5) All black pyranometers (which do not have a compensating thermopile) calibrated as described in (3) above, *and used to measure sky diffuse radiation*, will still have inherent thermal offsets on the order of 20 W/m² which still must be accounted (corrected) for.

RCC software was also modified to correct for Y2K problems, and was upgraded with an improved algorithm for calculating solar position. These changes will not significantly affect the calibration results.

4.3.5.6   Recommendations
It is recommended that the responsivities from BORCALs performed after event 2000-01 be used to update network radiometers as they are deployed in the field. The results from the same instruments in BORCAL 1999-03 should not be used. As in the past, the *Composite Responsivities* from the tables in the BORCAL report should be used.

The results of the new diffuse measurement methodology will continue to be a subject of study in the future.   One important outcome of the continued research will be a recommendation on whether or not to reprocess existing network global and diffuse data that were collected with instruments calibrated using the old method of measuring diffuse.

4.3.5.7   Discussion of Historical Data Discontinuity
Previous BORCAL reports have discussed an apparent discontinuity in the control instrument responsivities between BORCALs 1996-02 and 1996-03. Since the last report, the Helios data logger was calibrated at the NREL metrology lab and a short-test was conducted of the data acquisition system before the Helios was removed from service for calibration. The short-test revealed some small irregularities, but none that could cause the observed discontinuity.   In summary, the discontinuity has not been explained.

4.4 Application of Zenith Angle Corrections to Network Data

Given that RCC produces information on the zenith angle response of pyranometers, that the variation in response for instantaneous data can approach 5% or more, and that the data collected from the field use the composite (cosine weighted) single responsivity; NREL evaluated the impact of correcting previously measured network global horizontal data to account for varying responsivity throughout the diurnal cycle of measurements.

4.4.1 Correction Method

Figure 4.6 illustrates the magnitude and direction of data corrections for a single pyranometer used to measure global horizontal irradiance at one site (Qassim) for winter (December) and summer (July) months of the year in 1999. The corrections vary due to the changing solar geometry through the year. Low sun elevation angles (high zenith angles) in December mean the radiation is underestimated up to 6 W/m² when using the composite responsivity. Data measured using the composite responsivity under high sun angles (low zenith angles) in July generally overestimate the irradiance near noon by up to 10 W/m² and underestimate the irradiance in the morning and afternoon by up to 5 W/m².

Figure 4.6. Absolute magnitude of corrections in global horizontal irradiance (W/m²) data measured with composite responsivity as a function of zenith angle for December (open circles) and July (points) at Qassim.

The advantages of the zenith angle dependent responsivities can be realized by applying them to data collected from field instruments. NREL devised a means of applying corrections derived from the RCC binned zenith angle responses and the clearness index, Kt, to the global horizontal data measured using the composite responsivities. [6]

Because the BORCAL is conducted under clear, cloudless skies, the vector responsivities can be applied directly only to global irradiance data collected under similar conditions. Under overcast skies when no direct beam is present, the composite responsivity should be used. Given this, the true responsivity of the instrument is a function of both the zenith vector and composite responsivities, scaled by the magnitude of the direct beam. A distinct disadvantage of this approach is that it requires the measurement of direct beam solar radiation coincident with the global radiation. However, because of a strong correlation between direct beam and global irradiance, we have developed an effective correction algorithm using only the global measurement from the pyranometer.

A clearness index, K, is derived by dividing the measured global irradiance by the ETR at the top of atmosphere. We determine the clearness index for the field data, the calibration data, and a value that represents a typical global irradiance below which there is no direct beam. We can then approximate the instrument responsivity as follows:

$$Rs = (K_{glo} - K_{min}) / (K_{cal} - K_{min}) * V_{rs} + (1 - (K_{glo} - K_{min}) / (K_{cal} - K_{min})) * C_{rs}$$

27

Where

K_{glo} = Clearness index of the measured global irradiance (single calibration factor)
K_{cal} = Clearness index of the global reference irradiance during calibration
K_{min} = The clearness index that corresponds to a direct beam irradiance of zero
Rs = Instrument responsivity
V_{rs} = Vector responsivity
C_{rs} = Composite responsivity

4.4.2 Corrected Results

We applied the vector corrections to the global data collected at the Solar Village network station. The effect of the corrections was analyzed using the SERI QC quality assessment software, which produces quality flags based on the departure from coupling in the three measurements. In the analysis, the degree of coupling for the entire test data set was determined both before and after the application of the corrections. The differences in data quality were binned by zenith angle and summarized in Table 4.1 below.

Table 4.1. Coupling errors as a percent of extraterrestrial radiation

Zenith angle bin	Average coupling error (% of ETR)	
	Original	Revised
0-9	0.3	0.1
9-18	0.3	0.1
18-27	0.3	0.2
27-36	0.2	0.2
36-45	0.2	0.2
45-54	0.3	0.2
54-63	0.7	0.4
63-72	0.9	0.6
72-81	1.3	0.7
81-90	0.0	0.0

In addition, the magnitude of the corrections in irradiance was analyzed by zenith angle, which is summarized in Table 4.2. The results show that the effect of the correction on total annual irradiance was less than 0.2%, nearly insignificant. This is because the original single calibration factor (composite) was adequate to represent the instrument responsivity under a variety of conditions. However, the table shows changes that are more significant to the irradiance at low and high zenith angles where the vector responsivities depart the greatest from the single calibration factors. Corrections on individual data points could likely be much higher than these averages, possibly as much as 25 or 30 W/m^2 at midday, depending on sky conditions, zenith angle, and the responsivity curve of the pyranometer in use.

Table 4.2. Effects of corrections on irradiance (W/m^2)

Zenith Angle Bin	Bin Average Irradiance		% Change
	Original	Revised	
0-9	1010	999	-1.09
9-18	964	955	-0.99
18-27	900	892	-0.84
27-36	825	821	-0.47
36-45	723	725	0.29
45-54	584	589	0.84
54-63	440	446	1.23
63-72	287	291	1.17
72-81	143	146	1.90
81-90	55	56	1.68
Total/Year*	2212965	2216850	0.18

* kWh/year

We have used this method to process data from the KACST Solar Monitoring Network as part of the NASA Mission to Planet Earth project. The corrected data are available at http://rredc.nrel.gov/solar/new_data/Saudi_Arabia/ [30].

For determining long-term monthly or annual total irradiance, the use of a single calibration factor optimized for all conditions cannot be significantly improved by the application of zenith angle-dependent calibration factors. However, when looking at subsets of data, such as midday or clear skies, the corrections described here are measurable and can result in an important uncertainty reduction in the estimate of the solar resource for some applications.

Figure 4.7 compares clear day uncorrected global horizontal measurements (made with a composite responsivity) with zenith angle corrected global horizontal measurements. Also shown is the global horizontal irradiance computed from direct normal irradiance measured with a normal incidence pyrheliometer and sky diffuse measured with a black-and-white pyranometer under a tracking shading disk. The zenith angle corrected data are much closer to the computed irradiance, and are about 20 W/m² lower than the uncorrected irradiance measured at noon.
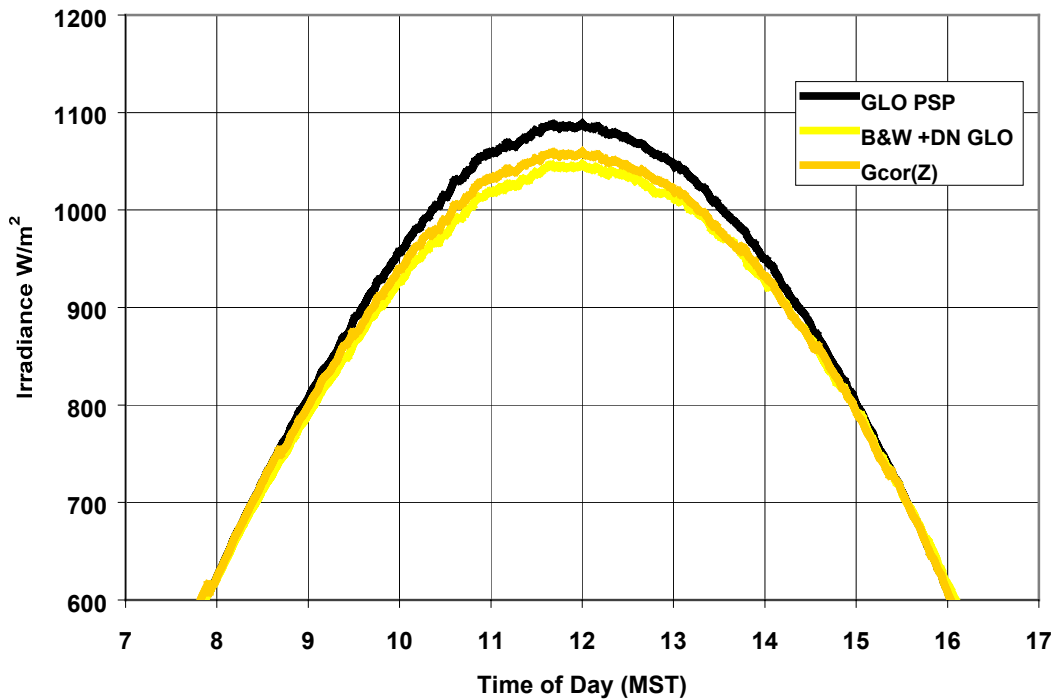
Figure 4.7. Comparison of global horizontal irradiance measured with single responsivity [GLO PSP, top black curve] with zenith angle corrected data [Gcor(z) 2nd curve from top] and with global horizontal computed from direct normal and black and white shaded pyranometer sky diffuse [B&W+DN GLO 3rd curve from top]

4.5 Pyranometer Aging

Anecdotal evidence has suggested that the sensitivity of thermopile radiometers changes at about 1% - 2% per year for pyranometers, and that the greatest rate of degradation occurs when the instrument is new. For pyrheliometers, the rate of degradation is much less. These observations have led to general recommendations that instruments be calibrated annually to properly characterize and compensate for the expected sensitivity changes.

4.5.1 Evaluating Sensitivity Changes

At startup, the KACST network was instrumented with new Eppley PSP and NIP radiometers for global and direct beam measurements, and shading disk trackers for measurement of diffuse with PSP radiometers. Prior to installation, all radiometers were calibrated with a procedure developed and implemented by NREL. Sufficient radiometers were purchased such that each site would receive newly calibrated radiometers once per year in an instrument exchange operation that would interrupt data acquisition for no more than a few minutes. Two to three calibration events are scheduled at the calibration facility each year to accomplish this procedure.

Calibration control instruments have been designated and are kept in dark storage except for the few days each year that they are required as part of the calibration process. These

instruments have shown stability well within the calibration uncertainty (approximately 1%) over the years, giving credence to the observation that exposure to the elements is a major factor in sensitivity degradation.

During instrument exchange operations, no effort is made to match radiometers with sites; instruments are taken from storage and assigned to sites as needed. Similarly, no effort is made to designate a PSP for either global or diffuse measurements. They are deployed as needed.

This procedure gives rise to the opportunity to investigate the aging characteristics of instruments in a variety of climates and deployments. The hypothesis is that the degradation is largely a function of exposure to the sun and possibly temperature, and can be correlated to the amount of radiation an instrument receives [7].

4.5.2 Quantifying Instrument Exposure

Data from the instrument itself are perfectly suited for this analysis. For each instrument in the network, the irradiance between calibrations was accumulated. No effort was made to filter the data with convention quality assessment methods usually used for the data. If the optics were dirty or a tracker misaligned, this would affect the amount of irradiance falling on the sensor and would be significant in our analysis. Given the variety of climates at the 12 stations of the network, and the use of the 39 instruments in both the global and diffuse positions, a wide range of irradiance has impinged the individual radiometers. At each calibration, an instrument's responsivity was ratioed with its original responsivity and plotted against the cumulative total irradiance exposure since the instrument was first deployed in the network.

4.5.3 Aging as a Function of Irradiance

The results of the analysis for five of the 39 network instruments are shown in Figure 4.8. After each calibration for each of the five instruments, the cumulative irradiance up to the date of calibration was calculated. The percent change from the original calibration was also computed, and plotted versus the cumulative irradiance total. The plot shows a distinct trend highly positively correlated to irradiance. Further, the trend indicates that the rate of change of the degradation may level off after a certain level of exposure is obtained. Although these data are insufficient to predict stable responsivity, experience with other older instruments at locations in the United States shows consistent stable responsivities over a period of several years. A similar analysis of the direct beam data from the KACST network shows that the degradation in NIP sensitivity is much smaller than that of PSPs.

A similar analysis could be conducted using the cumulative thermal dose due to temperature (i.e., cumulative degree days above a certain temperature). However, the project did not have the resources to conduct this analysis.

31
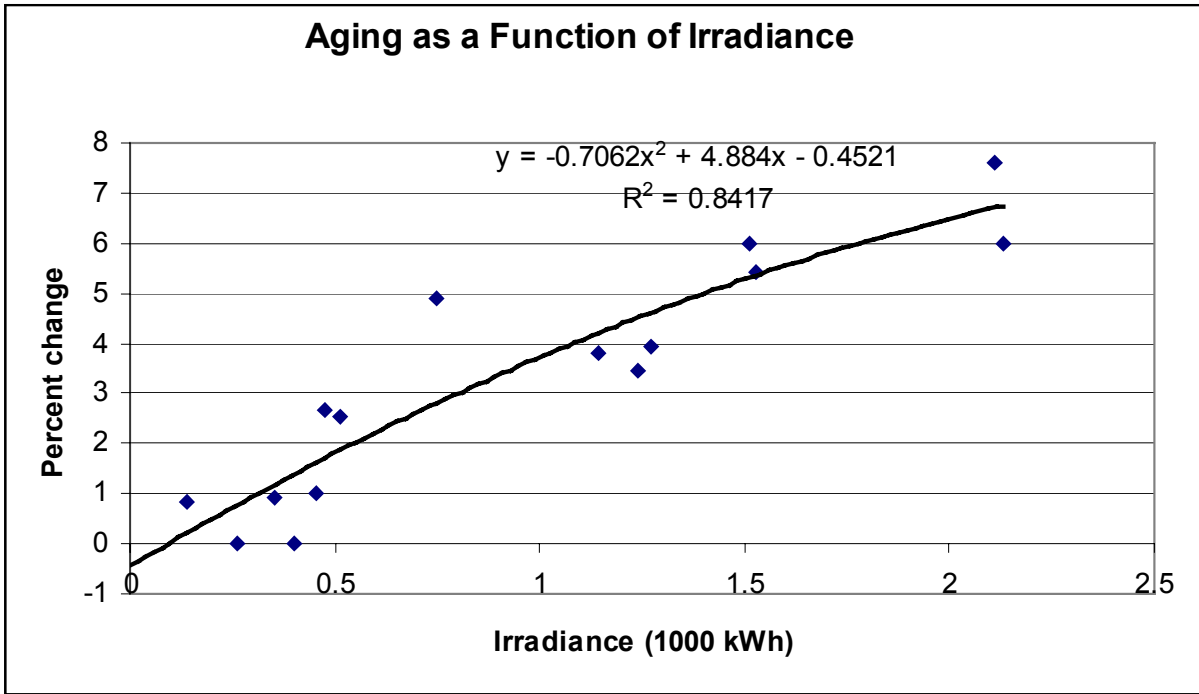
Figure 4.8. Percent change in responsivity for five pyranometers plotted as a function of cumulative irradiance in thousands of kilowatt-hours. The decreasing slope at higher irradiance values may indicate that the degradation eventually levels off at a certain (higher) cumulative irradiance level.

4.5.4 Conclusions on Pyranometer Aging

We have observed dependence of the degradation of pyranometer responsivities that is highly correlated with the total cumulative exposure of the radiometers, and possibly the thermal environment of the radiometers deployed in a Saudi Arabian solar monitoring network. A wide range of irradiance and thermal conditions is observed for the network stations; and a wide range of degradation values is observed.

It may be possible to establish or change the period for instrument calibrations through an analysis of the data that the instruments collect. By keeping a running total of the irradiance for each radiometer, a network administrator could schedule calibrations at more frequent intervals based on the conditions at the measurement site. However, significantly extending the customary one-year interval for calibrations may be unwise given that other factors can affect an instrument's sensitivity, such as optics, electrical malfunctions, or physical damage.

5.0 Data Quality Management and Assessment Software Upgrade

5.1 Year 2000 (Y2K) Revisions

On January 2000, several changes were made to solar position calculation (SOLPOS) and data quality assessment routines SERI QC and QCFIT to correct known problems and to bring certain calculations into line with current knowledge.

5.1.1 Updating Solar Geometry Computations

Solar geometry considerations are critical to evaluating the cosine response of pyranometers, for computing the balance of the radiation components in data quality assessment software. NREL reviewed and updated the solar position and solar geometry subroutines to address year 2000 problems, and provide more accurate computations based on the best algorithms available [26, 27]. Modifications to the SOLPOS routine accomplished include the following:

- Modularized the functions
- Changed from global variables to passed-parameter structure
- Added a selection mechanism to choose which functions to execute
- Replaced erroneous leap year algorithm with correct algorithm (3 places)
- Required input of year, day number, hour, minute, second, latitude, longitude,
- time zone, rather than defaults
- Increased maximum allowable time from 23:59 to 24:00
- Added interval parameter (up to 20 hours)
- Added 3 shadowband correction factor arguments rather than Eppley constants
- Removed error-checking text output
- Added a return value with error codes
- Added a decode function for checking return code
- Added an initialization function (since not using global variables)
- Added toggle for day/month or day number date input/output

5.1.2 Updating Quality Control and Assessment (SERI QC)

The SERI_QC software module is used to compare recently collected data with critically evaluated historical data that have been used to set boundaries within which acceptable data are expected to fall [9]. These boundaries are approximated by double exponential functions known as Gompertz Functions. The acceptable boundaries are saved in lookup files called QC-zero files, representing reasonable solar data regions for low, medium, and high air-mass conditions. As with the SOLPOS routines, year 2000 and other modifications were made to make the SERI_QC operations more accurate and flexible. Modifications included:

- Corrected improper read of QC-zero file during exchange between computer platforms
- Corrected leap year algorithm to correctly report 2000 as a leap year

- Corrected improper logical if block statement transfer to Augustyn executable
- Corrected improper low limits for global Kt and direct Kd
- Corrected calculation of zenith angles, ETR, and ETRN for partial sunup hours
- Corrected calculation for 1-minute data once per hour
- Adjust Extraterrestrial radiation for entire interval,[minute; hour] not just partial sunup portion
- Expanded valid times to include 24:00
- Corrected a floating point rounding problem; occasionally selected wrong index for Gompertz (QC_ZERO Boundary) curve
- Added Michalsky solar geometry calculation (SOLPOS)
- Changed method of selecting airmass regime from calculated AM to simple zenith angle cutoff
- Remapped two-digit years based on year-50 pivot. If (YY-50) < 0 data from 19YY; otherwise from 20YY
- Remapped out of bounds years to nominal values in valid range
- (1950-2050)

5.1.3 Updating Fit of Acceptable Data Boundaries (QCFIT)

QCFIT is a sub-module of the SERI_QC routine that fits the correct QC-zero Gompertz function to the boundary of the acceptable data envelope for historical data, using operator judgment and input. Year 2000 issues were corrected by incorporating the following:

- Added Michalsky SOLPOS
- Remapped two-digit years based on year-50 pivot
- Remapped out of bounds years to nominal values in valid range (1950-2050)

Table 5.1 is a summary of the changes and the effects on program operations. Note that though six changes are characterized as "minor" in impact. Within the resources of the project, it was impossible to evaluate every possible scenario for the impact of the changes. A conservative estimate of the impact of the minor changes might be 0.5% changes in the quality assessment results, or 10% of the 5% window of acceptance for "good" data, and 5% of the window of discrepancy (resolution of 1%) for flagging data error magnitudes. Implementing these corrections reduces the possibility of improper flagging of data and of accepting bad data (type I statistical error) or rejecting good data (type II statistical errors) by at least 10%.

Table 5.1. Summary of DQMS/SERI_QC/QC_FIT/SOLPOS changes and effects on program operations.

Action	Problem Description	Change in Behavior
Corrected a year 2000 leap year problem (QCFIT and SERI QC).	The original versions of SERI QC and QCFIT did not recognize the year 2000 as a leap year.	This corrects a small error in solar position calculations between February 29th and December 31st, 2000. The magnitude of the error in ETR irradiance ranges from 0.08% on the solstice to 0.7% on the equinox.
Corrected improper low limits to Kt and Kd (SERI QC).	The low limits for Kt and Kn were changed from 0.0 to 0.05 for Kt and 0.03 for Kd.	This will now correctly flag some very low daytime irradiance as below empirical limits (flag of 07). The occurrence of such low irradiance is very rare.
Corrected several problems with the calculation of zenith angle, ETR, and ETRN for partial sunup hours near sunrise and sunset (SERI QC).	Changed the routine to determine the average zenith angle. Changed the calculation of partial hour ETR values to consider only the sunup portion of the hour.	The most significant effect of these changes will be on one-minute data, where the zenith angle calculation was grossly in error for one minute near the top of each hour. The effect on other data will be minimal but possibly noticeable as either 1) a rare change in flagging by one level or 2) the correct flagging of slightly more data during sunrise/sunset periods as above empirical limits (flag 08).
Expanded the valid times to include 00:00 (SERI QC).	The program would not allow the time 00:00 as a valid input time, but instead rigidly enforced a 00:01 – 24:00 time range.	The program now accepts 00:00 as a valid time, but treats it internally as time 24:00 of the previous day. This affects only data from the parts of the world where the sun is up at midnight, and only affects data on a monthly boundary. In such cases, the program will use the QC0 file entry from the previous month for data from time 00:00 on the first day of the month.
Table 5.1 Continued...		

Table 5.1 Continued...		
Corrected a floating point rounding problem (SERI QC).	Due to improper rounding of floating point decimal representation, the program would select the incorrect boundary.	This problem was extremely rare. When encountered, it will result in a one-step change in the flag.
Added the Michalsky solar position algorithms (SERI QC and QCFIT).	Implements a more accurate solar position routine.	QCFIT will display a few data points in slightly different locations on the scatter plot, and will likely show slightly different boundary statistics. Some points near an air mass boundary may appear on another air mass plot. SERI QC will show an occasional one-step change in flagging. The errors of the old algorithm are generally less than one percent, and this change is not expected to have a significant impact on the characterization of data quality.
Changed the method of handling year data (SERI QC and QCFIT).	The new solar position algorithms are valid only for years 1950 to 2050. A pivot was added to accommodate two-digit year data that would otherwise clearly lie outside bounds. Additionally, the default year of 1901 in QCFIT was changed to 2001, and in both programs, out of bounds years are remapped rather than rejected.	The effect will be minimal, largely lost in the effects of the new solar position algorithm. But the user should know that two-digit years will be pivoted at year 50 in the following manner: For input years 0-49, the program will interpret them as year+2000. For input years 50-99 the program will interpret them as year+1900. If four-digit years beyond the valid range of 1950-2050 are submitted, they will be remapped to 1950 or 2050, whichever is closer, or to 1952 or 2048 for leap years. In QCFIT when no year is specified, the default year becomes 2001. The errors introduced by re-mapping years that are out of bounds have not been quantified, but are expected to be of a smaller magnitude than the errors in the old solar position algorithms.

6.0 Training for MEPA Observers at the Solar Radiation Network

A training course for the MEPA operators who conduct operation of the eleven network sites was held at the solar village, Riyadh in May 2000. Two operators from each participated in the course. The course included the following topics:

- Overview of the solar energy fundamentals and applications
- Overview of the renewable energy research and development at KACST Energy Research Institute
- Solar radiation fundamentals, applications, measurements and instrumentation
- Network stations components, design, instrumentation, and parameters recorded
- Hands-on training on the operation and maintenance of network stations

7.0 Evaluation of Solar Radiation Atlases for Saudi Arabia

As was described in Section 2.8, a primary objective of the project was to develop a solar radiation atlas for the Kingdom of Saudi Arabia. Initially, meteorological satellite data were envisioned as the source of data for such an atlas. A lack of resources and suitable models for converting the satellite images into solar radiation values forced an approach based on the CSR also described in Section 2.8. The data grids developed under the CSR model were used in conjunction with a modified METSTAT model and GIS processes to produce full color "contour" maps of monthly mean daily total solar radiation for each of the global, direct, and diffuse radiation components, as shown in Figure 2.5. The new atlas [12] was published to update a previous, first edition of a solar radiation atlas developed in 1983 [23].

7.1 First and Second Edition of Solar Radiation Atlas for Saudi Arabia

The first edition of the Saudi Arabian Solar Radiation Atlas was produced by the Saudi Arabian National Center for Science and Technology (SANCST), later renamed KACST in honor of King Abdulaziz. SANCST obtained data from the archives of the Saudi Arabian Ministry of Agriculture and Water for the period 1971 to 1980. Sunshine duration was measured at 17 stations, and global horizontal irradiance was measured at 41 stations. The global horizontal solar irradiance was measured by the mechanical pyranographs described in Section 2.6.

The first edition atlas contained contour maps and data tables for monthly mean sunshine duration in hours and monthly mean daily total global horizontal irradiance in W/m². The Angstrom relation between duration of sunshine (S) and global irradiance (G) was used to convert relevant data to the appropriate units. The Angstrom relation requires determination of the slope, B, and intercept, A, of a linear relation between G and S, given as $G/Go = A + B\, S/So$, where Go is the extraterrestrial irradiance on a horizontal surface, and So is the maximum possible sunshine duration. The coefficients are often site and time dependant. The coefficients used are reported along with the data in the atlas data tables.

To generate contours for the maps, data were interpolated to a 2.5 ° grid, using the three nearest stations, inversely weighted by distance from the grid point. The gridded data were reported for each month in tables, as well. Note that the 2.5° grid represents approximately 160 mile, or 260 kilometer, spatial resolution at the central latitude of 22.5° for the Kingdom. Figure 7.1 is the Global Horizontal Contour plot for October from the first edition atlas. Contour lines are in units of Kwh/m²/Day (compare with Figure 2.5).
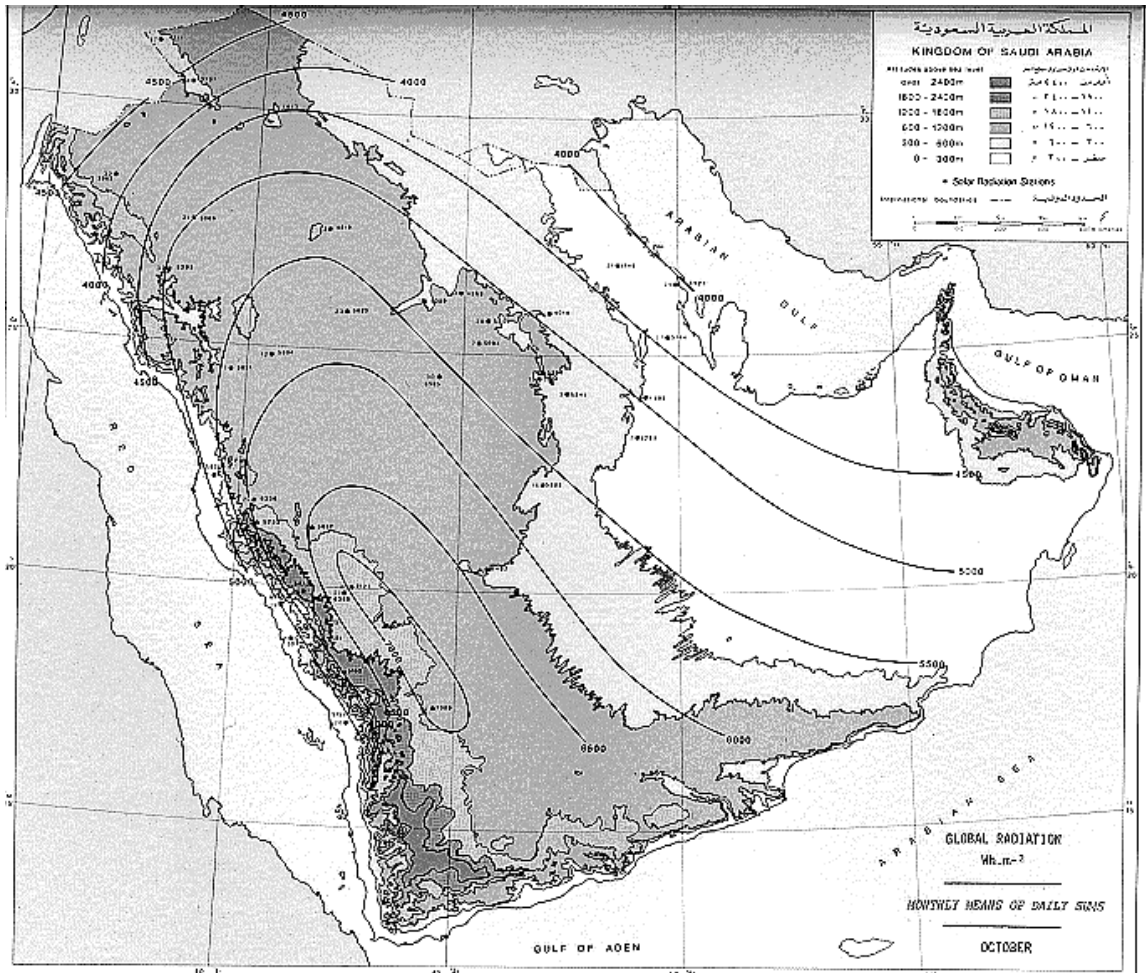
Figure 7.1. October contour lines of monthly mean daily total global horizontal radiation overlaying shaded elevation map of Saudi Arabia, as presented in the first edition of the Saudi Arabian Solar Radiation Atlas. Contours are in increments of 500 W-hr/m²/day, beginning at 4000 W-h/m²/day at upper left to 7000 W-h/m²/day at the top of the plateau near the east coast.

The second edition solar radiation atlas generated under this project used the 40 kilometer resolution cloud cover data (RTNEPH), representing both ground and satellite derived cloud cover information as the fundamental resolution for the data gridding. Other satellite derived inputs to the CSR (ozone, albedo, water vapor, etc.) were sub-sampled or interpolated to the 40 km resolution.

Monthly means of the CSR input parameters were computed on an hourly basis, to preserve diurnal patterns. These data were then assumed to hold for a single day, the midpoint of the month. The "midpoint" day was selected based on the available extraterrestrial solar radiation. The day that was selected produced the daily total extraterrestrial radiation closest to the mean for that month [11].

The METSTAT model, modified to calculate the solar radiation in 5-minute intervals though the representative day, was used to compute the monthly mean diurnal profile of solar radiation. This daily profile was then integrated to produce the monthly mean daily total for the month. The color of each grid cell was assigned based on the value of the resulting integration. This process was repeated at every point in the 40-km grid covering the region, resulting in maps such as shown in Figure 2.5. The second edition atlas provides data for direct and diffuse solar radiation, as well as global horizontal irradiance. The second edition atlas also contains tables showing the monthly mean daily totals of each component measured at the 12 network stations during the first three years of network operation, and comparisons with the CSR model results for each station.

7.2 Comparing Atlases and Saudi Solar Radiation Network Data

The only data that are common to both editions of the Saudi Arabian Solar Radiation Atlas are global horizontal irradiance; presented as monthly mean daily totals. In this section, we compare the data presented in each edition with the first five years of measured network data. Since the purpose of the atlases is to present climatological data, it can be argued that the five years of measured data may no adequately represent the "true" solar radiation "climate" of the kingdom. However, our analysis highlights significant differences between the two editions, and substantial improvements in accuracy in the second edition of the atlas.

Not every station in the network appears in the first edition of the atlas. Only four stations (Riyadh, Abha, Tabouk, and Madinah) are common to both the KACST measurement network and stations used to generate the first edition atlas. Surrogate, or substitute stations with data tabulated were chosen from the first edition atlas. The substitute stations selected were those nearest the current network stations, in latitude and longitude, as shown in Table 7.1.

Using the measured network data from 1996 to 2000, we first show that these data compare fairly well with the second edition atlas climatological summary. We then compare the five years of measured data with the first edition atlas data, noting where the differences are large. The differences between the measured data and the first edition atlas data then should be representative of differences between the two versions of the atlas.

39

Table 7.1. Network Station Substitutes from First Edition Atlas

STATION	LATITUDE	Substitute Station	Substitute Location
Solar Village	24.91 N 46.41 E	COMMON (Riyadh)	
Qassim	26.31 N 43.77 E	Unayzah	26.07 N 43.98 E
Al Ahsa	25.30 N 49.48 E	Harad	24.07 N 49.02 E
Wadi Al-Dawasser	20.44 N 44.68 E	Al-Aflat	22.28 N 46.73 E
Abha	18.23 N 42.66 E	COMMON	
Gizan	16.90 N 42.58 E	Sabya	18.17 N 42.62 E
Sharurah	17.47 N 47.11 E	Najran	17.55 N 44.23 E
Jouf	29.79 N 40.10 E	Sakaka	29.96 N 40.20 E
Qaisumah	28.32 N 46.13 E	Maaqala	22.36 N 47.36 E
Tabouk	28.38 N 36.61 E	COMMON	
Madinah	24.55 N 39.70 E	COMMON	
Jeddah	21.68 N 39.15 E	Taif	21.23 N 40.35 E

7.2.1 Measured and 2nd Edition Atlas Global Horizontal

We compared the tabulated monthly mean daily totals from the second edition atlas with the upper and lower boundaries of the range represented by the color of the cell containing a station. Figure 7.2 shows how well the measured values fall within the upper and lower limits for each station month. Each panel of the plot contains the data for the 12 station months for the station indicated.
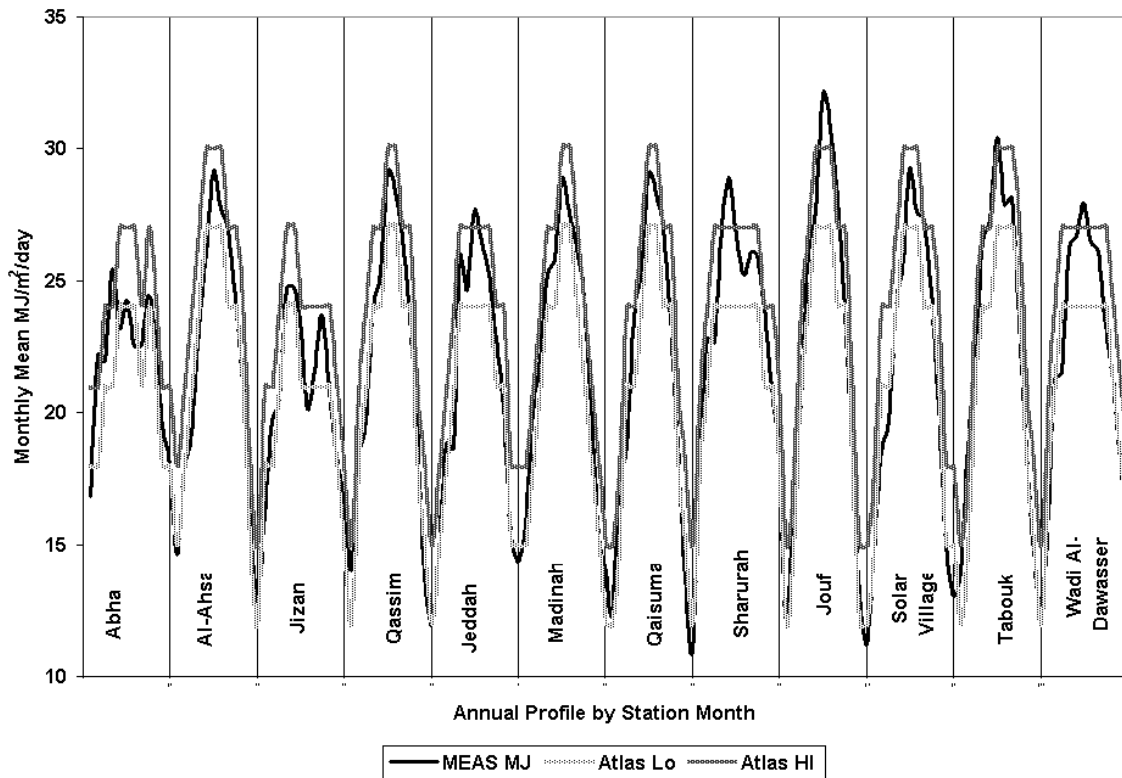
Figure 7.2. Plot of monthly upper (dark gray) and lower (light gray) bounds of CSR modeled irradiance data and monthly mean measured (black) data.

In Figure 7.2, the black curve is the monthly mean daily total computed from the 1996-2000 measured data. Each panel contains the 12 monthly data points for the station indicated.

The measured data follow the envelope of the upper and lower bounds very well, except for a few excursions above the upper limit (the summer peaks at Jeddah, Sharurah, Jouf, and Wadi Al-Dawasser). In a few cases, as at Jizan and Abha, the measured data fall only slightly below the lower boundaries. However, the measured data follow the station dependent seasonal variations quite well, and mainly within the range of values given by the atlas.

7.2.2 Measured and 1st Edition Atlas Global Horizontal

Figure 7.3 compares the first edition atlas data to the measured data from 1996 to 2000 in a manner similar to that in Figure 7.2. Each panel shows the 12 monthly measured and the first edition tabulated monthly mean total radiation data.
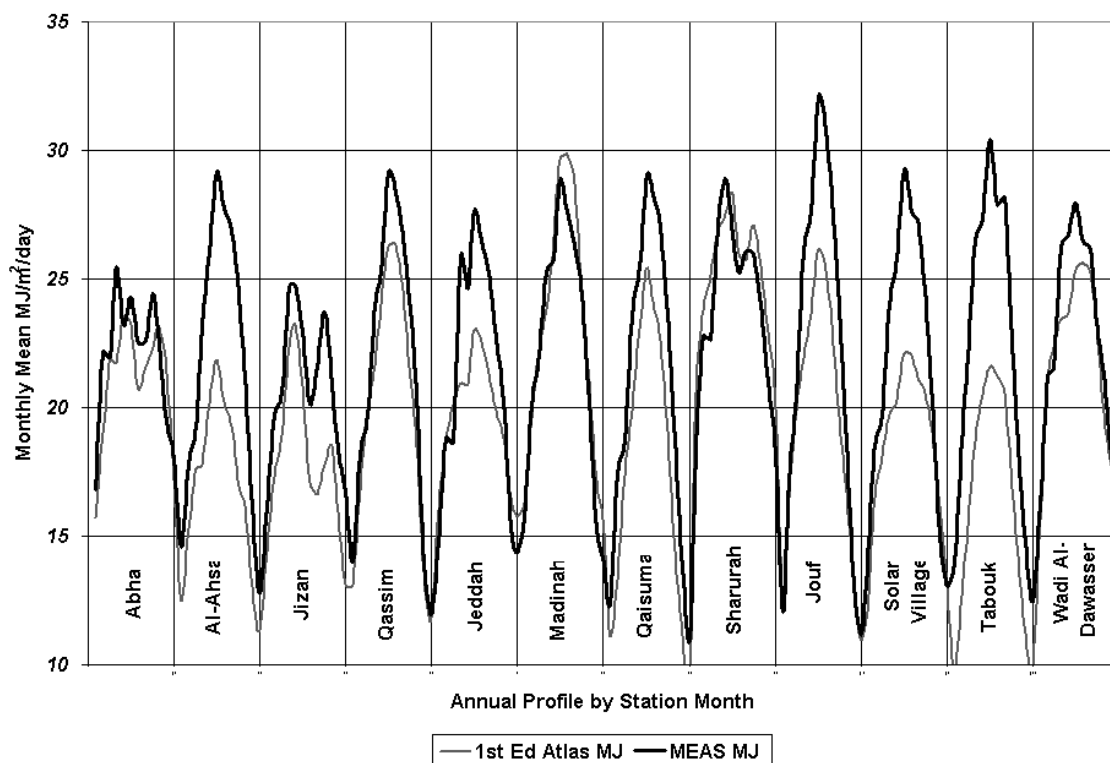
Figure 7.3. Measured monthly mean daily totals (black line) compared with first edition atlas (gray line) tabulated monthly mean daily totals. Note that nearby substitute stations were used as shown in Table 7.1, where applicable.

In Figure 7.3, we observe substantial differences for Riyadh (the Solar Village), Tabouk, Jeddah, Al-Ahsa, and Jizan. In each case, there are several months where the first edition atlas data are lower than the measured data by more than the 3 MJ/m²/day range increment for the second edition atlas.

Figure 7.4 is a histogram of the differences between the measured and first edition atlas monthly mean daily totals. The histogram bins are one MJ/m²/day wide. The figure shows that measured data exceed the first edition data by more than one second edition atlas range bin, or 3 MJ/m²/day for 72 station months, or 50% of the station months. Measured data exceeded the first edition data by more than two second edition atlas range bins (6 MJ/m²/day) for 12 station months, or 8% of the station months. Since the measured data and second edition data are closer to each other, these differences represent the difference between the first and second edition atlas. Namely, about 50% of the time the first edition atlas underestimated the monthly mean daily total global solar radiation by more than 3 MJ/m²/day.
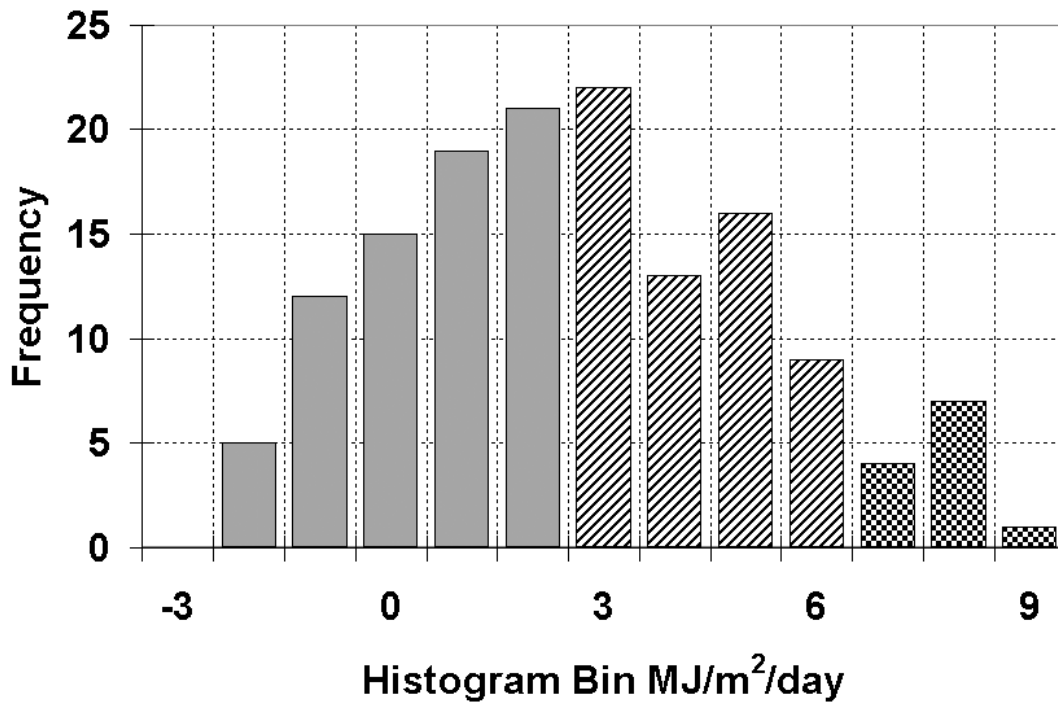
Figure 7.4. Histogram of the difference (Measured) - (First Edition Atlas) for data monthly mean totals for KACST network stations. Solid bars show differences less than one second-edition atlas range bin of 3 MJ/m²/day. Diagonal shaded bars are for differences exceeding 3 MJ/m²/day, and cross hatched bars are for differences greater than 6 MJ/m²/day. Fifty percent of the first edition atlas data are lower than measured data by more than 3 MJ/m²/day.

The annual average monthly mean daily total over all station months in the KACST network is 21.8 MJ/m²/day. The 3 MJ/m²/day resolution of the second edition, CSR model based atlas represents a resolution of 15% with respect to this average. Thus the first edition atlas can be said to have underestimated global solar radiation monthly mean daily totals by more than 15% about half the time, and by 30% or more about 8% of the time. These differences highlight the improvement in accuracy made since 1981 in modeling and validation of modeled solar radiation resources.

7.2.3 Measured and 2nd Edition Atlas Direct Normal

As might be expected from the close agreement shown in Figure 7.2 of the global horizontal measured monthly mean daily totals and the 2nd edition atlas data for global horizontal, measured and CSR modeled direct normal data are in good agreement, as well. Because direct-normal radiation is more sensitive to cloud cover and atmospheric conditions, the agreement between the measured and CSR modeled (2nd edition Atlas) data are not quite as strong. For example, due to operational problems with some of the stations (Jizan, Jeddah), especially tracker maintenance problems, the measured direct normal data are much lower than the CSR modeled second edition atlas "low boundary" for the site, as shown for these sites in Figure 7.5.
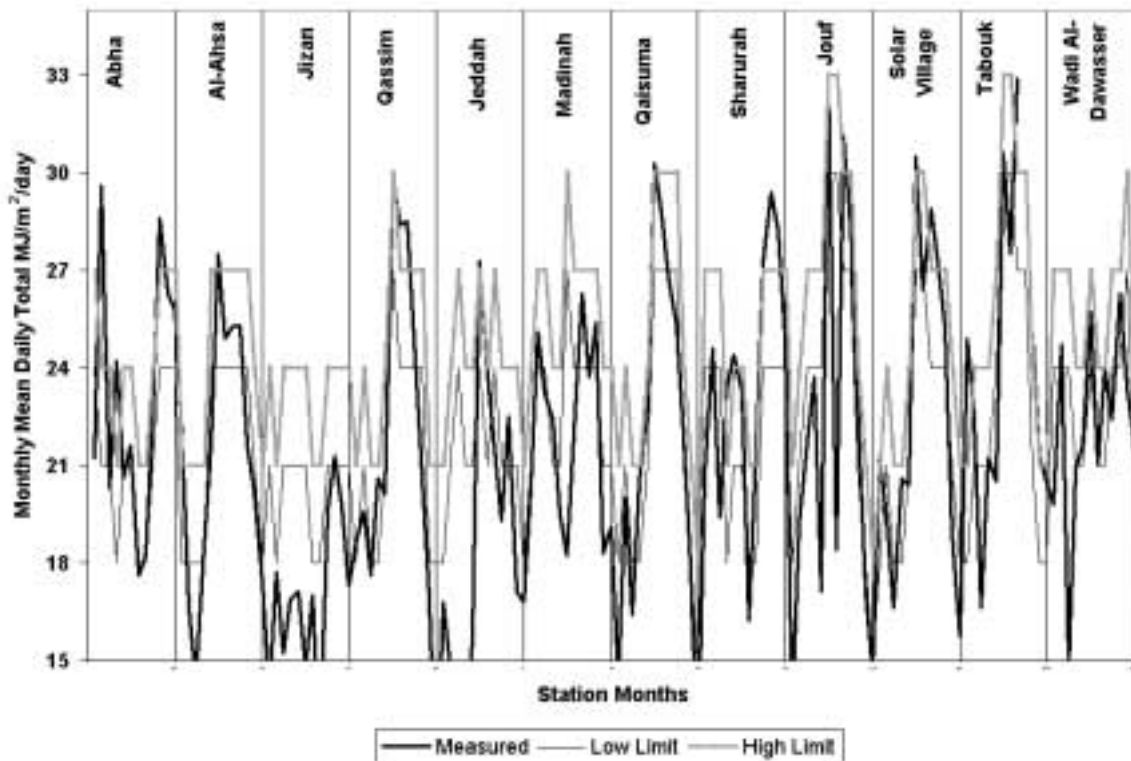
Figure 7.5. Comparison of direct normal monthly mean daily totals computed from network data (black) and CSR modeled second edition atlas upper (dark gray) and lower (light gray) range bounds on by site month. Jizan and Jeddah reported data are considerably lower than lower bounds, mainly due to tracker maintenance problems.

However, for the other 10 stations, the measured data fall near or within the bounds computed for the CSR modeled data used in the second edition atlas.

8.0 Expanding Measurement Capabilities at the Solar Village

Part of the technology transferred to KACST involved the expansion of solar radiation measurement capability and scope. The high quality of the Saudi solar radiation network

data were the basis for a joint project between the NASA EOS satellite remote sensing validation project, KACST, and NREL [30]. The scope of this project was to provide NASA/EOS investigators with ground based measurement data for the Saudi environment to validate satellite derived data products. The project was enhanced by the addition of a Baseline Surface Radiation Network (BSRN) measurement station at the Solar Village station, and NASA loan of a sunphotometer to KACST for aerosol optical depth measurements.

In addition, KACST purchased multiple Ultraviolet (UV) monitoring sensors for installation at the Solar Village. NREL performed calibration of the UV sensors at NREL before shipping them to KACST for installation. These activities are described in more detail below.

8.1 Baseline Surface Radiation Network (BSRN) Station

The BSRN activity is a voluntary, co-operative project managed by the WMO. BSRN is a project of the World Climate Research Program (WCRP) aimed at detecting important changes in the earth's energy balance that may cause climate changes [31]. At a small number of stations (fewer than 40) in contrasting climatic zones, covering a latitude range from 80°N to 90°S (see station maps), solar and atmospheric radiation is measured with instruments of the highest available accuracy and at a very high frequency (one minute). Radiation data are stored together with collocated surface and upper-air observations and station metadata in an integrated database at the WRMC. The project history and description are available on the World Wide Web at **http://bsrn.ethz.ch**. Figure 8.1 is a map of showing the distribution of BSRN stations around the world. The Solar Village station is circled and labeled as RIY.
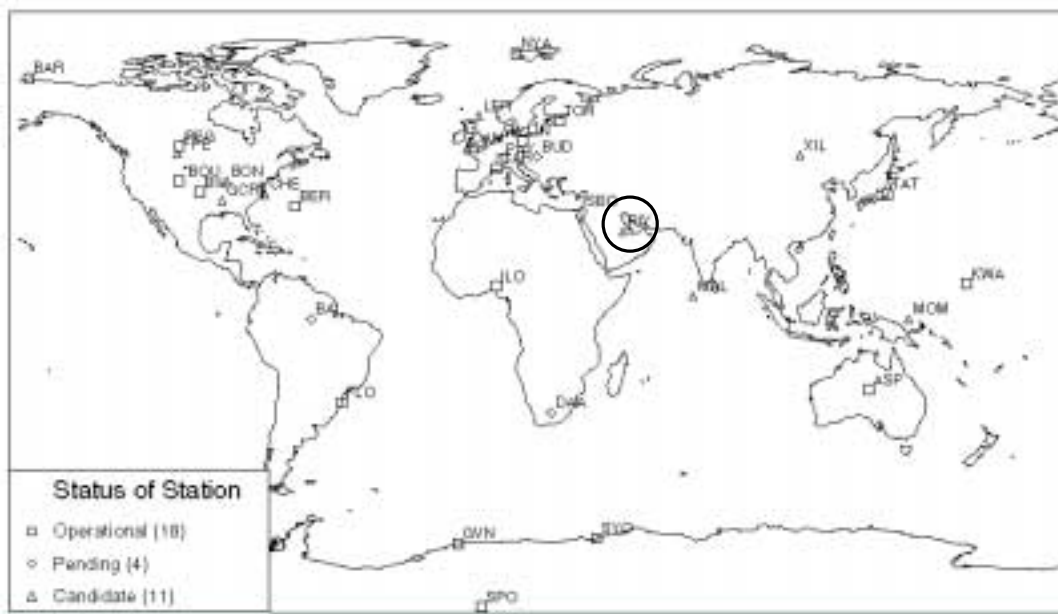
Figure 8.1. BSRN station locations worldwide as of 1999. Solar Village station circled and labeled as RIY.

The measurement scheme for BSRN stations is documented in the BSRN Operations Manual [32]. Primary measurement parameters are global, direct, and diffuse radiation, along with upwelling and downwelling infrared radiation. Accuracy requirements of the BSRN station are best met by measuring the direct radiation with an absolute cavity radiometer and measuring diffuse sky irradiance with a pyranometer under a tracking-shading disk. Global irradiance is measured with pyranometers. A global horizontal irradiance computed from the direct beam and diffuse measurements is required. The BSRN data are collected at a high frequency (at least 2-second sampling and 1-minute averaged data). The 1-minute averaged data are processed by the site scientist, quality assessed, and formatted into a stringent BSRN mandated format for submission to the BSRN Archive via electronic mail or file transfer protocol (ftp). Data are submitted on a monthly basis. BSRN quality assessment software processes submitted data files and rejects those that do not meet format specifications.

NREL assisted KACST to assemble a BSRN station at the Solar Village by specifying an absolute cavity radiometer system for continuous outdoor operation, as well as longwave instrumentation (pyrgeometers) for infrared measurements, and a suitable tracking platform for the cavity radiometer and shading devices for longwave downwelling measurements. Table 8.1 lists the BSRN instrument complement. NREL designed the appropriate mounting hardware for upwelling shortwave (albedo) and longwave on a 33-meter tower about 1.5 km from the main solar village site. Figures 8.2 and 8.3 show the cavity radiometer and downwelling IR radiometer installation and the installation of the upwelling IR radiometer on the tower before raising the tower. Figure 8.4 is an overall view of the upwelling shortwave and IR monitoring site, showing the tower.

Figure 8.2. All-weather absolute cavity radiometer (right) and shaded infrared radiometer (top left) on BSRN Brusag tracker at the Solar Village.

Figure 8.3. Installing IR radiometer in NREL-designed fixture for upwelling IR measurements. Shortwave upwelling radiometer (PSP) on opposite arm.

TABLE 8.1. Solar Village BSRN Radiometric Instrumentation

PARAMETER	UNITS	SENSOR	MANF.	MODEL	UNCERTAINTY	COMMENTS
Direct Beam Absolute Cavity Pyrheliometer	W/m²	Wire wound Type T Thermopile solid silver inverted cone cavity	Eppley Laboratory	AHF Auto-matic Hickey-Frieden	+/- 0.45%	@ 1kW/m² Corning 7940 fused silica window correction factor additional 0.8% uncertainty. Tracking by BRUSAG tracker
Downwelling longwave (sky irradiance) under Shading Disk	W/m²	Pyrgeometer Type T Thermopiles	Eppley Laboratory	PIR	+/- 10 W/m²	Silicon dome with thin film interference filter passing longwave (wavelength > 8 micron) infrared Shade disk mounted on BRUSAG tracker
Upwelling Longwave (ground emission)	W/m²	Pyrgeometer Type T Thermopiles	Eppley Laboratory	PIR	+/- 10 W/m²	As above, mounted at 100 ft (33 m) level at 3 ft (1 m) from 1 ft (0.3 m) diameter tower; body shaded from direct sun, downward looking
Upwelling shortwave radiation	W/m²	Type T Thermopiles	Eppley Laboratory	PSP	+/- 3.0% @ 1 kW/m²	100 ft (33 m) level at 3 ft (1 m) from 1 ft (0.3 m) diameter tower; body shaded from direct sun, downward looking
Solar Tracker: Cavity radiometer Direct Beam and downwelling longwave shade disk	n/a	Stepping motor drive	BRUSAG	INTRA	+/- 0.2° per day	autonomous, self correcting based on quad Silicon solar sensor input on clear days
Aerosol Optical Depth	n/a	filtered silicon cell sunphoto-meter(*)	CIMEL Electronique	CE-318	+/- 0.01 OD	Wavelengths at 340, 380,440,500,670,870,1020 nm. Autonomous collection at 0.5 air mass intervals. Real time collection via METEOSAT at NASA Langley

Figure 8.5 on the next page is a plot of the additional BSRN instrumentation data for March 2-3, 1999. The BSRN all weather cavity data, up- and down-welling longwave radiation, and upwelling (reflected) shortwave radiation are shown. Vertical lines associated with the cavity radiometer data are where the cavity radiometer is programmed to perform electrical calibrations. Figure 8.6 shows the June 1999 downwelling infrared radiation at the KACST Solar Village BSRN site compared with the same measurement made at the NREL Solar Radiation Research Laboratory at Golden, Colorado.

Figure 8.4. Tower installation for upwelling shortwave and longwave radiometers. Radiometers mounted on cross arms (inside circle) at 30 m above ground.

46
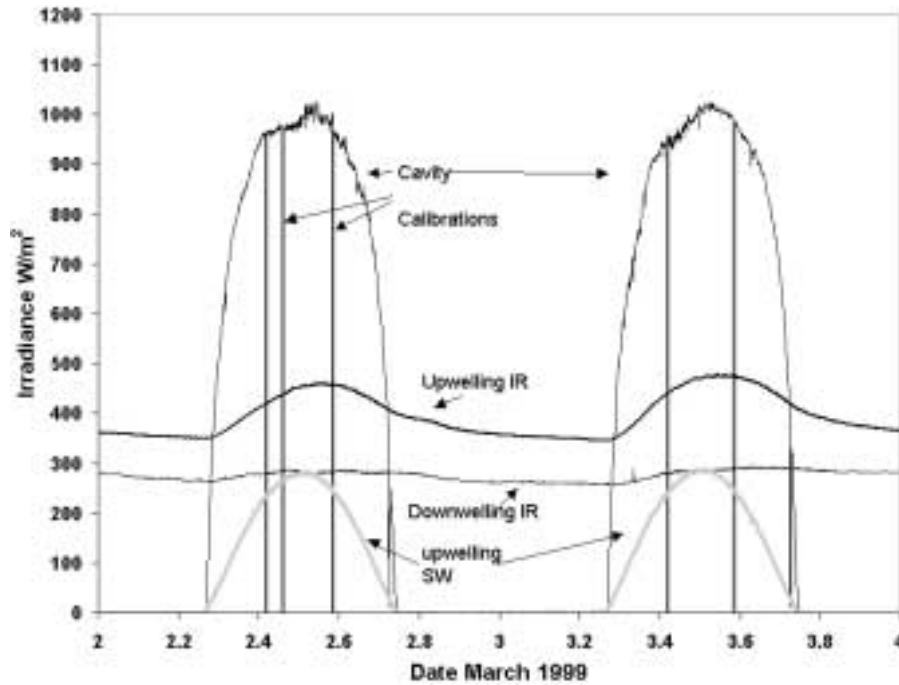
Figure 8.5. Plot of BSRN data for all-weather cavity radiometer (direct beam), up-and downwelling longwave (infrared) and upwelling (reflected) shortwave radiation for March 2-3, 1999, at the Solar Village
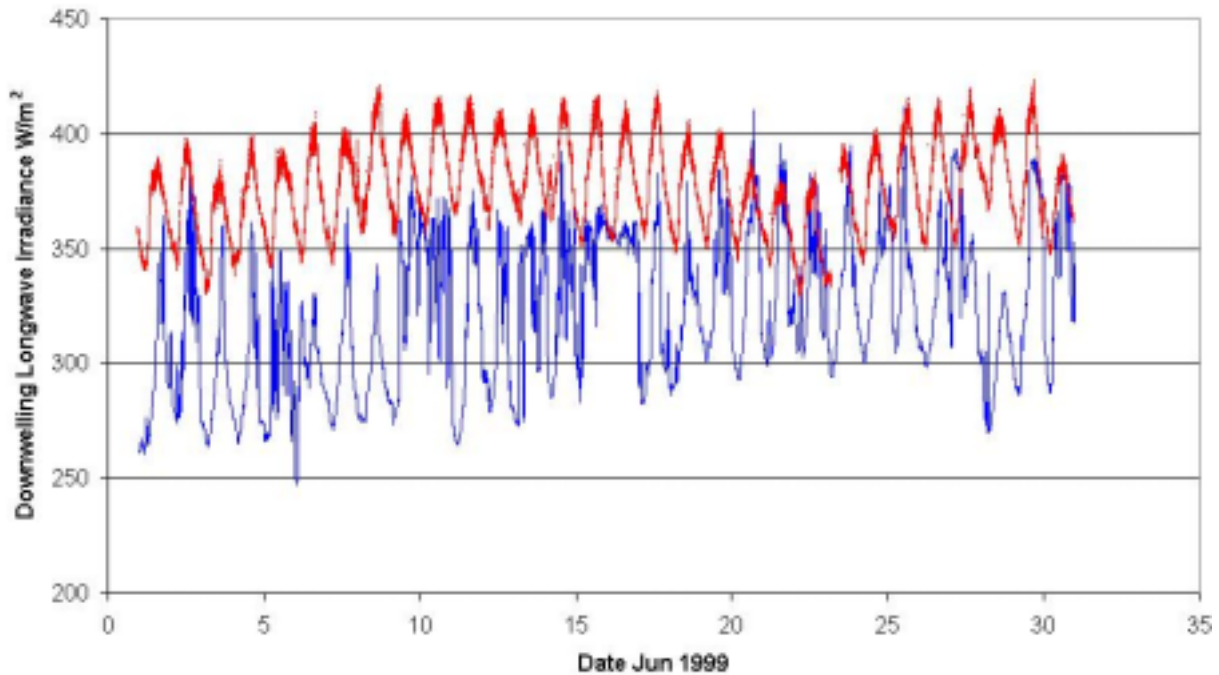
Figure 8.6. Comparison of downwelling infrared radiation at the KACST Solar Village (top curve) and at the NREL (bottom curve) Solar Radiation Research Laboratory at Golden, Colorado, for the month of June 1999.
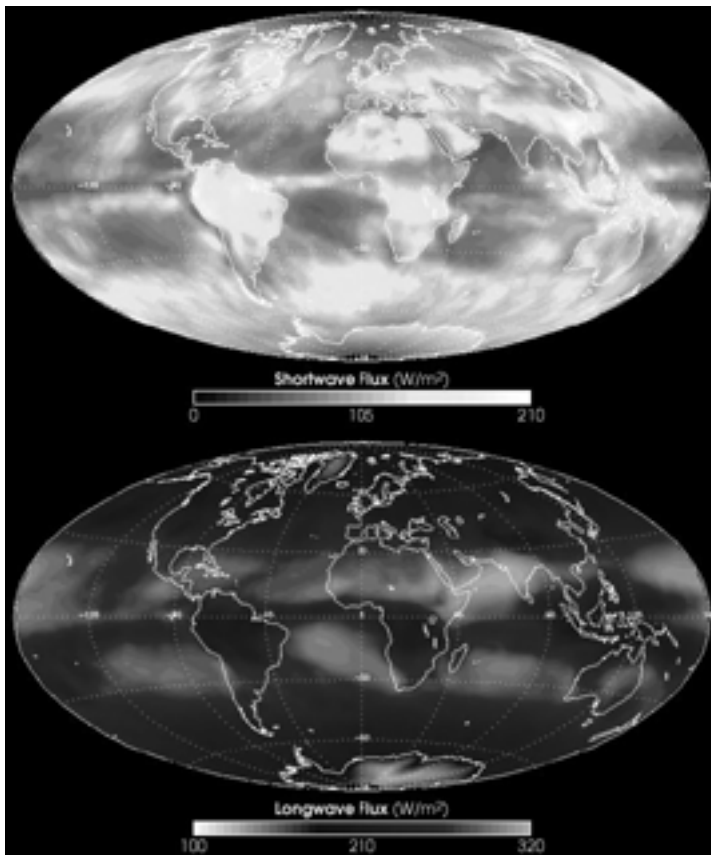
These measurements will provide significant ground truth data for comparison with the orbiting NASA sensors, which can be used to derive global radiation fluxes as shown in Figure 8.7. On-board satellite calibrations and ground-based measurements of these fluxes can be used to produce more accurate quantitative values for the satellite-derived data.

Figure 8.7. Shortwave and longwave fluxes for March 2000, derived from NASA Terra satellite sensor for the Clouds and Earth Radiant Energy Sensor (CERES) instrument.

8.2 Ultraviolet Measurements at the Solar Village

In addition to the BSRN instrumentation described above, the project also purchased three new instruments to measure the ultraviolet energy at the Solar Village site. NREL assisted with the specification and selection of the instrumentation, and performed calibrations for the instruments before shipment to KACST. Figure 8.8 depicts the three instruments. The instruments selected were an Eppley Laboratories Total Ultraviolet Radiometer (TUVR), a Yankee Environmental Systems (YES) Ultraviolet B (UVB) pyranometer, and an EKO Instruments Ultraviolet A (UVA) pyranometer. Figure 8.9 shows the nominal measurement passbands for the three instruments in relation to the spectroradiometric measurement of the outdoor solar ultraviolet during the NREL calibrations. As figure 8.9 shows, the three units were selected to provide overlapping coverage of the three UV spectral regions, UV-A (315 nm to 385 nm), UV-B (285 nm to 315 nm) and the so-called "total UV" (285 nm to 385 nm) commonly measured with the TUVR.

48

Figure 8.8. Ultraviolet Instruments purchased by KACST, calibrated by NREL, and installed at the Solar Village measurement station. Left to right: Eplab Total Ultraviolet Radiometer (TUVR), Yankee Environmental Systems UV-B, EKO instruments UV-B.
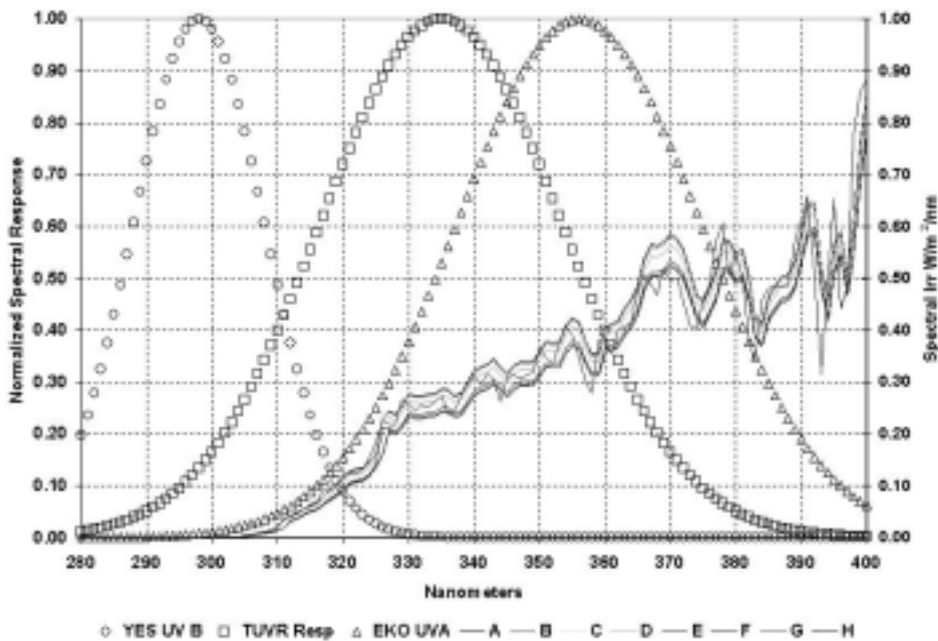
Figure 8.9. Nominal spectral response curves (symbols) for the three UV radiometers purchased by KACST, calibrated by NREL, and installed at the Solar Village station in 2000. The lines show spectroradiometric measurements of the solar UV during the NREL calibrations of the radiometers.

The radiometers were calibrated using an Optronic Laboratories OL-754 UV spectrometer to measure the spectral distribution of the solar radiation while the millivolt output of the radiometers was recorded. The spectrometer data were then integrated over the passband appropriate for the specific radiometer. The calibration data were taken Dec 9, 1999. The results are shown in table 8.2.

49

Table 8.2. Ultraviolet radiometer calibration data and results at NREL, Dec 9, 1999.

Spectral Scan	OL-754 SPECTRAL INTEGRAL W/m²			TEST UNIT mV DATA			CAL FACTOR W/m²/mV		
	UVB 280-315	UVA 315-385	TUVR 285-385	TMET	EKO	YES	TUVR TMET	UVA EKO	UVB YES
A	0.321	25.237	25.494	3.138	3.379	444.000	8.124	7.469	7.222E-04
B	0.313	24.981	25.232	3.097	3.338	433.900	8.147	7.484	7.220E-04
C	0.298	24.258	24.496	3.066	3.299	423.300	7.990	7.353	7.043E-04
D	0.293	24.090	24.324	3.031	3.262	408.000	8.025	7.385	7.180E-04
E	0.315	23.404	23.658	2.884	3.114	369.700	8.203	7.516	8.532E-04
F	0.238	22.556	22.744	2.852	3.078	357.600	7.975	7.328	6.669E-04
G	0.232	22.134	22.317	2.806	3.029	347.300	7.953	7.307	6.689E-04
H	0.228	21.952	22.131	2.773	3.003	341.200	7.981	7.310	6.694E-04
						Average	8.050	7.394	7.156E-04
						Std. Dev.	0.094	0.084	6.075E-05

These results are typical for outdoor calibrations of UV radiometers. The UVA and UVB radiometers produce a relatively low signal to noise ratio, so the standard deviation of the mean calibration factor for them is about 10%, while the broader band UVA and TUVR standard deviations are on the order of 2%.

8.3 NASA AERONET Sunphotometer at the Solar Village

NASA/EOS investigators were interested in measuring the aerosol optical depths in a desert environment, so provided the loan of a CIMEL (Cimel Electronique 172, rue de Charonne 75011 Paris, France) C-318 sunphotometer to KACST for direct aerosol optical depth and precipitable water vapor measurements. Figure 8.10 shows the instrument as installed on the Solar Village calibration facility roof. Data are collected periodically and transmitted via satellite to the Aeronet data processing site at Goddard Space Flight Center in Greenbelt Maryland [33].

Figure 8.10. CIMEL C-318 Sunphotometer (lower right) as installed on Solar Village Calibration facility roof.

Data have been collected and archived since October 1998, and are available at the NASA Aeronet internet site at **http://aeronet.gsfc.nasa.gov:8080/.**

Figure 8.11 shows the Solar Village data for June 2000, as presented on the Aeronet Internet site. The CIMEL instrument provided NREL and KACST with an opportunity to evaluate estimation techniques for aerosol optical depth and water vapor content by comparing our estimates with the sunphotometer measurements.
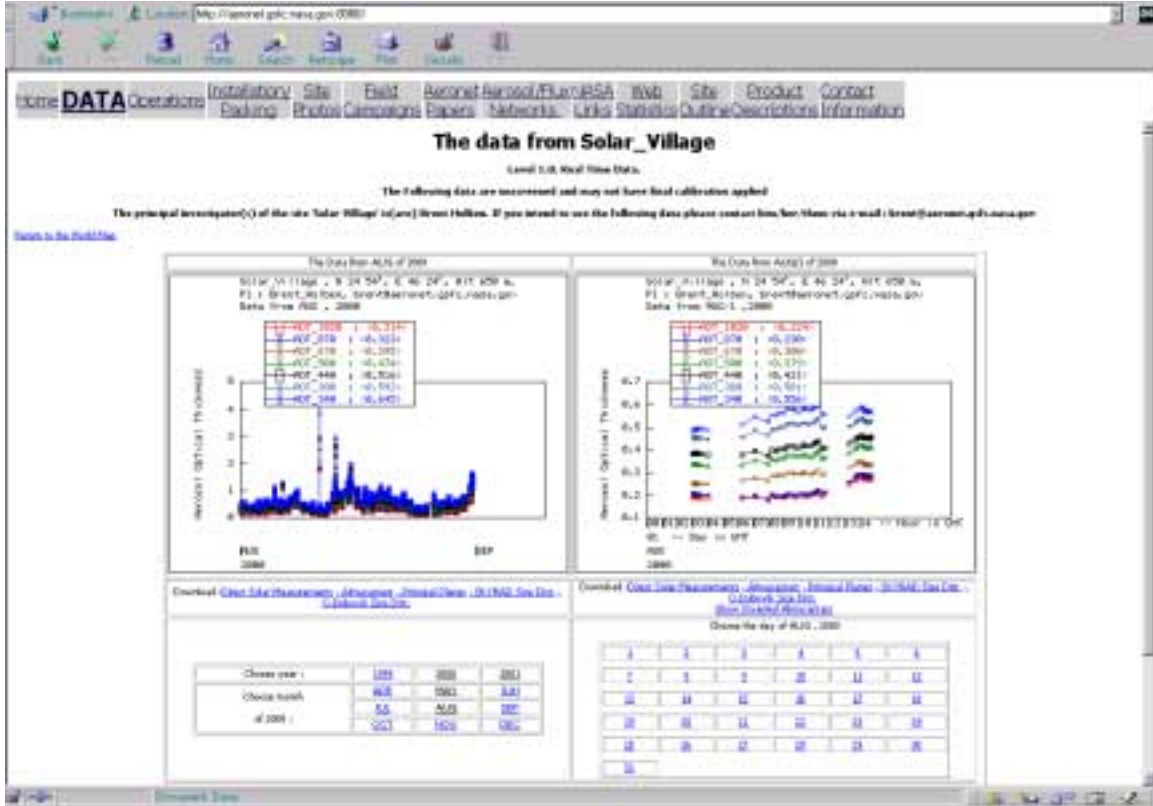
Figure 8.11. KACST Solar Village aerosol optical depth data presented on the Aeronet Internet site.

This validation of the estimation techniques is valuable for two reasons. First, it validates the techniques used to estimate solar radiation using NREL's METSTAT model for developing solar radiation databases from meteorological and available measured solar radiation (see Section 9.0 below). Secondly, our estimation techniques can then be used to compute aerosol optical depths from ground-based data to compare with NASA/EOS Terra based derived optical depths.

Figures 8.12 and 8.13 show the correlation between one month (March 2000) of the Solar Village quality assured sunphotometer measurements and NREL estimates of aerosol optical depth (AOD) and total precipitable water vapor. The correlation of NREL AOD estimates with the NASA measurements is better than 0.96. The correlation between total water vapor estimates is low (0.4), since the "signal" for water vapor at the Solar Village station is low (less than 2.5 cm). However, the linear relationship between the two measurements and estimates has a slope within 0.8% of unity.
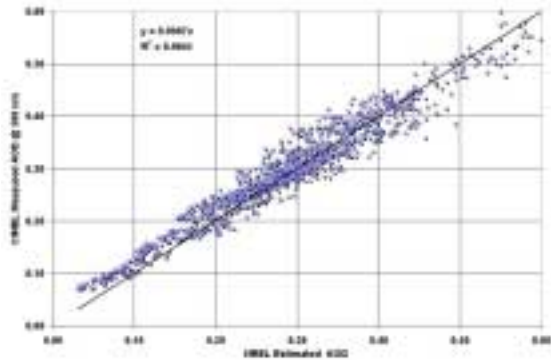
Figure 8.12. Correlation of NREL and CIMEL estimates of AOD.
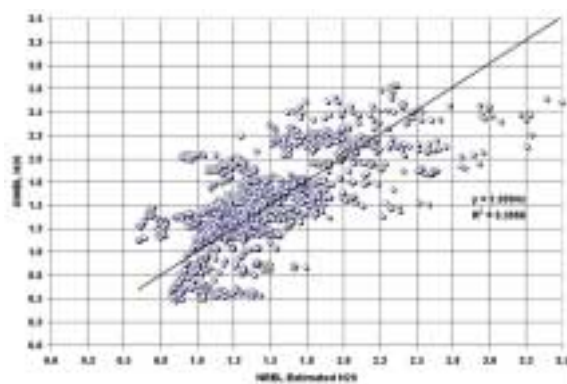
Figure 8.13. Correlation of NREL and CIMEL estimates of total water vapor.

Figure 8.14 is a histogram of the differences between the NREL- and CIMEL-based estimates of AOD, showing that the mean difference is 0.01 optical depths (OD); and 98% of the NREL estimates are within 0.05 in OD. Most measured optical depths are considered very accurate if they have uncertainty of 0.03 OD or less.
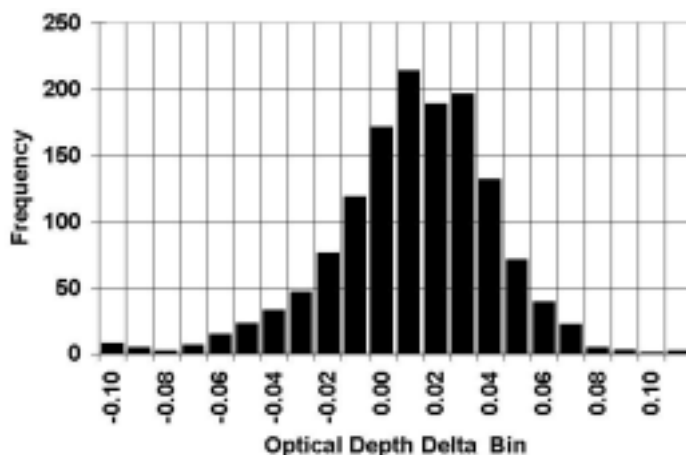
Figure 8.14. Histogram of differences between CIMEL measurements and NREL estimates of aerosol optical depth for March 2000.

These results improve our confidence in the application of the NREL estimation techniques used in METSTAT modeling of solar radiation for database development purposes described below.

9.0 Developing a Solar Radiation Database for Saudi Arabia

An important objective for the Annex II project was the development of the capability for KACST to generate a long-term solar radiation database (SRDB) for their country. The first requirement in developing a SRDB is the vision for the applications. The applications should determine what data are available in the SRDB.

9.1 Design of the Solar Radiation Database

9.1.1 Applications

Based on our experience with the 1961-1990 US National SRDB, KACST was encouraged to consider that applications require a data set with the following properties:

(1) Contain data pertinent to the application envisioned,

(2) Is serially complete, with no missing data or data gaps in the periods of record,

(3) Is of a duration or period long enough to capture and faithfully represent monthly, seasonal, annual, and long term (ten to 30 year or more) variation in the data,

(4) Is suitable as input, perhaps with some format changes, into simulation software to simulate various time frames from 1 day to multiple years with hourly resolution, and

(5) Is of known uncertainty,

(6) Is well documented, and

(7) Is easy to access, interpret, and include in research activities.

Applications foreseen included:

Design, performance evaluation, and simulation for photovoltaic (PV) energy conversion systems. Besides converting radiation resources, these systems are spectrally sensitive and knowledge of atmospheric parameters affecting spectral distributions are important.

Design and performance of solar thermal energy conversion systems.

Building energy system balancing, design, and performance. Radiation and environmental loads are important in energy analysis and requirements for modern buildings.

Alternatives to energy intensive building infrastructures: daylighting, passive solar cooling and heating, and other energy conservation techniques applied to building design.

Investigation of long term climate change and earth radiation budget balances. Repetitive updating of long-term databases may be helpful in investigating climate trends in terms of radiation balance and meteorological parameters.

Investigation of environmental parameters associated with agricultural and medical issues: human and plant interactions with solar radiation (evapo-transporation models, Photosynthetic ally Active Radiation -PAR-, medical problems such as human and animal skin aging, cancer, and deterioration).

9.1.2 Database Components

Based on the possible areas of application, the minimum data requirements recognized as meeting the needs of these diverse interests are shown in Table 9.1. These constituents are for the most part measured parameters. The elements in Table 1 represent a merging of typical meteorological data and routinely measured solar radiation data as well as some derived components, (marked with * in the table) discussed below.

Table 9.1. Solar Radiation Database Minimal Contents

Data Element	Comments
Global (horizontal surface)	Building Loads, Daylighting, conversion model input
Direct Beam Irradiance	Thermal and PV Concentrator technology
Diffuse (horizontal surface)	Daylighting, Flat plate vs. Concentrator technology
Ambient Temperature	Heating/cooling loads, PV system sensitivities
Barometric Pressure	Bulk atmospheric tranmisttance, Air Mass corrections
Wind Speed	Building heat transfer, Hybrid (PV/WIND) systems
Wind Direction	As above
Relative Humidity	Spectral impacts on PV; heating loads
Total Column Water Vapor (*)	Spectral impact on PV; heating loads
Turbidity/Optical Depth(*)	Spectral impact Direct beam key input for spectral modeling
Total Cloud Cover	Overall resource availability
Opaque Cloud Cover	Translucent and opaque transmission properties vary

9.1.3 Database Station Selection

In light of the applications desired, and the availability of data, a selection of database stations is required. The 12 stations of the Saudi solar radiation-monitoring network were

carefully selected to represent the variety of environments encountered in the kingdom. They are obvious candidates for database stations.

There is much wider distribution of MEPA meteorological sites at which synoptic (periodic daily) meteorological observations are recorded, and agricultural measurement stations the measure radiation for estimating evapo-transpiration and other radiation dependant parameters important to crops. NREL suggests these stations could also be included in the database, despite the lack of measured solar radiation data, since solar radiation estimates can be generated for these stations, if suitable input data exist. NREL acquired a complete set of DATSAV2 [34] data covering the period from 1973 to 2000, as part of other DOE renewable energy programs. The DATSAV2 surface meteorological database provides a means for expanding the number of station locations and to provide multi-year data sets of hourly solar radiation and meteorological data. DATSAV2 data are surface weather observations archived by the U.S. Air Force. Worldwide, there are more than 20,000 DATSAV2 stations. The locations of these stations are shown in Figure 9.1. Not all of the stations will have the quantity or quality of data needed for solar radiation modeling, but many of them will have acceptable data. The Annex II project extracted data for all Saudi MEPA stations and evaluated the period of record and quality of the data for each of the stations in the Saudi data set.
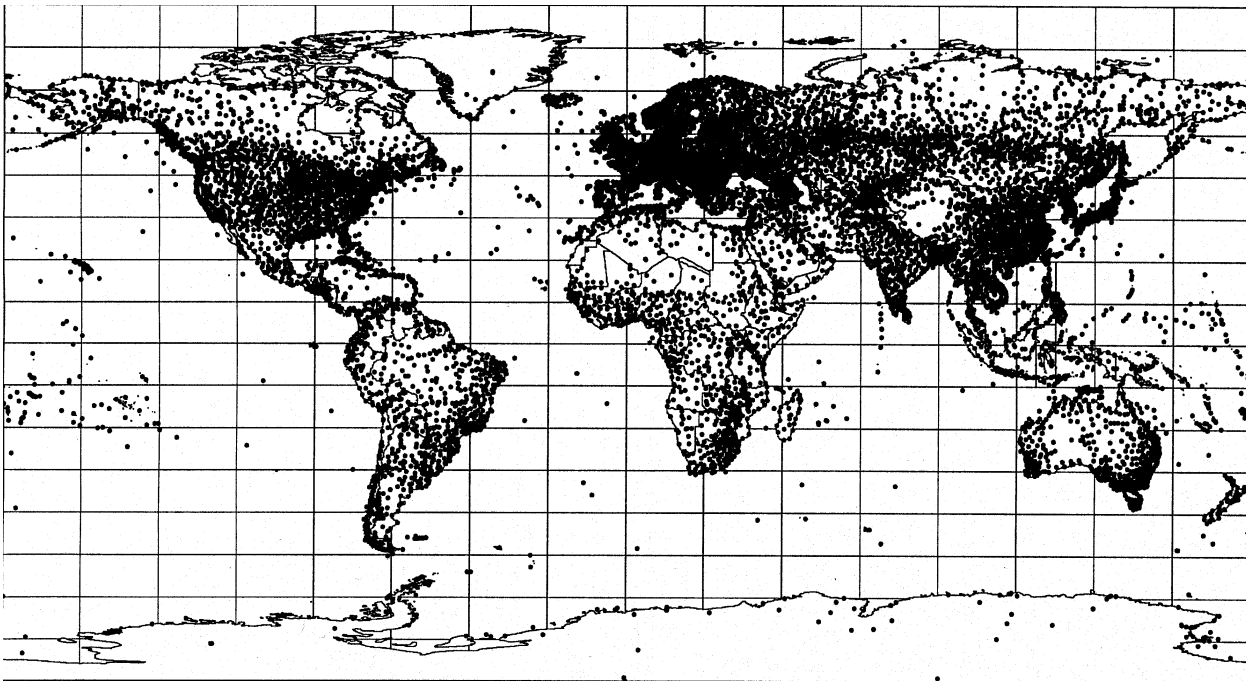
Figure 9.1. Distribution of DATSAV2 surface meteorological stations.

Table 9.2 summarizes the assessment of the stations in the Saudi DATSAV2 data set. Table 9.3 is a filtered version of Table 9.2, where only stations with more than 10 years of high quality data have been identified.

From the original DATSAV2 files, data fields of interest were extracted from the data tapes and transferred to CD-ROM. For each station, there exist two files of hourly data, one with the file extension .TXT and the other with the file extension .ADD. Tables 9.4 and 9.5 describe the elements contained in these comma-separated files. These data structures were provided to KACST for possible use as input to a database generating process.

Three programs were used to process data and model solar radiation. Data gaps greater than 8 hours are not filled; consequently, data files created are not serially complete. Depending on the location of the input data, small editing changes were required to run the programs. Output formats are specified in the comment sections of the programs. The programs developed were working versions subject to change as improvements are incorporated.

SA_DATS1.C: This program calculated quality assessment information by month for about 70 parameters to indicate sources and quantities of good input data for daylight hours. This information is written to files named p_xxxxxx.dat where xxxxxx is the station number. Using Grapher's (Golden Software) automated scriptor, these data may be quickly graphed for ease of interpretation. The program creates a file z_xxxxxx.his that contains the date when the station location is initiated and dates when changes in location occur. The program creates a file z_xxxxxx.cld that has the number and average cloud amount by cloud layer and type classification. These data are used in SA_DATS3.C for calculating opaque cloud cover.

SA_DATS3.C_:_ This program creates a file z_xxxxxx.inp for input to the solar radiation modeling program SA_MSDRV.C. Data gaps up to 8 hours are filled by linear interpretation. The longitude sign is changed to conform to NSRDB convention (west negative).

SA_MSDRV.C: This is the driver program that reads the input file created by SA_DATS3.C and calls METSTAT2.C to model solar radiation. Hourly solar radiation and meteorological data are output to file z_xxxxxx.dat. Calculates hourly water vapor from dew point temperature and daily aerosol optical depth from sine function relationship. Aerosol function coefficients, monthly albedos, and terrain factor are read from an independent file.

Table 9.2. DATSAV2 stations for Saudi Arabia with daytime Cloud Cover and Meteorological Observation interval and estimated total and sequential years of observations with sufficient quality data for solar radiation modeling.

WMO#	Station	Lat		Long		Elev	Cloud Obs. Interval	Met. Obs. Interval	Good Data	Sequential Good Data
		Deg	Min	Deg	Min	(m)	(hrs)	(hrs)	(yrs)	(yrs)
403560	TURAIF	31	41	-38	40	813	3	1.5	25	25
403570	ARAR	30	54	-41	8	552	3	1.5	25	25
403584	ARAR	30	54	-41	8	552	0	1.5	0	0
403600	GURIAT	31	25	-37	16	499	3	1.2	13	13
403610	AL-JOUF_(CIV/MIL)	29	47	-40	6	684	3	1.5	20	20
403620	RAFHA_(PRIVATE)	29	38	-43	29	447	3	1.5	25	25
403730	HAFR_AL-BATIN_ARPT	28	20	-46	7	355	3	1.5	20	20
403740	BOGUS_SAUDI_ARABIA	0	0	0	0	0	0	0	0	0
403750	TABUK_(SAUD-AFB)	28	22	-36	38	770	3	1.5	25	25
403760	TAYMA_(AUT)	27	36	-38	36	860	0	3	0	0
403770	KING_KHALID_MIL_CTY	27	54	-45	32	413	6	2	7	7
403800	AL-KHAFJI_(AUT)	28	24	-48	30	8	0	0	0	0
403940	HAIL	27	26	-41	41	1013	3	1.2	20	20
403950	AN_NU_AYRIYAH	27	28	-48	27	55	10	10	0	0
404000	WEJH	26	12	-36	28	16	3	1.2	20	20
404050	GASSIM	26	18	-43	46	650	3	1.5	25	18
404100	KHAYBER	25	42	-39	12	754	6	6	5	5
404160	DHAHRAN_INTL_(MIL)	26	16	-50	9	17	3	1.2	30	25
404184	AL-HASA	25	24	-49	29	178	0	1.2	0	0
404190	DAMMAM_(AUT)	26	24	-50	6	10	0	3	0	0
404200	AL_AHSA	25	17	-49	29	172	3	1.5	16	16
404210	HUFUF_(AUT)	25	18	-49	42	151	0	4	0	0
404300	MADINAH_INTL_ARPT	24	33	-39	42	631	3	1.2	25	25
404320	UQLAT_AS_SUQUR(AUT)	25	48	-42	0	783	0	4	0	0
404350	DAWADMI	24	30	-44	24	990	10	10	0	0
404370	RIYADH/KING_KHALID	24	56	-46	43	612	3	1.2	15	15
404375	KING_KHALID_MIL_CTY	27	54	-45	32	413	0	1.5	0	0
404380	RIYADH_(SAUD-AFB)	24	43	-46	43	612	3	1.2	25	25
404384	AL_AHSA	25	17	-49	29	172	0	0	0	0
404390	YENBO	24	9	-38	4	1	3	1.5	20	20
404400	YANBU_(AUT)	24	0	-38	12	11	0	0	0	0
404450	AL-KHARJ_(AUT)	24	12	-47	18	439	3	3	5	5
404500	AL-KHUSARIA_(AUT)	23	42	-44	36	1080	0	3	0	0
404540	OBAYLAH	22	0	-49	55	150	0	0	0	0
404560	SHAWALAH	22	20	-54	0	50	10	10	0	0
404760	JEDDAH/ABUL_AZIZ	21	40	-39	9	8	3	1.5	1	1
404770	JEDDAH_INTL	21	30	-39	12	11	3	3	15	10
404800	TAIF/AT_TAIF	21	29	-40	32	1457	3	1.5	6	6
404950	SULAYEL/ASSULAYYIL	20	28	-45	40	612	3	1.5	5	5
404980	BISHA	19	58	-42	40	1161	3	2	7	7
405690	KHAMIS_MUSHAIT/ABHA	18	18	-42	48	2057	3	2	7	7
405710	SHARORAH	17	20	-47	10	900	0	3	0	0
405720	GEZAN/GIZAN	16	52	-42	35	3	3	1.5	5	5
410060	MUWAIH	22	43	-41	37	970	0	0	0	0
410100	LAYLA_(AUT)	22	18	-46	42	543	0	3	0	0
410140	OBAYLAH_(AUT)	22	13	-50	53	588	0	0	0	0
410160	SHAWALAH_(AUT)	22	20	-54	0	468	0	0	0	0
410200	JEDDAH/I.E._(AUT)	21	24	-39	12	10	0	0	0	0
410240	JEDDAH/KING_ABDUL	21	40	-39	9	12	3	1	16	16
410260	JEDDAH	21	30	-39	12	15	3	1.5	1	1
410300	MAKKAH/MECCA	21	29	-39	50	310	3	1.5	14	14
410350	AL-HADA_(AUT)	21	18	-40	18	2089	0	6	0	0
410360	TAIF_(CIV/MIL)	21	29	-40	33	1449	3	1.5	16	16
410550	AL_BAHA	20	18	-41	38	1656	3	1.5	16	16
410610	WADI_AL_DAWASER	20	30	-45	12	617	3	1.5	8	8
410620	SULAYEL	20	28	-45	37	609	3	3	7	7
410800	AL-QUNFUDAH(AUT)	19	6	-41	12	1	0	6	0	0
410840	BISHA_(CIV/MIL)	19	59	-42	37	1157	3	1.5	16	16
411120	ABHA	18	14	-42	39	2084	3	1.5	16	16
411140	KHAMIS_MUSHAIT_AFB	18	18	-42	48	2054	3	1.5	16	16
411280	NEJRAN	17	37	-44	26	1203	3	1.5	16	16
411360	SHARURAH_(CIV/MIL)	17	28	-47	7	722	3	2	15	15
411363	SHARURAH_(CIV/MIL)	17	28	-47	7	722	0	2	0	0
411400	GIZAN	16	54	-42	35	3	3	1.5	16	16
411410	GIZAN(AUT)	16	54	-42	30	6	3	3	1	1

Table 9.3. Reordering of Table 9.2 from greatest to least years of sequential good data for stations with a minimum of 10 years of sequential good data. Stations with an asterisk (*) are co-located with a solar monitoring network station (Wadi Al-Dawaser is not included because DATSAV2 data began in 1990.)

WMO#	Station	Latitude		Longitude		Elev	Cloud Obs. Interval	Met. Obs. Interval	Good Data	Sequential Good Data
		Deg	Min	Deg	Min	(m)	(hrs)	(hrs)	(yrs)	(yrs)
404380*	RIYADH_(SAUD-AFB)	24	43	-46	43	612	3	1.2	25	25
404300*	MADINAH_INTL_ARPT	24	33	-39	42	631	3	1.2	25	25
404160	DHAHRAN_INTL_(MIL)	26	16	-50	9	17	3	1.2	30	25
403750*	TABUK_(SAUD-AFB)	28	22	-36	38	770	3	1.5	25	25
403620	RAFHA_(PRIVATE)	29	38	-43	29	447	3	1.5	25	25
403570	ARAR	30	54	-41	8	552	3	1.5	25	25
403560	TURAIF	31	41	-38	40	813	3	1.5	25	25
404390	YENBO	24	9	-38	4	1	3	1.5	20	20
404000	WEJH	26	12	-36	28	16	3	1.2	20	20
403940	HAIL	27	26	-41	41	1013	3	1.2	20	20
403730*	HAFR_AL-BATIN_ARPT	28	20	-46	7	355	3	1.5	20	20
403610*	AL-JOUF_(CIV/MIL)	29	47	-40	6	684	3	1.5	20	20
404050*	GASSIM	26	18	-43	46	650	3	1.5	25	18
411400*	GIZAN	16	54	-42	35	3	3	1.5	16	16
411280	NEJRAN	17	37	-44	26	1203	3	1.5	16	16
411140	KHAMIS_MUSHAIT_AFB	18	18	-42	48	2054	3	1.5	16	16
411120*	ABHA	18	14	-42	39	2084	3	1.5	16	16
410840	BISHA_(CIV/MIL)	19	59	-42	37	1157	3	1.5	16	16
410550	AL_BAHA	20	18	-41	38	1656	3	1.5	16	16
410360	TAIF_(CIV/MIL)	21	29	-40	33	1449	3	1.5	16	16
410240*	JEDDAH/KING_ABDUL	21	40	-39	9	12	3	1.2	16	16
404200*	AL_AHSA	25	17	-49	29	172	3	1.5	16	16
411360*	SHARURAH_(CIV/MIL)	17	28	-47	7	722	3	2	15	15
404370	RIYADH/KING_KHALID	24	56	-46	43	612	3	1.2	15	15
410300	MAKKAH/MECCA	21	29	-39	50	310	3	1.5	14	14
403600	GURIAT	31	25	-37	16	499	3	1.2	13	13
404770	JEDDAH_INTL	21	30	-39	12	11	3	3	15	10

Table 9.4. Format of NREL DATSAV2 Files with File Extension .TXT

Field No.	Description	Data Type	Units	Missing Data Value	DATSAV2 Field No.
1	Pseudo Station No.	Long integer			
2	Original Station No.	Long integer			
3	Greenwich Mean Time	Long integer	yyyymmddhh		
4	Latitude, north positive	Integer	ddmm		
5	Longitude, east negative	Integer	dddmm		
6	Elevation	Integer	m		
7	Wind direction	Integer	°	999	M01
8	Wind speed	Float	m/s	99.99	M02
9	Dry bulb temperature	Float	°K	999.9	M21
10	Sea level pressure	Float	Mb	9999.9	M23
11	Altimeter setting	Float	Inches	99.99	M26
12	Dew point temperature	Float	°K	999.9	M22
13	Observation type	Integer		15	C14
14	Cloud flag	Integer		15	M05
15	Total sky cover	Integer		15	M06
16	Low cloud amount	Integer	Octas	15	M07
17	Type of low cloud	Integer		15	M08
18	Type of middle cloud	Integer		15	M10
19	Type of high cloud	Integer		15	M11
20	Lowest cloud height	Integer		999	M09
21	Visibility	Long integer	M	999999	M12

Table 9.5. Format of NREL DATSAV2 Files with File Extension .ADD

Field No.	Description	Data Type	Units	Missing Data Value	DATSAV2 Field No.
1	Original Station No.	Long integer			
2	Greenwich Mean Time	Long integer	yyyymmddhhmm		
3	Observation type	Integer		99	C14
4	Type of automatic stn.	Integer		99	C27
5	Ceiling	Integer		999	M04
6	Present weather	Integer		999	M14
7	Present weather	Integer		999	M15
8	Present weather	Integer		999	M16
9	Present weather	Integer		999	M17
10	# additional data groups	Integer			
Varies	Additional data groups – Present weather, snow data, cloud layer data, state-of-ground	12 char. Per group			Group EA, CA,GA, & IA

9.2 The METSTAT Model

The DATSAV2 data are used for input to METSTAT, a solar radiation model developed by Maxwell [11] to model hourly solar radiation values for the 1961-1990 National Solar Radiation Database (NSRDB). Because the DATSAV2 data are slightly different than the input data used for the NSRDB, METSTAT was revised to accommodate the DATSAV2 data.

9.2.1 METSTAT Inputs and Requires Modifications

DATSAV2 does not include opaque sky cover, which is one of the inputs to the METSTAT solar radiation model. Consequently, opaque sky cover is determined as a function of the DATSAV2 amounts and types of low, middle, and high clouds present. The function was developed using coincident DATSAV2 and NSRDB data for the United States. (Results showed that low clouds are essentially opaque, middle clouds are 90% or greater opaque, and high clouds are 25%-60% opaque, depending on their type.)

The DATSAV2 present weather field was rarely reported after 1985. Present weather indicates the weather conditions for the hour and is used in METSTAT to reduce the diffuse radiation by 40% if rain occurs. It had previously been suggested that ceiling height, which is available from DATSAV2, might be a better indicator of a reduction in diffuse radiation [11]. Consequently, a step function based on ceiling height was developed to reduce diffuse radiation for overcast conditions. This eliminated the need for the present weather field and yielded a slight improvement in model performance.

With these modifications, all the needed model inputs for METSTAT are available from DATSAV2 and other existing data sources. Table 9.6 lists these model inputs. Besides the DATSAV2 elements described in Table 9.6, DATSAV2 includes wind speed and wind direction that is included in the processed solar radiation and meteorological hourly data sets.

Table 9.6. METSTAT Model Inputs and Their Source

Model Input Parameter	Source
Total sky cover	DATSAV2
Opaque sky cover	Calculated from DATSAV2 layered cloud cover amounts and types
Ceiling height	DATSAV2
Atmospheric pressure	Calculated from either DATSAV2 altimeter setting and station elevation, or DATSAV2 sea level pressure, dry bulb temperature, and station elevation
Precipitable water vapor	Calculated from DATSAV2 dew point temperature using equation by Wright et al. (1989)
Ozone	Calculated from day of year and station latitude and longitude using equation by Van Heuklon (1979)
Aerosol optical depth (AOD)	Calculated from sine function relationship (Maxwell, 1998) with the mean, amplitude, and phase angle estimated from AVHRR ($1°$ grid over water) and GADS (550 km grid over land) data
Albedo	Monthly averages from Canadian Center for Remote Sensing (280 km grid)

The data set for deriving the ceiling height function was the 1977-1980 solar radiation data for 28 U.S. stations (same stations as listed in Table 3-11 of NSRDB Volume 2). This data set played a major role in the original development of METSTAT. The hourly data were screened to exclude hours when global and direct were not measured or a quality assessment flag for these two elements was greater than 3.

The data were binned at various ceiling height intervals and for 8, 9, and 10 tenths opaque cloud covers. METSTAT was run using the binned data and with the precipitation switch turned off. METSTAT modeled diffuse was then compared with database diffuse values to determine which bins required a reduction in the modeled diffuse values. Based on mean-bias-error (MBE), bins with 8 and 9 tenths opaque cloud cover required no reduction. As expected, the amount of required reduction for 10 tenths opaque cloud cover increased with a decrease in ceiling height. The amount of reduction was determined using an iterative procedure to minimize the root-mean-square-error (RMSE) for each bin.

To implement in METSTAT, the precipitation switch variable, psw, is replaced by the ceiling height variable, cfactor, which is determined using the following code:

```
if( iopq > 9 )
        {
        if( mdat->ceiling <= 200 )
                cfactor = 0.56;
        else if( mdat->ceiling <= 400 )
                cfactor = 0.67;
        else if( mdat->ceiling <= 3000 )
                cfactor = 0.80;
        else
                cfactor = 1.00;
        }
else
        cfactor = 1.00;
```

where:

    iopq   = opaque cloud cover in tenths
    mdat->ceiling = ceiling height in meters

Using the 1977-1980 data for the 28 stations, three versions of METSTAT were compared for modeling global and diffuse horizontal radiation. These versions are:

METSTAT – Original version as used for the NSRDB

METSTAT w/Vignola – Revised to include Vignola's ASES 1997 recommendations to eliminate the procedure that modifies the random number for consecutive hours of cloudy or clear hours and that changes the value of cvsopq from 0.05 to 0.10.

METSTAT w/Vignola and cfactor– Revised to include Vignola's ASES 1997 recommendations and replaces the precipitation switch with the ceiling height step function.

The modeling was performed with the "statistics on" for all models and the precipitation switch operable for the METSTAT and the METSTAT w/Vignola models. The Vignola change for cvsopq resulted in numerous negative kd and kt errors. Restricting the ksopq values to non-negative numbers with the conditional statement eliminated these errors:

```
if( ksopq < 0.0 )
        ksopq = 0.0;
```

Gueymard originally proposed this fix for kd and kt errors he observed at high air mass. However, in his implementation he located it prior to where ksopq is modified by cvsopq and other terms. It should be located after the point of modification.

Table 9.7 compares MBEs for modeling diffuse horizontal radiation for opaque cloud cover values of 8, 9, and 10 tenths. The use of the ceiling height function reduced the bias error by up to 30% over the original version of METSTAT. Because the cfactors were derived from the evaluation data set, MBEs close to zero for this method are not unexpected. However, it should be noted that the cfactors are not applied for opaque cloud cover values other than 10 tenths, yet the MBE for opaque cloud covers of 8, 9, and 10 tenths remained near zero for this method.

Table 9.7. MBE (%) by Model Revision for Diffuse Horizontal Radiation

Opaque Cloud Cover (tenths)	Number of Hourly Values	METSTAT	METSTAT w/Vignola	METSTAT w/Vignola and cfactor
8, 9, or 10	20,342	12.5	6.5	0.2
10	11,651	29.8	16.6	0.6

Table 9.8 presents results using modeled and measured four-year monthly average solar radiation for the 28 stations for all opaque cloud cover values. Only monthly averages based on a minimum of 200 hours were used to determine the statistics. For example, if there were less than 200 hours of data meeting the quality assessment criteria from the Januarys of 1977, 1978, 1979, and 1980 for Boulder, then a January average monthly value for Boulder was not used in determining the statistics.

When the models are run for all hours in the data set, their statistics are comparable. The primary advantage of the revised METSTAT versions is the improvement for opaque cloud covers of 8 tenths or more, a situation where solar radiation values are low and they play a smaller role in determining the monthly average. Relative to the original METSTAT, the METSTAT version with the Vignola changes and the ceiling height function reduced the average global horizontal radiation by 1.7% and the average diffuse horizontal radiation by 4.2%.

Table 9.8. Statistics for the Differences of Modeled and Measured Four-Year Monthly Average Solar Radiation

Model	Element	Measured Average (Wh/m^2)	Statistics for Modeled Minus Measured Monthly Averages			
			Average Difference (Wh/m^2)	Standard Deviation (Wh/m^2)	Low Difference (Wh/m^2)	High Difference (Wh/m^2)
METSTAT	Global Hor.	454	5.0	21.1	-74.4	45.8
	Diffuse Hor.	153	5.5	17.8	-51.2	45.9
METSTAT w/Vignola	Global Hor.	454	0.7	20.0	-75.8	36.5
	Diffuse Hor.	153	2.4	17.4	-53.6	44.4
METSTAT w/Vignola and cfactor	Global Hor.	454	-2.8	19.5	-75.9	30.5
	Diffuse Hor.	153	-1.0	18.3	-50.8	44.4

Figure 9.2 shows the cumulative distribution functions (CDFs) for hourly diffuse horizontal for opaque cloud cover values of 10 tenths for all 28 stations. The METSTAT version with the Vignola changes and the ceiling height function has the CDF closest to that of the measured data.
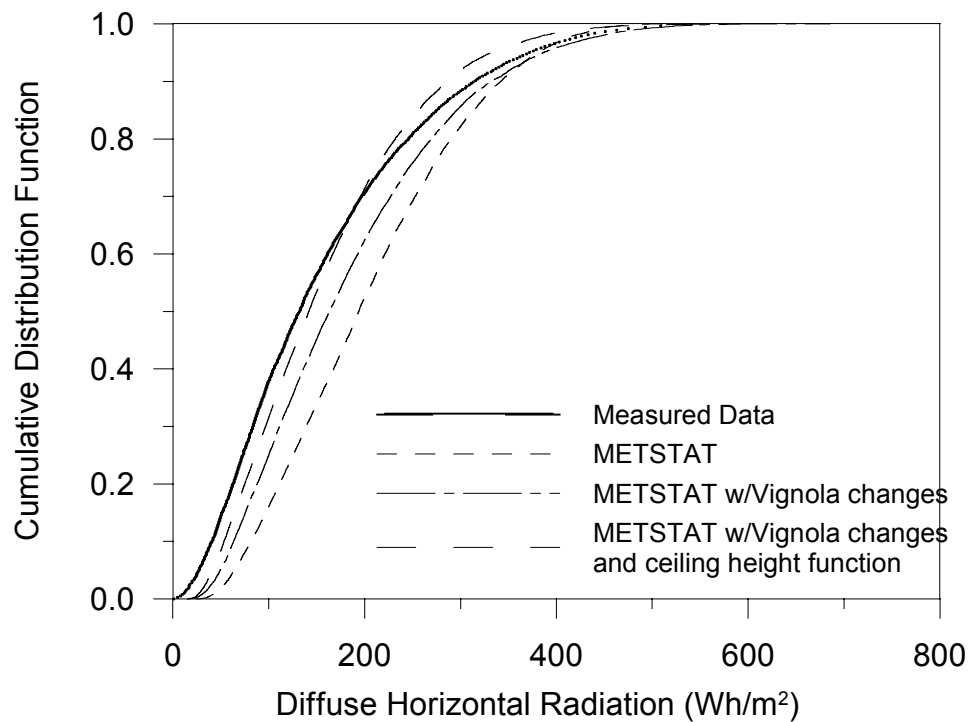
Figure 9.2. CDFs for hourly diffuse horizontal radiation for opaque cloud cover equal to 10 tenths.

9.2.2 Evaluating the METSTAT Model for Saudi Arabia

Measured and modeled daily values of global horizontal and direct normal radiation were compared for the period January 1996 to August 1998 for each of the Saudi network stations. Solar radiation for the same days were modeled using METSTAT with statistics

turned "ON" and with aerosol coefficients from the data grid. For reference only, the tables contain the number of present weather observations of smoke or volcanic ash, haze, and dust, duststorms, sand, and sandstorm. This information may be useful for determining the aerosol climate.

For two stations, Solar Village and Wadi Al-Dawser, their DATSAV2 station was 25-35 miles distant. However, this did not appear to adversely affect results. In general, the results were favorable with station overall MBEs of ±5% or less for global horizontal and ±10% or less for direct normal. Overall MBEs were higher for Gizan: +6% for global horizontal and +26% for direct normal. This may be a consequence of the aerosol input data, which were the lowest aerosol optical depths assigned to any of the stations. Also, errors in the measured data may have played a part. For all stations, calendar months showed larger errors, particularly for direct normal. Comparison of monthly measured and model results are displayed in tables 9.9-9.20

Table 9.9. MBEs and RMSEs for Solar Village

Month	Days of Data	Global Horizontal			Direct Normal			Number of Present Weather Observations Containing:		
		Ave. (kWh/ m^2/day)	MBE (%)	RMSE (%)	Ave. (kWh/ m^2/day)	MBE (%)	RMSE (%)	Smoke or Ash	Haze	Dust or Sand
Jan	81	4.01	4.0	14.2	5.69	-11.4	27.5	0	8	0
Feb	84	5.19	3.8	10.3	6.02	-0.7	28.3	0	3	7
Mar	84	5.47	7.3	16.9	4.69	6.7	40.6	0	7	38
Apr	81	6.83	4.4	10.2	6.25	-1.2	26.5	0	16	23
May	84	7.26	5.3	11.4	6.17	1.0	34.1	0	10	19
Jun	76	7.98	1.5	4.8	8.26	-14.5	25.0	0	4	3
Jul	82	7.62	4.7	7.4	7.31	-2.1	19.7	0	14	19
Aug	89	7.39	2.9	5.4	7.64	-8.5	22.7	0	14	13
Sep	59	6.70	4.7	7.6	7.35	-2.7	26.1	0	19	9
Oct	58	5.57	5.6	8.9	6.70	-1.3	21.3	0	11	4
Nov	51	3.96	6.5	15.0	4.71	-5.0	33.1	0	9	2
Dec	50	3.99	4.5	8.7	5.91	-8.4	24.7	0	3	0
All	879	6.13	4.4	9.9	6.43	-4.3	27.1	0	118	137

Table 9.10. MBEs and RMSEs for Al-Madinah

Month	Days of Data	Global Horizontal			Direct Normal			Number of Present Weather Observations Containing:		
		Ave. (kWh/ m^2/day)	MBE (%)	RMSE (%)	Ave. (kWh/ m^2/day)	MBE (%)	RMSE (%)	Smoke or Ash	Haze	Dust or Sand
Jan	76	4.42	-1.4	9.0	6.58	-11.1	21.9	0	0	7
Feb	72	5.58	-1.9	5.0	7.58	-9.9	20.3	0	0	22
Mar	79	6.18	0.1	12.0	6.73	-6.9	30.0	0	3	27
Apr	52	7.05	1.2	8.3	6.95	-0.9	26.1	0	0	46
May	34	6.79	5.8	13.1	5.48	5.0	33.7	0	0	15
Jun	9	7.24	5.2	7.5	5.72	12.0	15.9	0	0	0
Jul	23	7.07	4.7	10.0	6.25	-4.4	25.6	0	0	8
Aug	63	7.27	1.1	4.9	7.34	-9.6	22.5	0	0	19
Sep	48	6.46	3.9	6.8	6.46	3.6	25.2	0	0	18
Oct	54	5.61	1.9	6.7	6.84	-2.9	22.4	0	0	11
Nov	48	4.16	4.8	15.2	5.49	-4.5	27.5	0	2	5
Dec	57	3.92	4.5	12.0	5.69	-1.2	23.1	0	0	8
All	615	5.77	1.7	9.3	6.58	-4.9	24.8	0	5	186

Table 9.11. MBEs and RMSEs for Tabouk

Month	Days of Data	Global Horizontal			Direct Normal			Number of Present Weather Observations Containing:		
		Ave. (kWh/ m^2/day)	MBE (%)	RMSE (%)	Ave. (kWh/ m^2/day)	MBE (%)	RMSE (%)	Smoke or Ash	Haze	Dust or Sand
Jan	43	3.93	-2.1	10.2	6.26	-15.8	27.8	0	20	4
Feb	40	5.04	-1.6	6.1	6.89	-7.6	26.9	0	13	19
Mar	17	5.19	2.5	16.3	4.94	4.3	40.1	0	4	10
Apr	18	7.26	-1.5	4.6	7.46	-1.2	20.0	0	5	12
May	26	7.26	0.5	6.7	6.63	-5.1	20.1	0	9	7
Jun	34	8.16	0.1	3.8	9.33	-13.5	19.0	0	5	1
Jul	30	7.86	0.8	4.4	8.80	-13.4	20.8	0	7	2
Aug	50	7.35	3.2	5.3	8.25	-5.3	18.6	0	2	2
Sep	11	6.29	2.7	5.7	6.60	6.6	26.4	0	8	1
Oct	25	5.17	-2.0	6.4	6.84	-17.0	26.2	0	7	7
Nov	32	3.96	-4.6	9.9	5.46	-20.5	28.8	0	21	2
Dec	33	3.65	-2.7	10.5	6.21	-19.0	31.0	0	13	2
All	359	5.86	-0.1	6.9	7.11	-10.5	24.2	0	114	69

Table 9.12. MBEs and RMSEs for Al-Jouf

Month	Days of Data	Global Horizontal			Direct Normal			Number of Present Weather Observations Containing:		
		Ave. (kWh/ m^2/day)	MBE (%)	RMSE (%)	Ave. (kWh/ m^2/day)	MBE (%)	RMSE (%)	Smoke or Ash	Haze	Dust or Sand
Jan	70	3.50	1.7	10.7	5.20	-7.2	23.2	0	1	4
Feb	64	4.77	1.0	6.8	6.43	-5.4	25.3	0	0	30
Mar	35	5.16	3.6	13.8	5.17	3.9	35.4	0	0	31
Apr	5	4.53	34.3	40.8	1.88	69.3	92.6	0	0	7
May	5	4.80	29.0	32.8	1.51	148.1	164.6	0	0	7
Jun	0									
Jul	2	6.69	17.8	17.8	4.31	61.1	63.6	0	0	4
Aug	2	6.51	6.4	12.2	4.58	21.9	34.7	0	0	0
Sep	6	5.68	11.8	12.4	4.83	53.9	62.5	0	1	13
Oct	53	5.02	4.0	7.9	6.31	-0.4	24.7	0	2	21
Nov	47	3.53	4.7	13.0	4.69	-7.2	29.4	0	0	12
Dec	56	3.31	2.3	9.0	5.17	-9.0	22.2	0	0	11
All	345	4.22	4.0	12.4	5.41	-2.3	28.2	0	4	140

Table 9.13. MBEs and RMSEs for Qassim

Month	Days of Data	Global Horizontal			Direct Normal			Number of Present Weather Observations Containing:		
		Ave. (kWh/ m^2/day)	MBE (%)	RMSE (%)	Ave. (kWh/ m^2/day)	MBE (%)	RMSE (%)	Smoke or Ash	Haze	Dust or Sand
Jan	72	3.88	3.6	10.4	5.42	-2.0	20.9	0	0	0
Feb	66	5.25	3.0	6.5	6.80	0.8	27.2	0	0	3
Mar	67	5.48	6.1	15.1	4.94	9.9	34.9	0	1	22
Apr	60	6.71	3.9	11.3	6.02	6.5	29.6	0	6	10
May	91	7.37	3.7	8.6	6.57	-0.7	26.1	0	1	16
Jun	88	8.01	3.1	5.3	8.25	-5.3	18.4	0	4	2
Jul	92	7.75	3.9	6.2	7.76	-4.6	21.7	0	0	6
Aug	83	7.30	4.6	5.9	7.56	-2.4	15.7	0	1	1
Sep	52	6.49	7.6	9.3	6.55	17.1	31.1	0	6	9
Oct	52	5.28	6.2	10.7	5.84	7.4	23.5	0	0	2
Nov	35	3.60	8.3	15.6	4.20	1.5	32.2	0	0	1
Dec	49	3.52	6.8	11.9	4.85	0.5	24.9	0	0	1
All	807	6.20	4.5	8.9	6.48	0.9	24.3	0	19	73

Table 9.14. MBEs and RMSEs for Gizan

Month	Days of Data	Global Horizontal			Direct Normal			Number of Present Weather Observations Containing:		
		Ave. (kWh/ m²/day)	MBE (%)	RMSE (%)	Ave. (kWh/ m²/day)	MBE (%)	RMSE (%)	Smoke or Ash	Haze	Dust or Sand
Jan	54	4.37	7.4	14.4	3.68	33.0	46.9	2	0	0
Feb	42	5.32	5.5	12.4	4.41	31.4	40.9	5	0	0
Mar	29	5.59	9.4	15.1	4.05	31.6	48.5	2	1	0
Apr	29	6.83	2.0	5.8	5.51	21.1	30.9	1	0	3
May	23	6.77	3.4	7.4	5.22	11.3	32.0	2	1	3
Jun	22	6.58	4.4	6.7	4.52	25.1	38.3	0	2	7
Jul	34	5.91	15.5	18.9	2.79	92.0	106.3	1	3	62
Aug	29	5.91	13.8	19.5	3.37	62.1	78.5	0	2	21
Sep	25	6.51	1.8	4.8	5.40	13.8	23.7	0	0	1
Oct	32	5.66	0.6	17.3	5.40	-3.6	31.0	0	0	0
Nov	26	4.87	3.6	14.7	4.62	17.6	35.0	0	0	2
Dec	25	4.65	1.0	12.1	4.96	10.1	29.2	0	0	2
All	370	5.62	6.0	13.4	4.39	26.3	43.9	13	9	101

Table 9.15. MBEs and RMSEs for Abha

Month	Days of Data	Global Horizontal			Direct Normal			Number of Present Weather Observations Containing:		
		Ave. (kWh/ m²/day)	MBE (%)	RMSE (%)	Ave. (kWh/ m²/day)	MBE (%)	RMSE (%)	Smoke or Ash	Haze	Dust or Sand
Jan	68	4.65	-3.7	14.7	5.39	-16.8	31.3	0	0	0
Feb	62	6.11	-7.2	10.9	7.73	-20.2	25.7	0	0	0
Mar	63	6.03	-1.7	17.5	6.21	-14.1	32.7	0	0	4
Apr	56	7.14	-3.1	12.3	7.14	-13.0	26.6	0	0	2
May	79	6.61	3.3	12.2	5.96	-9.8	25.9	0	0	2
Jun	78	6.64	5.4	13.0	5.74	-4.0	29.5	2	0	13
Jul	82	6.27	11.0	15.7	4.78	17.8	31.2	0	0	49
Aug	60	6.02	12.8	18.7	4.62	17.3	36.9	0	0	16
Sep	44	6.82	-0.4	6.3	6.93	-3.1	17.8	0	1	3
Oct	47	5.90	-1.3	13.9	6.85	-17.7	30.9	0	0	0
Nov	40	5.02	-3.0	11.3	6.39	-17.1	28.3	0	1	0
Dec	36	5.12	-6.8	9.2	7.39	-19.0	23.7	0	0	0
All	715	6.09	1.5	13.7	6.11	-8.5	28.6	2	2	89

Table 9.16. MBEs and RMSEs for Jeddah

Month	Days of Data	Global Horizontal			Direct Normal			Number of Present Weather Observations Containing:		
		Ave. (kWh/ m^2/day)	MBE (%)	RMSE (%)	Ave. (kWh/ m^2/day)	MBE (%)	RMSE (%)	Smoke or Ash	Haze	Dust or Sand
Jan	24	4.16	4.5	9.1	4.72	6.0	28.7	0	2	0
Feb	21	5.44	-0.7	6.4	5.98	-12.8	32.6	0	0	2
Mar	26	5.44	6.0	14.4	4.37	14.1	43.7	0	0	12
Apr	22	6.96	1.9	6.2	6.05	4.5	33.8	0	0	3
May	38	7.14	0.7	6.7	6.28	-7.1	31.1	0	0	6
Jun	41	7.39	-0.5	6.6	6.62	-11.8	28.2	0	0	1
Jul	43	7.26	2.4	7.9	6.27	3.5	35.6	0	9	15
Aug	36	6.70	3.0	5.9	5.07	9.6	31.7	0	1	12
Sep	9	6.20	4.5	9.8	5.11	9.3	25.4	0	0	0
Oct	28	5.45	0.6	5.5	5.53	-4.1	24.3	0	1	0
Nov	40	4.44	3.4	15.5	5.46	-12.4	25.7	0	0	2
Dec	56	3.99	1.1	9.0	4.64	-5.5	24.2	0	0	7
All	384	5.85	1.9	8.6	5.54	-2.5	30.8	0	13	60

Table 9.17. MBEs and RMSEs for Al-Qaisumah

Month	Days of Data	Global Horizontal			Direct Normal			Number of Present Weather Observations Containing:		
		Ave. (kWh/ m^2/day)	MBE (%)	RMSE (%)	Ave. (kWh/ m^2/day)	MBE (%)	RMSE (%)	Smoke or Ash	Haze	Dust or Sand
Jan	55	3.51	-0.0	12.0	4.62	-9.8	28.2	0	0	2
Feb	40	4.84	-0.2	11.6	6.11	-2.0	35.2	0	0	12
Mar	32	4.92	5.2	15.0	3.92	10.3	52.4	0	0	25
Apr	17	6.75	3.4	9.4	5.93	10.2	28.8	0	0	16
May	20	7.51	2.6	5.0	7.06	-0.8	18.6	0	0	4
Jun	27	8.14	1.5	4.1	8.43	-6.1	22.3	0	0	3
Jul	29	7.87	2.6	5.1	7.93	-2.4	24.2	0	0	17
Aug	21	7.44	3.4	6.0	7.40	-0.3	19.3	0	0	10
Sep	28	6.47	3.4	6.1	6.82	11.2	25.8	0	0	12
Oct	25	5.21	4.2	10.5	5.60	15.7	32.6	0	0	0
Nov	32	3.67	-0.1	15.9	4.54	-8.4	33.9	0	0	1
Dec	25	3.39	1.4	13.7	4.74	-8.7	33.0	0	0	0
All	351	5.49	2.2	9.2	5.91	-0.3	29.3	0	0	102

Table 9.18. MBEs and RMSEs for Al-Ahsa

Month	Days of Data	Global Horizontal			Direct Normal			Number of Present Weather Observations Containing:		
		Ave. (kWh/ m^2/day)	MBE (%)	RMSE (%)	Ave. (kWh/ m^2/day)	MBE (%)	RMSE (%)	Smoke or Ash	Haze	Dust or Sand
Jan	78	4.03	1.9	10.6	5.63	-5.8	22.8	0	4	2
Feb	73	4.96	0.9	7.1	5.25	5.6	29.7	0	6	12
Mar	59	5.32	2.1	9.9	4.54	4.7	34.2	0	18	19
Apr	53	6.77	1.1	5.7	5.81	1.7	23.7	0	4	19
May	53	7.20	3.5	8.2	5.71	11.7	28.0	0	8	9
Jun	72	7.92	0.5	4.0	7.65	-3.6	21.7	0	1	18
Jul	85	7.68	2.1	4.9	6.88	6.2	24.9	0	11	30
Aug	75	7.22	2.6	4.5	6.65	3.8	21.7	0	14	27
Sep	51	6.67	3.3	6.2	6.96	5.2	24.7	0	9	11
Oct	50	6.32	-10.5	20.6	7.00	-8.2	27.7	0	10	1
Nov	46	4.49	-3.9	18.1	5.22	-6.4	30.2	0	7	1
Dec	54	3.97	1.5	6.7	5.64	-4.5	22.1	0	6	7
All	749	6.10	0.8	8.9	6.12	1.0	25.5	0	98	156

Table 9.19. MBEs and RMSEs for Sharurah

Month	Days of Data	Global Horizontal			Direct Normal			Number of Present Weather Observations Containing:		
		Ave. (kWh/ m^2/day)	MBE (%)	RMSE (%)	Ave. (kWh/ m^2/day)	MBE (%)	RMSE (%)	Smoke or Ash	Haze	Dust or Sand
Jan	51	5.07	6.9	12.2	6.41	5.8	28.2	0	1	9
Feb	39	6.10	3.5	6.3	6.84	4.0	28.5	0	0	16
Mar	44	6.42	5.2	9.5	5.72	11.4	32.9	0	8	33
Apr	29	7.24	4.4	7.1	6.12	14.2	39.3	0	6	23
May	24	6.98	4.0	9.5	6.07	-6.2	33.9	0	0	15
Jun	27	6.99	4.9	9.1	5.58	9.3	36.3	0	4	13
Jul	45	6.90	10.2	13.1	4.77	35.7	57.7	0	12	35
Aug	39	7.05	5.7	8.8	5.90	7.2	29.0	0	2	17
Sep	35	7.08	1.5	5.8	6.98	-2.3	24.0	0	0	3
Oct	21	6.42	-1.5	4.6	7.71	-16.0	21.5	0	0	0
Nov	24	5.37	0.1	6.7	6.91	-12.6	24.2	0	0	1
Dec	26	5.21	1.5	4.0	7.69	-11.4	18.4	0	1	3
All	404	6.38	4.5	9.0	6.28	4.2	31.5	0	34	168

Table 9.20. MBEs and RMSEs for Wadi Al-Dawaser

Month	Days of Data	Global Horizontal			Direct Normal			Number of Present Weather Observations Containing:		
		Ave. (kWh/ m^2/day)	MBE (%)	RMSE (%)	Ave. (kWh/ m^2/day)	MBE (%)	RMSE (%)	Smoke or Ash	Haze	Dust or Sand
Jan	72	4.66	3.6	10.0	5.84	-2.7	24.7	0	0	8
Feb	67	5.89	3.6	6.1	6.97	3.3	22.2	0	0	29
Mar	64	5.93	6.5	11.2	5.11	18.6	35.6	0	4	57
Apr	65	7.18	4.4	7.9	6.07	11.4	38.8	0	3	79
May	56	7.17	6.2	11.1	5.82	11.6	30.9	0	0	37
Jun	59	7.52	4.1	7.5	6.76	-0.3	23.2	0	0	17
Jul	80	7.33	6.4	8.9	6.12	9.9	30.3	0	0	42
Aug	60	7.15	4.9	7.9	6.49	-0.7	27.7	0	0	9
Sep	50	6.86	3.9	6.4	6.91	2.8	28.4	0	0	15
Oct	41	6.06	0.1	9.5	7.44	-15.3	29.4	0	0	4
Nov	43	5.03	0.4	6.5	6.30	-10.0	24.8	0	0	6
Dec	46	4.77	1.9	6.5	6.87	-6.6	22.4	0	0	0
All	703	6.35	4.3	8.7	6.33	2.4	28.5	0	7	303

These results reflect the current status of the software and the input data. To improve results, the following elements require further investigation:

- Update aerosol coefficients based on more recent direct normal measurements
- Use monthly averages of aerosol optical depth instead of the sine curve relationship to see if that better accommodates changes in aerosol optical depths for Saudi Arabia.
- Use measured values of precipitable water vapor and ozone, instead of the equations, to see what, if any, improvements in the results are possible.

After completing the initial study discussed above, questions arose as to whether the appropriate aerosol coefficients were used and if the larger RMSEs for direct normal were reasonable. Aerosol coefficients selected from the data grid used for the initial study were compared with those used for the 1997 workshop. Two stations had notable differences for average Aerosol Optical Depth (AOD): Gizan with an AOD of 0.160 from the data grid and 0.320 from the workshop; and Abha with an AOD of 0.160 from the data grid and 0.108 from the workshop.

After changing the average AOD to 0.320, solar radiation for Gizan was remodeled and new statistics were computed. The results are shown in Table 9.21. Increasing the AOD reduced the overall MBE for direct normal from +26.3% to –1.7%.

Table 9.21. MBEs and RMSEs for Gizan for Average AOD = 0.320

Month	Days of Data	Global Horizontal			Direct Normal			Number of Present Weather Observations Containing:		
		Ave. (kWh/ m^2/day)	MBE (%)	RMSE (%)	Ave. (kWh/ m^2/day)	MBE (%)	RMSE (%)	Smoke or Ash	Haze	Dust or Sand
Jan	54	4.37	3.3	13.5	3.68	-1.6	40.5	2	0	0
Feb	42	5.32	2.1	11.2	4.41	0.8	28.7	5	0	0
Mar	29	5.59	5.7	13.5	4.05	-1.1	41.8	2	1	0
Apr	29	6.83	-0.5	5.3	5.51	-1.7	23.2	1	0	3
May	23	6.77	0.7	7.5	5.22	-12.0	35.3	2	1	3
Jun	22	6.58	2.2	5.7	4.52	1.6	29.5	0	2	7
Jul	34	5.91	13.5	17.2	2.79	56.5	77.0	1	3	62
Aug	29	5.91	11.5	17.9	3.37	32.1	58.5	0	2	21
Sep	25	6.51	-0.7	5.0	5.40	-8.6	24.8	0	0	1
Oct	32	5.66	-2.7	17.5	5.40	-25.6	41.0	0	0	0
Nov	26	4.87	-0.5	14.5	4.62	-11.7	35.1	0	0	2
Dec	25	4.65	-3.7	13.0	4.96	-19.8	35.9	0	0	2
All	370	5.62	2.9	12.6	4.39	-1.7	38.4	13	9	101

Insight for the larger RMSEs for direct normal were examined by rerunning the data for the Solar Village with METSTAT statistics turned "OFF". These results are shown in Table 9.22. Overall RMSEs for daily values of direct normal were reduced from 27.1% to 21.6%. Apparently, there are day-to-day variations in real AODs that keep the RMSEs for direct normal about twice those for global horizontal even when the statistics are turned "OFF". With the statistics turned "ON", the modeled AODs are varied from the average and the difference between real and modeled AOD may increase, resulting in a larger RMSE.

Figure 9.2 illustrates this point. Modeled direct normal radiation and AODs, for both statistics "ON" and "OFF", were plotted along with the measured direct normal radiation for a two week cloud free period in September 1997. With statistics "OFF", the modeled direct normal radiation was closer to measured values, but the modeled values with statistics "ON" better represented the range of measured values encountered.

These results indicated that the METSTAT model, as modified to account for the input data structure and different mix of observation variables in the DATSAV2 data set, could be used to model solar radiation data for DATSAV2 stations with mean bias errors of less than 10% and root mean square errors of less than 15% with respect to measured data. The objective of the METSTAT model is to produce solar radiation data with the statistical properties of long term measured solar radiation data, and not precise hour-by-hour computation of solar radiation data. Thus the accuracies achieved in this comparison justify the use of modified METSTAT algorithms and DATSAV2 data to produce a solar radiation database for Saudi Arabia comprised of both measured and modeled solar radiation and meteorological data.

Table 9.22. MBEs and RMSEs for the Solar Village with METSTAT statistics turned "OFF".

| Month	Days of Data	Global Horizontal			Direct Normal			Number of Present Weather Observations Containing:		
		Ave. (kWh/ m^2/day)	MBE (%)	RMSE (%)	Ave. (kWh/ m^2/day)	MBE (%)	RMSE (%)	Smoke or Ash	Haze	Dust or Sand
Jan	81	4.01	4.0	12.6	5.69	-13.2	24.3	0	8	0
Feb	84	5.19	4.1	10.0	6.02	-2.0	25.8	0	3	7
Mar	84	5.47	8.3	16.1	4.69	4.6	36.9	0	7	38
Apr	81	6.83	5.4	9.9	6.25	-2.0	22.4	0	16	23
May	84	7.26	5.8	10.1	6.17	-0.3	24.2	0	10	19
Jun	76	7.98	3.1	4.9	8.26	-12.1	17.8	0	4	3
Jul	82	7.62	4.8	6.7	7.31	-7.4	14.9	0	14	19
Aug	89	7.39	4.0	5.2	7.64	-9.5	14.7	0	14	13
Sep	59	6.70	6.3	7.9	7.35	-0.5	19.6	0	19	9
Oct	58	5.57	6.0	8.6	6.70	-3.4	16.9	0	11	4
Nov	51	3.96	6.8	14.5	4.71	-7.4	28.6	0	9	2
Dec	50	3.99	4.5	7.7	5.91	-9.7	20.0	0	3	0
All	879	6.13	5.1	9.3	6.43	-5.5	21.6	0	118	137
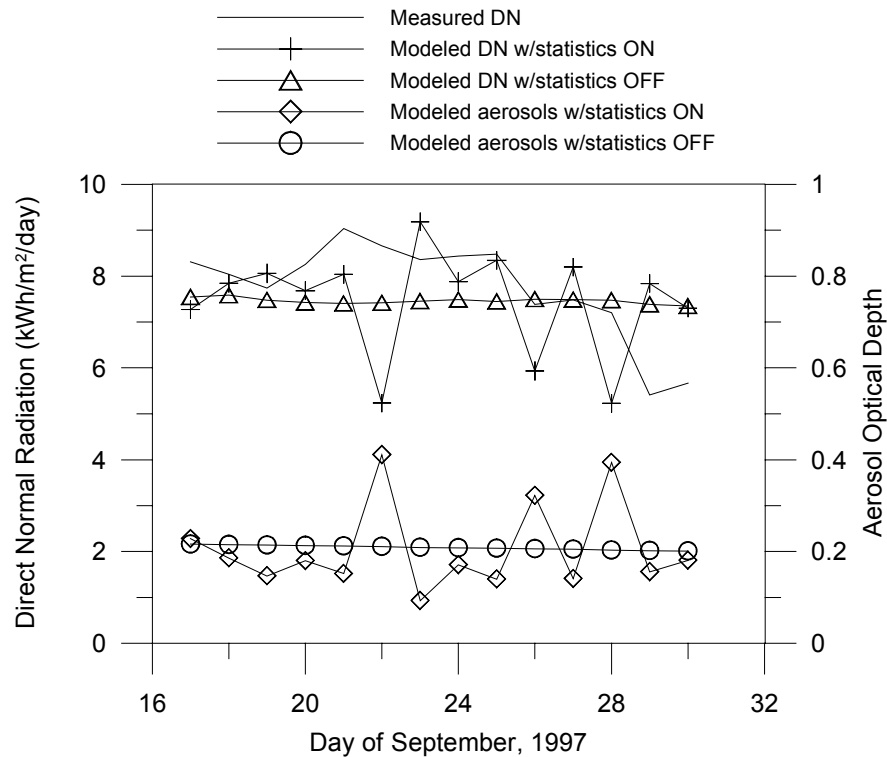
Figure 9.3. Comparison of modeled direct normal radiation and AODs and measured direct normal radiation for a two week cloud free period for the Solar Village with METSTAT statistics turned "OFF" and "ON".

9.3 SQL Implementation of the Database

After consultation with NREL, KACST decided that rather than repeat verbatim the "custom software" approach NREL used in producing the US 1961-1990 database, they would use commercially available, standardized software and database packages to produce both tools and products to support dynamic, flexible, useful national (and possibly international) solar radiation and meteorological databases for their country. The commercial package selected by KACST was Microsoft SQL Server.

SQL stands for "Structured Query Language". This language allows users to pose complex questions of a database. It also provides a means of creating databases. "SQL Server" is a database software package, analogous to Oracle, or MS Access. SQL is a standardized product that is very widely used. Many database products support SQL. This means that if you learn how to use SQL you can apply this knowledge to MS Access, SQL Server, Oracle and countless other databases. No other database language has found such wide acceptance among such a broad range of products. Since it was first standardized in 1986, SQL has become universally adopted. Even non-relational database systems support a SQL interface. Programmers, database administrators, and business analysts alike use SQL to access information. A working knowledge of the language is valuable to anyone who uses a database.

SQL works with *relational databases*. The relational model was first introduced in a paper published in 1970 by Dr. E. F. Codd. [35], providing a mathematical basis for structuring, manipulating, and controlling data, and it abstracted data from any physical implementation. A relational database stores data in tables (relations). A database is a collection of tables. A table consists a list of records - each record in a table has the same structure, each has a fixed number of "fields" of a given type; similar to the "flat" or "fixed" structure in the present US National Solar Radiation Database. Most important, relational databases have the mathematical property of **closure**: any operation performed on a relation yields another relation. This lets one perform *mathematical operations on relations with predictable results*. It also allows operations to be abstracted into variable expressions and nested.

The advantages of the relational approach espoused by KACST included the ability to easily update and augment a previously generated database; change and add in computational algorithms as improved models were developed, produce customized products, and easily produce "default" or "nominal" products. The eventual capability for user-interactive (i.e., over the Internet) production of customized data sets and products was envisioned as well. (SQL is the basis of most Internet business shopping software).

KACST had begun to implement their strategy using the SQL Server package, NREL-supplied algorithms, input data (DATSAV2 Saudi data subset), quality assessment software, and expert advice when the Annex II project was terminated in June 2000. Under the then-operative Annex II project, NREL purchased an identical copy of SQL server using KACST funds. Both institutions planned to share in the development and evaluation of the 'queries,' the language of SQL, to perform ALL of the operations which NREL

spent four years (1988-1991) in programming custom software, debugging, and iterating multiple times to produce the NSRDB. With the termination of the Annex II project, KACST will be proceeding to implement these plans, relying on NREL for occasional technical consultation under a no-cost joint Memorandum of Understanding (see Appendix A).

10.0 Conclusion

This *Final Report* summarizes the accomplishment of work performed, results achieved, and products produced under Annex II, a project established under the Agreement for Cooperation in the Field of Renewable Energy Research and Development between the Kingdom of Saudi Arabia and the United States. The report covers work and accomplishments from January 1998 to December 2000. A previous progress report, *Progress Report for Annex II – Assessment of Solar Radiation Resources in Saudi Arabia 1993-1997*, NREL/TP-560-29374, summarizes earlier work and technical transfer of information under the project. A brief synopsis of the progress report is contained in this final report. The work was performed at NREL in Golden, Colorado, at KACST in Riyadh, Saudi Arabia, and at selected weather stations of MEPA. The primary objectives of Annex II were to upgrade the assessment of solar radiation resources in Saudi Arabia, and to transfer NREL's solar radiation resource assessment technology to KACST in the form of hardware, software, and staff training.

The original objectives of the project, set out in 1993, included the following tasks:

Task 1.   Update Solar radiation measurements in Saudi Arabia

Task 2.   Assemble a database of concurrent solar radiation, satellite (METEOSAT) and meteorological data (with a period of record of 10 years, to the extent possible)

Task 3.   Adapt NREL model and other software for use in Saudi Arabia

Task 4.   Develop procedures, algorithms, and software to estimate solar irradiance at locations and times for which measured solar radiation was not available.

Task 5.   Prepare a uniformly spaced grid of solar radiation data to prepare maps and atlases, and to estimate solar radiation resources and system performance at any location in Saudi Arabia.

These objectives have been substantially achieved by:

1. The design, procurement, and deployment of high quality solar radiation instrumentation in the KACST solar radiation monitoring network
2. The development of a 2nd edition of a solar radiation atlas for the Kingdom of Saudi Arabia, including all of the solar radiation modeling, geographical information system procedures and data needed to produce future updates

3. Transfer of NREL-developed METSTAT and CSR models to KACST for their use
4. The transfer of large, decadal data sets of DATSAV2 meteorological data suitable for input to modified METSTAT algorithms for producing a Saudi National Solar Radiation Database
5. Significant upgrades of KACST Solar Village for BSRN, UV, IR , and sunphotometer measurements
6. Development of software to reformat Saudi BSRN data for submission to the BSRN archive
7. Twelve joint publications regarding the project and scientific results derived from the project [3,5-8,11-13,17-19,30].

With the termination of the JECOR Annex II agreement in June 2001, KACST and NREL realized the advantages of continued cooperation on a collegial basis. The two institutions then developed a no-cost Memorandum of Understanding concerning this research area. This document, reproduced in Appendix A, sets the foundation for continued joint work and exchange of data and research results of importance to both institutions and both country's renewable energy efforts.

The success of the Annex II project documented here is the result of concerted professional effort of all participants from all involved entities, including the Saudi Ministry of Finance and the National Economy, the U.S. Department of Treasury, the U.S. Department of Energy Headquarters in Washington, D.C., The U.S. Department of Energy Golden Field Office, the members of the Joint Economic Commission, and the scientists, researchers and technicians in the KACST Energy Research Institute and NREL Distributed Energy Resources Center.

11.0 References

1. Anon, *Project Agreement Between the Saudi Arabian National Center for Science and Technology and the Saudi Arabian Ministry of Finance and the National Economy, Jointly, and the United States Department of Energy and United States Department of Treasury, Jointly, for Cooperation in the Field of Solar Energy.* 1977, U.S. Department of Energy: Washington, D.C. and Riyadh, KSA.
2. Anon, *Saudi Arabian - United States Joint Commission on Economic Cooperation Project Agreement Between the King Abdulaziz City for Science and Technology and the Ministry of Finance and National Economy Kingdom of Saudi Arabia and the Department of Energy and the Department of Treasury United States of America for Cooperation in the Field of Renewable Energy Research and Development.* 1987, U.S. Department of Energy: Washington D.C., USA and Riyadh, KSA.
3. Maxwell, E.L., S.M. Wilcox, C. Cornwall, B. Marion, S. H. ALawaji, M. bin Mahfoodh, A. Al-Amoudi, *Progress Report for Annex II- Assessment of Solar Radiation Resources in Saudi Arabia 1993-1997 NREL/TP-560-25374.* 1999, National Renewable Energy Laboratory: Golden CO. p. 100.

4. WMO, *International Pyrheliometer Comparison VIII*. 1996, World Meteorological Organization: Davos and Zurich, Switzerland.

5. Al-Abbadi, N., M.,S.H. Alawaji, M.Y. bin Mahfoodh, D.R. Myers, S. Wilcox, M. Landenberg, *Saudi Arabian Solar Radiation Network Operation Data Collection and Quality Assessment*. Renewable Energy, 2002. **25**: p. 219-234.

6. Wilcox, S., M bin Mahfoodh, N Al-Abbadi, S Alawaji, D Myers. *Improving Global Solar Radiation Measurements Using Zenith Angle Dependent Calibration Factors*. in *Forum 2001 Solar Energy, the Power to Choose*. 2001. Washington D.C: American Solar Energy Society.

7. Wilcox, S., D Myers, N Al-Abbadi, M Y Bin Mahfoodh. *Using Irradiance and Temperature to Determine the Need for Radiometer Calibrations*. in *Forum 2001 Solar Energy The Power to Choose*. 2001. Washington, D.C.: American Solar Energy Society.

8. Anon, *RCC-Radiometer Calibration and Characterization Data Acquisition and Data Base Software for the Calibration and Characterization of Pyranometers and Pyrheliometers*. 1994, National Renewable Energy Laboratory: Golden CO. p. 95.

9. NREL, *Users Manual for Quality Assessment of Solar Radiation Data NREL /TP-463-5608*. 1993, National Renewable Energy Laboratory: Golden CO.

10. Maxwell, E.L., *METSTAT The Solar Radiation Model Used in the Production of the National Solar Radiation Data Base (NSRDB)*. Solar Energy, 1998. **62**(4): p. 263-279.

11. Maxwell, E.L., George, R.L., Wilcox, S.M. *A Climatological Solar Radiation Model*. in *1998 Annual Conference- American Solar Energy Society*. 1998. Albuquerque, NM: American Solar Energy Society.

12. Anon, *Solar Radiation Atlas for the Kingdom of Saudi Arabia*. 2nd ed. 1999, Riyadh, Kingdom of Saudi Arabia: King Abdulaziz City for Science and Technology.

13. Maxwell, E.L., C. Cornwall, S. Wilcox, M. bin Mahfoodh. *Assessment of Solar Radiation Resources in Saudi Arabia*. in *World Renewable Energy Conference*. 1996. Denver, Co: Pergamon.

14. WMO, *OMM No. 8 Guide to Meteorological Instruments and Methods of Observation*. 5th ed. OMM. Vol. No. 8. 1983, Geneva, Switzerland: Secretariat of the World Meteorological Organization.

15. Reda, I., *Calibration of a Solar Absolute Cavity Radiometer with Traceability to the World Radiometric Reference NREL/TP-463-20619*. 1996, National Renewable Energy Laboratory: Golden CO. p. 79.

16. Myers, D., et al., *Improved Radiometric Calibrations and Measurements for Evaluating Photovoltaic Devices NREL TP-520-28941*. 2000, National Renewable Energy Laboratory: Golden CO. p. 34.

17. Myers, D.R., T L Stoffel, S Wilcox, I Reda, A Andreas, *Recent Progress in Reducing the Uncertainty in and Improving Pyranometer Calibrations*. Journal of Solar Energy Engineering, 2002. **in press**.

18. Reda, I., *Improving the Accuracy of Using Pyranometers to Measure Clear Sky Global Irradiance NREL/TP-560-24833*. 1998, National Renewable Energy Laboratory: Golden CO. p. 24.

19. Reda, I., Myers, D, *Calculating the Diffuse Responsivity of Solar Pyranometers NREL/TP-560-26483*. 1999, National Renewable Energy Laboratory: Golden CO. p. 15.

20. NREL, *Final Technical Report National Solar Radiation Data Base (1961-1990) NREL TP-463-5784*. 1995, National Renewable Energy Laboratory, Golden, CO.

21. NSRDB, *Vol 1 Users Manual-National Solar Radiation Data Base (1961-1990)*. 1992, National Renewable Energy Laboratory: Golden CO.

22. Faiman, D., Feuerermann, D., Zemmel, A., *Site Independent Algorithm for Obtaining the Direct Beam Insolation from a Multipyranometer Instrument.* Solar Energy, 1993. **50**(1): p. 53-58.

23. Anon, *Kingdom of Saudi Arabia Saudi Arabian Solar Radiation Atlas*. first ed. 1983, Riyadh, Saudi Arabia: The Saudi Arabian National Center for Science and Technology. 95.

24. Walraven, R., *Calculating the Position of the Sun.* Solar Energy, 1978. **20**: p. 393-397.

25. Walraven, R., *ERRATUM "Calculating the Position of the Sun.* Solar Energy, 1979. **22**: p. 195.

26. Michalsky, J., *ERRATA: The Astronomical Almanac's Algorithm for Approximate Solar Position (1950-2050).* Solar Energy, 1988. **41**(1): p. 113.

27. Michalsky, J., *The Astronomical Almanac's Algorithm for Approximate Solar Position (1950-2050).* Solar Energy, 1988. **40**(3): p. 227-235.

28. Gulbrandsen, A., *On the Use of Pyranometers in the Study of Spectral Solar Radiation and Atmospheric Aerosols.* Journal of Applied Meteorology, 1978. **17**: p. 899-904.

29. Dutton, E.G., J. J. Michalsky, T. Stoffel, B. W. Forgan, J. Hickey, T. L. Alberta, I. Reda, *Measurement of Broadband Diffuse Solar Irradiance Using Current Commercial Instrumentation with a Correction for Thermal Offset Errors.* Journal of Atmospheric and Oceanic Technology, 2001. **18**(3): p. 297-314.

30. Myers, D.R., S. Wilcox, M. Anderberg, S. Alawaji, N. Al-Abbadi, M. bin Mahfoodh. *Saudi Arabian Solar Radiation Network for Validating Satellite Remote Sensing Systems*. in *Earth Observing Systems IV, Annual Meeting of Photo-optical Instrumentation Engineers # 3750*. 1999. Denver Co: Society of Photo-optical Instrumentation Engineers.

31. Ohmura A., E.D., B. Forgan, C. Fröhlich, H. Gilgen, H. Hegner, A. Heimo, G. König-Langlo, B. McArthur, G. Muller, R. Phillapona, R. Pinker, C. Whitlock, K. Dehne, M. Wild, *Baseline Surface Radiation Network (BSRN/WCRP): New Precision Radiometry for Climate Change Research.* Bulletin of the American Meteorological Society, 1998. **79**(10): p. 2115-2136.

32. McArthur, B., *Baseline Surface Radiation Network (BSRN) Operations Manual Ver. 1.0 WMO TD-No. 879*. 1998, World Climate Research Program, World Meteorological Organization: Geneva Switzerland.

33. Holben, B.N., T F Eck, I Slutsker, D Tanre, J P Buis, A Setzer, E Vermote, J.A. Reagan, Y.F. Kaufmann, T Nakajima, F. Lavenu, I Jankowiak, A. Smirnov, *AERONET-A Federated Instrument Network and Data Archive for Aerosol Characterization.* Remote Sensing of the Environment, 1998. **66**: p. 1-16.

34.   Anon, *National Climatic Data Center Temporary Data Documentation for DATSAV2 Surface TD-9950*. 1998, National Climatic Data Center http://www4.ncdc.noaa.gov/ol/documentlibrary/datasets.html: Asheville, NC.

35.   Codd, E.F., *A Relational Model of Data for Large Shared Data Banks.* Communications of the Association for Computing Machinery, 1970. **13**(6): p. 377-387.

Appendix A.

Joint Memorandum of Understanding Between NREL and KACST

MEMORANDUM OF UNDERSTANDING
between
The National Renewable Energy Laboratory
and
The King Abdulaziz City for Science and Technology
Energy Research Institute

SUBJECT.   Memorandum of Understanding on Renewable Energy Resource Assessment between the King Abdulaziz City for Science and Technology Energy Research Institute, and The National Renewable Energy Laboratory of the U.S. Department of Energy, hereinafter the "Participants". This memorandum facilitates cooperation in the area of research, development, validation, and application of renewable energy resource assessment models, assessment tools, and data products

1.   Purpose

a.   The National Renewable Energy Laboratory (NREL) is a U.S. Department of Energy Laboratory dedicated to research, development and deployment of renewable energy systems. The NREL Distributed Energy Resources Center conducts research and development of assessment data, models, and tools for evaluating the success of renewable energy systems. The King Abdulaziz City for Science and Technology (KACST) is the national laboratory for scientific and technological development in the Kingdom of Saudi Arabia. The Energy Research Institute (ERI) of KACST conducts research and development of assessment data, models, and tools for evaluating the success of renewable energy systems in the Kingdom.

b.   This Memorandum is a mechanism for both KACST/ERI and NREL to collaborate to exchange information and apply data and research results for performing renewable energy resource assessments. These assessments can promote and foster deployment of successful renewable energy technologies as alternatives to fossil energy sources, climate change and air pollution mitigation options, and improving environmental security world-wide. From 1993-2000 the Participants executed a joint project conducted under Annex II to the *Agreement between the Department of Energy and the Department of Treasury of the United States of America and the King Abdulaziz City for Science and Technology and the Ministry of Finance and National Economy of the Kingdom of Saudi Arabia*. As a result, the Participants have developed extensive expertise, improved instrument calibration and measurement capabilities, data sets and data quality assessment tools, and resource assessment products. The Participants plan to collect additional data, conduct further research, and

produce new tools and products of mutual benefit in these areas. This Memorandum will facilitate continued cooperation and technical exchange in these areas of mutual interest and benefit.

    c.   This Memorandum is a non-binding statement of mutual interest by KACST and NREL in cooperation in the area of renewable energy resource assessment. This Memorandum is not a contract, shall not be used to obligate or commit funds, and will not be used as a basis for the transfer of funds.

2.   Scope of Cooperation

    a.   The general area of research and development covered by this memorandum include:

- Exchanges of data, research results, models, validation results, and staff (visits) between KACST/ERI and NREL.

- Technical discussions and exchanges of solar and meteorological data, methodologies and information that lead to the development of improved resource assessment tools and products of direct use to the renewable energy community.

- Identifying, acquiring or developing data sets for meteorological and aerosol optical depths data for modeling or estimating solar energy resources at high temporal and spatial resolution.

- Validation of satellite-based solar resource estimation algorithms based on the application of the above mentioned data sets and/or models.

    b.   The activities described herein benefit the DOE Photovoltaic (PV), Buildings and Solar Thermal, Wind Energy, and Distributed Energy Resources research and development (R&D) programs. They benefit the KACST/ERI activities in renewable energy research directed to assessing the deployment of renewable energy system in the Kingdom of Saudi Arabia. These research activities require accurate, appropriate resource data tools, products, and models to properly design, size, and deploy economically viable renewable energy systems, as well as predict and evaluate installed performance. Currently, only the PV R&D program provides direct funding support through NREL tasks on Solar Resource Characterization and PV Solar Radiometric Measurements. Other programs access NREL expertise through local NREL program managers on an as-needed basis.

3.   Term

    a.   Cooperation under this Memorandum may commence on the later date of the signatures of the Participants

b.   The term of this Memorandum is 5 years, from the effective date, and the intent is to renew annually by the anniversary of the effective date.

c.   Either Participant may terminate the Memorandum by giving sixty (60) days written notice to the other Participant.

4.   Role of the Parties

a.   The following personnel are designated as the principal points of contact:

KACST/ERI	NREL
Dr. Naif Al-Abbadi.	Mr. Daryl R. Myers
Energy Research Institute	Sr. Scientist
KACST	NREL
P.O. Box 6086	1617 Cole Boulevard
Riyadh 11442 Kingdom of Saudi Arabia	Golden, CO 80401-3393
Telephone: 966-1-481-3487	Telephone: (303) 384-6768

The principal point of contact from each Participant will be responsible for implementation of this memorandum. These contacts will also be responsible for resolution of issues cutting across organizational lines in their respective organizations.

b.   The Participants may each propose to each other separate individual, joint, or collaborative projects related to the subject matter of this Memorandum.

5.   Disclosure of Information

The Participants intend to cooperate in a manner that facilitates exchanges of non-proprietary information.

6.   Review Meetings

a.   Meetings to review plans and evaluate subsequent performance of activities undertaken pursuant to this Memorandum may be conducted on an annual basis, within the constraints of the resources available for the Participants to attend such meetings.

b.   When practical, the principal contacts will arrange and attend the review meetings, and are free to include technical experts in appropriate fields when necessary, within the constraints of the resources available to the Participants

7.   Intellectual Property

Activities that may involve sharing of proprietary information and allocation of rights and interest in intellectual property are excluded from the purview of this

Memorandum. In the event it becomes necessary to share proprietary information, separate nondisclosure agreements will be put in place.

8. **Future Collaboration**

    a.   This Memorandum does not create legally binding obligations between the Participants. It serves only as a record of the intentions of the Participants to identify areas of joint interest and possible cooperation.

    b.   If the Participants agree to undertake joint projects, they intend to develop a separate written agreement for each project, setting out each Participant's contribution, deliverables, responsibilities, and intellectual property rights and obligations.

Signatures

FOR THE NATIONAL RENEWABLE   FOR   THE KING ABDULAZIZ CITY FOR
ENERGY LABORATORY: SCIENCE AND TECHNOLOGY

By_____   By_____

Title_____   Title_____

Date_____   Date_____

REPORT DOCUMENTATION PAGE

1. AGENCY USE ONLY (Leave blank)	2. REPORT DATE April 2002	3. REPORT TYPE AND DATES COVERED Technical report; 1998-2001

4. TITLE AND SUBTITLE
Final Report for Annex II – Assessment of Solar Radiation Resources in Saudi Arabia 1998-2000

5. FUNDING NUMBERS
Task #: PVP27401

6. AUTHOR(S)
Daryl R. Myers; Stephen M. Wilcox; William F. Marion; Naif M. Al-Abbadi; Mohammed bin Mahfoodh; Zaid Al-Otaibi

7. PERFORMING ORGANIZATION NAME(S) AND ADDRESS(ES)
NREL
1617 Cole Blvd.
Golden, CO 80401-3393

8. PERFORMING ORGANIZATION REPORT NUMBER

9. SPONSORING/MONITORING AGENCY NAME(S) AND ADDRESS(ES)
National Renewable Energy Laboratory
1617 Cole Blvd.
Golden, CO 80401-3393

10. SPONSORING/MONITORING AGENCY REPORT NUMBER
NREL/TP-560-31546

11. SUPPLEMENTARY NOTES

NREL Technical Monitor: Daryl Myers

12a. DISTRIBUTION/AVAILABILITY STATEMENT
National Technical Information Service
U.S. Department of Commerce
5285 Port Royal Road
Springfield, VA 22161

12b. DISTRIBUTION CODE

13. ABSTRACT *(Maximum 200 words)*
The Final Report for Annex II – Assessment of Solar Radiation Resources in Saudi Arabia 1998-2000 summarizes the accomplishment of work performed, results achieved, and products produced under Annex II, a project established under the Agreement for Cooperation in the Field of Renewable Energy Research and Development between the Kingdom of Saudi Arabia and the United States. The report covers work and accomplishments from January 1998 to December 2000. A previous progress report, Progress Report for Annex II – Assessment of Solar Radiation Resources in Saudi Arabia 1993-1997, NREL/TP-560-29374, summarizes earlier work and technical transfer of information under the project. The work was performed in at the National Renewable Energy Laboratory (NREL) in Golden, Colorado, at the King Abdulaziz City for Science and Technology (KACST) in Riyadh, Saudi Arabia, and at selected weather stations of the Saudi Meteorological and Environmental Protection Administration (MEPA).

14. SUBJECT TERMS
Solar radiation; renewable energy; Saudi Arabia; distributed energy resources; NREL; National Renewable Energy Laboratory; Annex II; King Abdulaziz City for Science and Technology; KACST; Joint Economic Commission Office; technical transfer

15. NUMBER OF PAGES

16. PRICE CODE

17. SECURITY CLASSIFICATION OF REPORT Unclassified	18. SECURITY CLASSIFICATION OF THIS PAGE Unclassified	19. SECURITY CLASSIFICATION OF ABSTRACT Unclassified	20. LIMITATION OF ABSTRACT UL